بسم الله الرحمن الرحيم

Kabul Polytechnic University
Vice-Chancellor in Academic Affairs

KPU International Journal of Engineering & Technology (KPU-iJET)

KPU Press, KPU Campus, 5th District, Kabul City, Afghanistan.

Chief Editor: Associate Prof. A. J. Niazi
Managing Director: Associate Prof. A. Faqiri
Cover & Page Designer: Associate Prof. A. J. Niazi

Email Address: ijet@kpu.edu.af
Website: www.kpu-ijet.af

Messages

Message from Editor in Chief

Education is a treasure that can never be stolen. Whoever seeks knowledge and finds it, Allah will give him the reward of paradise.

It is with great pleasure and pride that I present to you Volume 03, Issue 01 of the Kabul Polytechnic University International Journal of Engineering and Technology (KPUIJET). First and foremost, I would like to extend my heartfelt gratitude to all the staff members, officials, and esteemed professors of Kabul Polytechnic University and other universities who have contributed their valuable research articles to this edition.

I would like to express my deepest appreciation to each and every individual who has played a role in bringing this journal to fruition. From the diligent authors who have shared their groundbreaking research findings, to the dedicated reviewers who have provided invaluable feedback, and the tireless editorial team who has worked diligently to ensure the highest quality standards, this publication is a testament to your unwavering commitment and expertise.

The significance of the publication of recent research in engineering and technology cannot be overstated, particularly in the context of Afghanistan's development.

In conclusion, I would like to express my deepest gratitude to all the contributors, reviewers, and dedicated individuals who have made this publication possible. Your unwavering commitment to advancing knowledge and driving progress in engineering and technology is truly commendable.

I invite you to explore the pages of this journal and delve into the wealth of knowledge and insights it offers. Together, let us continue to strive for excellence and contribute to the development of Afghanistan through our collective efforts in research, innovation, and academic collaboration.

Thank you for your continued support and readership.

Sincerely,

Associate Prof. A. Jawad NIAZI, Ph.D.

Editor-in-Chief

Message from the Chancellor of KPU

Prof. Abdul Rashid Iqbal
Chancellor, KPU.

Kabul Polytechnic University is proud of conducting and playing a significant role and brining positive impacts in all its three targeted areas of Teaching, Research and Social Development within Afghan Society despite of various turbulence, conflicts and problems in different period in this country.

I am Pleased to announce publishing the first issue of third volume of Kabul Polytechnic University International Journal of Engineering & Technology (KPU-iJET). This achievement is indeed pride and honored which brings together academicians, scientists, and researchers from different walks of life on a single platform to present their innovative ideas and research findings concerning different spheres of engineering & technology.

With the dedicated efforts of Prof. Ahmad Jawad Niazi as an Editor-in-chief this journal, and all other staff, I am certain KPU-iJET will have great successes in their future initiative steps.

Regards,

Professor Abdul Rashid Iqbal

Chancellor of KPU

Message from the
Vice-Chancellor in Academic Affairs

Assist. Prof. Enayatullah Rahimi
Vice Chancellor in Academic Affairs, KPU.

Academic interaction is one the most efficient way within universities and educational institutions in order to accomplish their expectations of high standards. Universities in all over the globe are mandated to undertake the three main tasks Teaching, Research and social services & development. Researches and studies are brought about and outcomes of the findings are presented with the world as a means of contributing to the bulk of knowledge.

Kabul Polytechnic University is also not an exclusion in the act of the above three mentioned goals where the International Journal of Engineering & Technology is one of its major initiatives which sees as an address for better interaction, collaboration and cooperation among researchers, professors and professionals both locally and internationally, meanwhile it paved the way to present the result of researches finding with the world through this high-principled platform.

I would like to take this opportunity to applaud this achievement to the leadership of the University, right from the pioneer to the current and also to the Editorial team for their efforts reaching this level.

Regards,
Assist. Prof. Enayatullah Rahimi
KPU Vice-Chancellor in Academic Affairs

25	Qareeb Ullah Anwari	Assist. Prof. Kardan University, NUST, Islamabad, Pakistan
26	Zekrullah kochai	Researcher, Parul University (PU), Gujarat, India
27	Ahmad Javeed Faizi	Researcher, Parul University (PU), Gujarat, India
28	Jami Osmanyar	Assistant Professor, Kabul Polytechnic University (KPU)
29	Izatmand Halimzai	Assistant Professor, Kabul Polytechnic University (KPU)

Disclaimer

The views expressed in the manuscript/text by the author(s) are their own and KPU-iJET, KPU or Editor or Publishers do not take any responsibility for the same.

In this issue, texts are copied from the soft copies provided by the author(s). hence printing errors/omissions if any are regretted.

Editorial Committee
KPU-iJET, 2023

Contents

NO	TITLE	PAGE NO
1	**Construction Productivity Analysis, Using Work Sampling Technique, a Case Study in Afghanistan** ABADURAHMAN NASER, INAMULLAH INAM, MOHAMMAD KHALID NASIRY	1
2	**As study on the durability of concrete structures against carbonation in Afghanistan** INAMULLAH INAM, ABADURAHMAN NASER, MIRWAIS SEDIQMAL	15
3	**Evaluation of Underground Water Contamination with Toxic Elements (Arsenic, Manganese, Fluoride and Magnesium) in Khost City** NAQIB AHMAD NAEEMI , MOHAMMAD NOOR JAN AHMADI	31
4	**Copper mineral exploration and metamorphic rock investigation using remote sensing: A case study in the Shaida Copper Mine, Herat, Afghanistan** ABDULKHALIL KHALIL, FARID AHMAD MOHAMMADI, SAYED SHABUDDIN SADAT	41
5	**The Contribution of Coal Resources to Electrical Energy Production in Afghanistan** M. SHAHAB SHARIFI, M. SHUAIB MOHSINI, ALYAS ASLAMI, M. ARIF NOORI, M. HAMED PATMAL	٦١
6	**Avalanche Susceptibility Mapping Using GIS-based Multi-Criteria Decision Analysis: The Case of Shighnan District** AHMAD SHEKIB IQBAL, ABDULLAH NASER	73
7	**Comparing the Elongation and Tensile capacity of Khan steel Reinforcement bar with the Esfahan and Tashkent companies** AHMAD ZAKER MUDASER, MATIULLAH WAHEDI	91
8	**Climate Change Impacts and Surface Water Accessibility Analysis in the Ghorband Sub River Basin, Afghanistan** MUJEEBULLAH MUJEEB, KAWOON SAHAK, LUTFULLAH SAFI, MUJIBURAHMAN AHMADZAI, SHARIFULLAH PEROZ	105
9	**Evaluation of Asphalt Mixtures Containing Rejuvenated Reclaimed Asphalt Pavement** KAMALUDDIN KAMAL, MUJTABA AMIN	123

KPU International Journal of Engineering & Technology
Volume 3, Issue1, Sep. 2023
e-ISSN:2790-0819, p-ISSN:2790-0800

Date Received: **202**3-04-15
Date Accepted: **202**3-06-04
Date Published: 202**3**-09-15

Construction Productivity Analysis, Using Work Sampling Technique, a Case Study in Afghanistan

ABADURAHMAN NASER[1*], INAMULLAH INAM[2], MOHAMMAD KHALID NASIRY[3]

[1*]Teaching Assistant, Department of Civil Engineering, Engineering Faculty, Laghman University, Sultan Ghazi Baba Town, Mehtarlam, Afghanistan. Email: abadmehraban@gmail.com

[2]Teaching Assistant, Department of Civil Engineering, Engineering Faculty, Laghman University, Sultan Ghazi Baba Town, Mehtarlam, Afghanistan. Email: inam.azizi@gmail.com

[3] Teaching Assistant, Department of Civil Engineering, Engineering Faculty, Laghman University, Sultan Ghazi Baba Town, Mehtarlam, Afghanistan. Email: nasiryk1366@gmail.com

Abstract

In the construction industry, productivity is one of the most important key performance indicators and fundamental to project success. Productivity isn't everything, but it is pretty much everything in the long run. Improving construction productivity is therefore one of the priorities of the construction industry in many countries around the world. Productivity cannot be managed or improved without being measured, so it must first be measured and analyzed, and then productivity weaknesses identified and corrected. This paper aims to measure labor productivity in the construction industry and assess the percentage distribution of productive, semi-productive, and non-productive activities by observing construction work. The work sampling method was used to find out how labors spend their time during an eight-hours working day, and to identify percentage of the productive, semi-productive and nonproductive tasks on a working day. The required number of the observations was calculated, the procedure for making observations was determined, and data were collected through observations made on a construction project as a case study. based on this study, it is found that generally about 32.02% of laborers' working time is spent on productive (direct) work, 36.70% on semi-productive (supportive) work, and 31.28% was spent on nonproductive (delayed) work.

Keywords: Construction Productivity, Work Sampling, Productivity Analysis

* Corresponding Author

1. Introduction

The construction industry is vital to today's economy as it accounts for a significant portion of any country's economic output [1]. As in other developing countries, the construction sector in Afghanistan is one of the key sectors which provides one of the main sources of income for Afghans [2]. The construction sector has created employment for at least 30% of Afghanistan's workforce. Afghanistan's construction sector has risen in value from 8.7 billion Afghanis (AFN) in 2002-03 to 124.28 billion AFN in 2015-16, accounting for more than 10% of Afghanistan's economy. The contribution to GDP in 2013-14, 2014-15, and 2015-16 was 7.84, 8.89, and 10.03 respectively [3]. However, the important issue is the manner of implementation and management of the construction projects.

Productivity isn't everything, but in the long run it is almost everything. Krugman [4] has stated that higher productivity levels have a direct impact on long-term improvements in a country's standard of living. For every business Improving the productivity of team members should be a priority, because high productivity not only leads to quality results but also helps customers deliver on time [5]. Pan has argued that Although productivity plays such an important role, construction is still a low-productivity level industry, and this remains a problem not only in developing countries but also in more developed countries [6]. Therefore, increasing construction productivity is one of the priorities for construction sectors in many countries around the world.

In a construction project organization and management of those inputs which has a high-level correlation with each other such as materials, labor, and capital greatly affect the success of the project, Therefore, it is more difficult to control and manage these correlated inputs from project workers due to the different nature of people in each country and region [7]. The construction industry is a labor-intensive, craftsman-driven industry, so people's behavior has a significant impact on project performance. With this in mind, it is important to determine the extent of labor productivity and the factors that affect productivity to effectively manage the workforce. Therefore, organizational management must focus on labor productivity analysis and its improvement strategies.

Productivity cannot be managed or improved without being measured, so it is necessary to first analyze and identify low productivity points and correct them [8]. There are many different methods of measuring construction productivity, each with its own strengths and weaknesses. A more appropriate method of measuring construction productivity, which is also used in this study, is the Work Sampling method. The current situation in Afghanistan needs to usher in an improved construction management framework with efficient design and appropriate legal, administrative and pricing systems with appropriate construction materials. Until project managers are able to lead projects to success and assert themselves in a highly competitive environment. Achieving this requires a lot of attention to academic research to uncover weaknesses and suggest possible solutions. It is clear that the number of scientific studies in Afghanistan's construction sector in general and productivity analysis in particular is very low. Therefore, construction productivity measurement was chosen as the topic of this paper. This research will be useful in this field and will contribute to the literature in this area.

2. Theoretical Framework and Literature Review

Construction is one of the most important economic sectors in every country. Therefore, the planning, implementation, monitoring, and control of construction projects must be done with extreme caution. The performance of construction projects should be checked continuously to know how a project is going. Will it finish inside the constraints? Will it succeed or fail? So, the top management can take appropriate action. Measuring project performance is therefore one of the most important topics in project management, and several factors go into measuring project performance: Efficiency, Effectiveness, Schedule, Quality, Productivity, and Safety. Productivity is not only a measure of project performance, it has special meaning in the construction industry as it contributes to the growth and vitality of the industry [9].

Many studies have been conducted to demonstrate the importance of productivity. A study conducted by [10] explored the importance of productivity in project management and concluded that productivity is the cornerstone of successful projects. Dixit conducted another study explaining how project management can improve productivity [11]. In this article, researchers discussed why project management leads to increased productivity. Another research which has carried out by Hamza [12] to address the ways to accelerate productivity with project management software.

Productivity is one of the most crucial issues in construction project management in recent years and it can be defined in numerous ways. Simply put, productivity is a measure of the output you receive for the inputs you use in your process. Being productive means getting more output from the same or less input [13]. Productivity does not just characterize the volume of output, but output gotten in relation to the resources employed [14]. There are two main categories of productivity: Partial Factor Productivity (PFP) and Total Factor Productivity (TFP). In PFP, there is only one input such as labor, materials, and machines. But TFP has multiple inputs [15]. In the construction industry, productivity is usually understood as labor productivity, and that is, the units of work created or produced per man-hour. Depending on the case, it may be used in reverse, and man-hours per unit, this form is also often used [16].

In order to manage construction productivity, it must first be measured [17]. Labor productivity ignores equipment and material costs. These are difficult to change in the short term. Additionally, labor costs are affected by factors such as craftsmanship, experience, and project location. For this reason, labor productivity also ignores actual labor costs and instead considers the number of hours to produce a unit of production [18]. This is indicated in the following equation number 1.

$$\text{Labor Productivity} = \frac{\text{Unit of physical output}}{\text{Labor hours}} \text{.............(1)}$$

Choosing the right measurement technique is an important topic in productivity analysis. There are many methods that can be used to measure labor productivity. Each method has its own advantages and disadvantages. The current study used the work sampling method to measure labor productivity in a construction project as a case study. Randolph Thomas, a leading authority in the field of construction work sampling, defined the method as "a productivity measurement technique used to quantitatively analyze the activities of people and equipment with respect to time [19]. This method estimates the percentage of time craftsmen spend on activities like plumbing, installing materials, plastering, brick masonry, pouring concrete, etc.[20].

Work sampling is one technique used to measure productivity. This method has been used by several researchers to analyze productivity in various industries. A study used a labor sampling method to assess labor productivity in semi High-Rise building construction projects in Pakistan [21]. This study used the Work Sampling technique to evaluate labor productivity and to determine the proportion of productive, semi-productive, and, nonproductive activities. As a result of this research, it has found that semi-productive activities have a large percentage following productive activities and nonproductive activities.

The work sampling technique used by many [22]–[26] researchers to analyze labor productivity in construction. According to the above publications, the work sampling technique is an effective tool for determining the proportion of workers' productive, semi-productive, and unproductive tasks on the working day of a construction project. Regarding the previous discussion, it is pointed out that there are many studies around the world that analyze labor productivity in the construction industry. However, there are no studies in Afghanistan that analyze and measure construction productivity.

3. Research Scope and Methodology

The work sampling method is used to find out how the laborers spend their time during an eight-hour working day and measure the percentage of productive, semi-productive, and nonproductive work on a working day. The required number of observations was calculated, the procedure for making observations was determined and the data were collected through the observations which were made on a construction project as a case study.

In the application of the work sampling technique, sufficient numbers of observations must be taken at random to achieve reliable results. In this method, errors are likely to occur but increasing the number of observations can reduce the error. To calculate the number of observations required for achieving the desired accuracy, the following formula is used [27]:

$$n = \frac{z^2 . p(1-p)}{(s.p)^2} \quad \text{..........} (2)$$

n= Sample size (number of observations)

z= number of standard deviation from mean for the desired level of confidence, for example, z=1.96 for a confidence level of 95%.

s= standard error for example 5%

P= percentage of occurrence of an activity or delay, expressed in decimal e.g. 30%=0.3

3.1. Procedure for Work Sampling Study

Following steps was taken to conduct the Work Sampling study

i. Defining the Problem.

ii. Obtaining the approval of the responsible manager of the project in which study was to be made. For this purpose, the researcher personally visited the responsible manager of the pre-selected project to obtain their approval to conduct the study, moreover the researcher visited the project staff and workers prior to starting the study in order to inform them about purpose of the study and to obtain their co-operation.

iii. Determine the desired accuracy of the final results in the form of standard error or percentage. An accuracy of 5% was accepted for this study.

iv. Indicates the 95% confidence level accepted for this study.

v. Make a preliminary estimate of the percentage occurrence of the activity or delay to be measured for one day. To do this, researcher visited the project and calculate percentage of the delay of the labors at the project site which was 30%. It means that labors were delaying 30% of all the working hours.

vi. Designing the study. In this step of the study, the following activities were executed:

   a. the Number of observations has been determined, this is one of the most important points in this research. the required number of observations was calculated with formula 3. In this study 'z' was equal to 1.96 for the confidence level of 95%, 's' or a standard error was equal to 5%, and 'p' was 30% according to the calculation which was done during the site visit before start the study, then the number of observations “n” was founded as below:

$$n = \frac{z^2.p(1-p)}{(sxp)^2} = \frac{1.96^2 \times 0.3(1-0.3)}{(0.05x0.3)^2} = \frac{3.8416 \times 0.3 \times 0.7}{0.000225} = 3585 \ldots\ldots\ldots\ldots\ldots\ldots\ldots\ldots (3)$$

   Therefore, at least 3585 observations were required to obtain reliable data. This may seem like a large number, but in a real application, every glance at the work in progress is an observation, so, 3585 observations are not excessive.

   b. The number of days required for the survey was calculated based on the number of the laborers at the project site and observation rounds per day. The number of workers at the time of the survey was 50, and observations were made 10 times a day. Therefore, it was calculated that it took at least 8 days to complete 3585 observations. However, in order to obtain reliable data, the project was visited for ten days and about 5000 observations were made.

c. An observation form was designed to collect the data.

1. The observations were made randomly and data recorded. To ensure that the observations are in fact made at random, a random table was used.

The project selected for applying the work sampling method was a public building construction project in Jalalabad city. The case study project was selected based on available resources, ease of access, and suitability. The total duration of the project was one calendar year, and five months had passed since the start of the project at the time of data collection, but the completion rate of the project was less than 30%. The main ongoing activities observed were backfilling, bricklaying, steel fixing, formwork and concrete placement.

In work sampling study ten rounds of observations were recorded on daily bases for 10 days. The author randomly noted labors at different paths on site for each round by observing them, recording their activities into standard mention categories and denoted it by a mark in the corresponding portion. Thus 10 rounds were repeated for each day and the number of ticks at the end of the day was recorded to display the number of labors corresponding to each category. The same exercise was repeated for the days of observations for 10 days and eventually summed up to reveal the total observations in accordance with the standard work sampling procedure.

Furthermore, according to the [27] task type does not play role as the observation is restricted to the mentioned categories which are generalized and are common in all types of activities. So, the focus is not on what the person is doing, but on the specific categories that fall into each moment of observation. However, as already mentioned, observations were limited to common types of backfilling, bricklaying, steel fixing, formwork and concrete placement. The recorded observations are therefore related to the task types mentioned in light of the standard categories. Some project information, operational details, and data have been removed to respect stakeholder confidentiality and their confidentiality requirements.

Extensive data was collected to understand the patterns in which workers spend their time during working hours. Other information physically observable at the project site is recorded to aid in data analysis and related results. The extra key information that impacts project productivity, such as weather conditions, working environment, safety conditions, skills and expertise, construction phases, and ongoing activities recorded as well. Table 1. Shows the number of observations made each day during the survey.

Table 1: Number of the observations made each day during the study

Day	*Observation Numbers*
1	480
2	490
3	510
4	500
5	500
6	510
7	500
8	510
9	500
10	500
Total	5000

4. Results and Discussion

After data collection, the observations were classified into the seven categories mentioned above, as shown in Table 2. In this table, percentages for each work category are recorded for each individual day, with the last column showing the average percentage for each category.

Table 2: Percentages for each work category

	Days										**Average %**
Activity type	1	2	3	4	5	6	7	8	9	10	
Productive work %	28.9	29.5	33.1	30.5	33.4	33.9	32.6	32.5	33.1	32.7	32.02
Semi-productive work %	37.4	37.6	35.9	37.2	36.4	36.5	33.8	36.4	37.1	38.7	36.7
Non-productive work %	33.7	32.9	31	32.3	30.2	29.6	33.6	31.1	29.8	28.6	31.28
total %	100	100	100	100	100	100	100	100	100	100	100

Table 3. shows the percentage of three categories of work: productive, semi-productive and nonproductive for every single day of the study period. As evident from the table below that direct work is negatively correlated in some extent with supportive work and delays.

Table 3: Percentages for each work category

Activity type		1	2	3	4	5	6	7	8	9	10	Average %
		Days										
Direct work %		28.9	29.5	33.1	30.5	33.4	33.9	32.6	32.5	33.1	32.7	32.02
Supportive work %	preparatory work and instruction	10.3	8.9	10.4	11	10	10.5	12.1	10.2	11.2	11.1	10.57
	travelling	9.7	8.7	9.6	10.1	9.2	7.1	7.3	8.2	9.1	8.2	8.72
	tools & equipment	8.6	11.4	8.5	8.8	5.9	6.4	5.3	8.4	8.3	9.3	8.09
	materials handling	8.8	8.6	7.4	7.3	11.3	12.5	9.1	9.6	8.5	10.1	9.32
Delays %	personal	19.4	20.3	19.5	17.4	21.1	19.8	17.6	18.4	16.9	17.3	18.77
	waiting	14.3	12.6	11.5	14.9	9.1	9.8	16	12.7	12.9	11.3	12.51
Total %		100	100	100	100	100	100	100	100	100	100	100

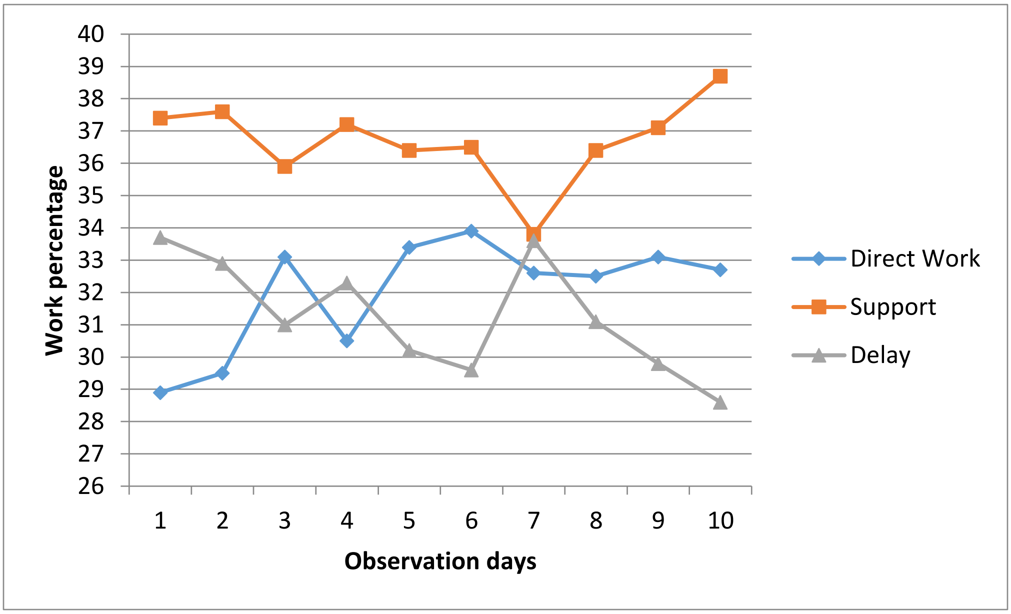

Fig 1: Percentages of each work category

To generalize the results of the study and measure labor productivity, all observations over 10 days are shown in Table 4. Each figure represents a characteristic of observed worker behavior, categorized into seven different types, which are further grouped into three main classes: direct (productive) work, support (semi-productive) work, and delay (non-productive) work.

Table 4: Percentages for each work category

Activities			%
Direct Work			32.02
Support	preparatory work and instruction	10.57	36.7
	travelling	8.72	
	tools & equipment	8.09	
	materials handling	9.32	
Delay	Personal	18.77	31.28
	waiting	12.51	

As shown in table 4. Supportive (semi-productive) activities were the largest number with 36.7%, following the direct (productive) work with 32.02% and the last one delay activities with value of 31.28%. First, the main categories of activity were analyzed in detail, and then the subcategories (secondary activities) in percentages were fully explored. According to Table 4, preparatory work and instruction shares the largest portion in support category, whereas in delay category, personal activities have the largest portion. It can be observed that secondary activities holding larger percentage after direct work are personal, preparatory work and instruction and waiting. Therefore, streamlining and managing these activities is necessary to increase direct work. Additionally, other related activities should be minimized as well because reducing them ultimately increases productive activities, which ultimately leads to increased construction labor productivity and increased project success.

Intuitively, to increase the overall productive (direct) work rate, areas of lower productivity should be minimized/avoided as much as possible throughout the project. And, this can be done by identifying factors that lead to decreased productivity during the project. Some of the reasons for the low percentage of direct (productive) work in case study project are lack of skills, lack of tools and equipment, improper use of scaffolding, unsuitable plywood for formwork, Improper planning, poor safety, design errors, etc. In addition, site management and responsible are encouraged to instruct the worker to work at appropriate times rather than starting work late or leaving the project site early.

5. Conclusion

By controlling costs in different parts of the project, construction companies become more profitable and they can compete in the market. These include labor costs, material costs, and overhead costs, of which labor costs differ the most. And this ultimately related to labor productivity, which needs to be managed and controlled strictly to ensure success of the project. This study is primarily focused on evaluating labor productivity in building construction project in Afghanistan.

The objective of the study was to analyze labor productivity on a construction project in Afghanistan. To analyze and measure productivity, a building construction project in

Jalalabad city, Afghanistan was selected as a case study. To find out how the laborers spend their time during working hours on a day and to measure the percentage of productive, semi-productive, and nonproductive work the Work Sampling technique was used. Which was the most relevant techniques identified in the literature. The required number of observations has been calculated. Procedures are established for conducting observations. Data were collected through observations made on a construction project selected for case study.

The study revealed that supportive (semi-productive) activities were the most common at 36.7%, followed by direct (productive) work at 32.02%, and delayed (nonproductive) activities at 31.28% accordingly. In addition, it was found that preparatory work and instruction share the largest portion in the supportive activities category, whereas in the delay category, personal activities have the largest portion.

For the success of the project, the labor productivity should be at the highest possible level, and this needs continuous monitoring of the site and determining the reasons for low labor productivity. The main reasons for the low percentage of direct (productive) work in case study projects were lack of skills of labors, lack of proper tools and equipment, improper use of scaffolding, unsuitable plywood for formwork, Improper planning, poor safety, design errors, etc. These factors can be the reasons for low labor productivity in other construction projects in Afghanistan as well.

This study forms the basis for assessing labor productivity in construction projects in Afghanistan. The work-sampling approach is used in the current research and can be further improved in the future by increasing the number of projects to add value to the existing body of knowledge.

6. Acknowledgement

The authors would like to thank the responsible persons for their permission and immense cooperation during the data collection at the project site.

7. Conflicts of Interest

All authors declare that they have no conflicts of interest to disclose.

References

[1] N. Wang, “The role of the construction industry in China’s sustainable urban development,” *Habitat Int.*, vol. 44, pp. 442–450, 2014.

[2] O. K. Hazrat and G. R. Kumar, “Construction Challenges in Afghanistan,” *i-Manager’s J. Manag.*, vol. 14, no. 2, p. 1, 2019.

[3] E. Grawert and F. Shirzad, “Conflict-sensitive employment in Afghan construction and transport companies,” 2017.

[4] P. Krugman, “Defining and measuring productivity,” *Age diminishing Expect.*, 1994.

[5] E. Dabla-Norris, G. Ho, K. Kochhar, A. Kyobe, and R. Tchaidze, “Anchoring growth: the importance of productivity-enhancing reforms in emerging market and developing economies,” *J. Int. Commer. Econ. Policy*, vol. 5, no. 02, p. 1450001, 2014.

[6] W. Pan, “Rethinking construction productivity theory and practice,” *Built Environ. Proj. asset Manag.*, vol. 8, no. 3, pp. 234–238, 2018.

[7] A. Kazaz and T. Acıkara, “Comparison of labor productivity perspectives of project managers and craft workers in Turkish construction industry,” *Procedia Comput. Sci.*, vol. 64, pp. 491–496, 2015.

[8] B. Vogl and M. Abdel-Wahab, “Measuring the construction industry’s productivity performance: Critique of international productivity comparisons at industry level,” *J. Constr. Eng. Manag.*, vol. 141, no. 4, p. 4014085, 2015.

[9] M. Jahangirian, S. J. E. Taylor, T. Young, and S. Robinson, “Key performance indicators for successful simulation projects,” *J. Oper. Res. Soc.*, vol. 68, no. 7, pp. 747–765, 2017.

[10] S. Dixit and K. Sharma, “An empirical study of major factors affecting productivity of construction projects,” in *Emerging Trends in Civil Engineering: Select Proceedings of ICETCE 2018*, 2020, pp. 121–129.

[11] S. Dixit, S. N. Mandal, J. V Thanikal, and K. Saurabh, “Evolution of studies in construction productivity: A systematic literature review (2006–2017),” *Ain Shams Eng. J.*, vol. 10, no. 3, pp. 555–564, 2019.

[12] M. Hamza, S. Shahid, M. R. Bin Hainin, and M. S. Nashwan, “Construction labour productivity: review of factors identified,” *Int. J. Constr. Manag.*, vol. 22, no. 3, pp. 413–425, 2022.

[13] A. Pekuri, H. Haapasalo, and M. Herrala, “Productivity and performance management–managerial practices in the construction industry,” *Int. J. Perform. Meas.*, vol. 1, no. 1, pp. 39–58, 2011.

[14] F. Barbosa, J. Woetzel, and J. Mischke, “Reinventing construction: A route of higher productivity,” McKinsey Global Institute, 2017.

[15] A. A. Tsehayae and A. R. Fayek, “System model for analysing construction labour productivity,” *Constr. Innov.*, vol. 16, no. 2, pp. 203–228, 2016.

[16] G. A. Bekr, “Study of significant factors affecting labor productivity at construction sites in Jordan: site survey,” *GSTF J. Eng. Technol.*, vol. 4, no. 1, p. 92, 2016.

[17] M. Abdel-Hamid and H. Mohamed Abdelhaleem, “Impact of poor labor productivity on construction project cost,” *Int. J. Constr. Manag.*, vol. 22, no. 12, pp. 2356–2363, 2022.

[18] S. Zheng, W. Sun, J. Wu, and M. E. Kahn, "The birth of edge cities in China: Measuring the effects of industrial parks policy," *J. Urban Econ.*, vol. 100, pp. 80–103, 2017.
[19] M. C. Gouett, "Activity analysis for continuous productivity improvement in construction." University of Waterloo, 2010.
[20] M. C. Gouett, C. T. Haas, P. M. Goodrum, and C. H. Caldas, "Activity analysis for direct-work rate improvement in construction," *J. Constr. Eng. Manag.*, vol. 137, no. 12, pp. 1117–1124, 2011.
[21] N. A. Sheikh, F. Ullah, B. Ayub, and M. J. Thaheem, "Labor productivity assessment using activity analysis on semi high-rise building projects in Pakistan," *Eng. J.*, vol. 21, no. 4, pp. 273–286, 2017.
[22] I. Loera-Hernández and G. Espinosa-Garza, "Labor productivity in projects of construction and industrial maintenance," in *Key Engineering Materials*, 2014, vol. 615, pp. 139–144.
[23] I. Loera, G. Espinosa, C. Enríquez, and J. Rodriguez, "Productivity in construction and industrial maintenance," *Procedia Eng.*, vol. 63, pp. 947–955, 2013.
[24] S. J. Motowidlo, W. C. Borman, and M. J. Schmit, "A theory of individual differences in task and contextual performance," in *Oraganizational Citizenship Behavior and Contextual Performance*, Psychology Press, 2014, pp. 71–83.
[25] N. Antonyán, I. de J. L. Hernández, and G. E. Garza, "Increase of productivity through the study of work activities in the construction sector," 2017.
[26] R. K. Akogbe, X. Feng, and J. Zhou, "Construction projects productivity in west african country of Benin: case of ground earthworks," *J. Constr. Eng. Proj. Manag.*, vol. 5, no. 2, pp. 16–23, 2015.
[27] E. Oddone, M. Weinberger, A. Hurder, W. Henderson, and D. Simel, "Measuring activities in clinical trials using random work sampling: implications for cost-effectiveness analysis and measurement of the intervention," *J. Clin. Epidemiol.*, vol. 48, no. 8, pp. 1011–1018, 1995.

Authors Profile

Abadurahman Naser received the BSc. degree in Civil Engineering from Nangarhar University in 2013 and completed MSc Civil Engineering (Project Management) in 2019, from Istanbul Kultur University, Istanbul City, Turkey. Currently, He is working as teaching assistant in the Department of Civil Engineering, Laghman University, Mehtarlam, Afghanistan. His areas of research include building construction materials and construction management.

Inamullah Inam received the BSc. degree in Civil Engineering from Nangarhar University in 2012 and in 2016, he completed his MSc. degree in Civil and Structural Engineering from Kyushu University in Japan. Currently, He is working as teaching assistant in the Department of Civil Engineering, Laghman University, Mehtarlam, Afghanistan. His areas of research include durability of concrete materials.

Mohammad Khalid Nasiry received the BSc. degree in Civil Engineering from Nangarhar University in 2013 and he received the M.Tech Civil Engineering (Hydraulic structures) 2020, from Z.H college of Engineering and Technology, Aligharh Muslim University in India. Currently, He is working as teaching assistant in the Department of Civil Engineering, Laghman University, Mehtarlam, Afghanistan. His areas of research include concrete and hydraulic concrete structures design.

KPU International Journal of Engineering & Technology
Volume 3, Issue1, Sep. 2023
e-ISSN:2790-0819, p-ISSN:2790-0800

Date Received: 2023-04-12
Date Accepted: 2023-06-04
Date Published: 2023-09-15

As study on the durability of concrete structures against carbonation in Afghanistan

INAMULLAH INAM[1*], ABADURAHMAN NASER[2], MIRWAIS SEDIQMAL[3]

[1*]Teaching Assistant, Department of Civil Engineering, Engineering Faculty, Laghman University, Sultan Ghazi Baba Town, Mehtarlam, Afghanistan. Email: inam.azizi@gmail.com

[2]Teaching Assistant, Department of Civil Engineering, Engineering Faculty, Laghman University, Sultan Ghazi Baba Town, Mehtarlam, Afghanistan. Email: abadmehraban@gmail.com

[3]Teaching Assistant, Department of Civil Engineering, Engineering Faculty, Laghman University, Sultan Ghazi Baba Town, Mehtarlam, Afghanistan. Email: msmm.200@gmail.com

Abstract

The durability of reinforced concrete is significantly affected by the corrosion of reinforcing bars, and carbonation is a major factor in the corrosion of steel bars in concrete. However, In Afghanistan, according to the Afghanistan Building Code (ABC), the major concerns regarding the durability of concrete structures are defined in terms of freezing/thawing, sulfate attack, and chloride-induced corrosion. However, there is no defined exposure class for carbonation-induced corrosion. Therefore, in this study, carbonation rate of concrete in Afghanistan is evaluated, and the carbonation prediction model is used to predict rate of concrete based on environmental and climate conditions. To evaluate the carbonation rate of concrete, 75x75x75mm concrete cubes were prepared and exposed in four different regions; namely Afghanistan, Japan, Indonesia and Malaysia. To predict the carbonation rate of concrete, the Papadakis model was used to estimate the carbonation rate in terms of environmental conditions (relative humidity, temperature, the concentration of CO2) and concrete composition. The carbonation depths of the concrete were measured at 6 months and 1 year after exposure. It was observed that climatic and environmental conditions influenced carbonation progress. Higher carbonation was observed in Afghanistan. Moreover, the prediction of carbonation rate based on atmospheric parameters and concrete composition matched actual carbonation depth measurements in four different regions. Furthermore, the applicability of the model is also confirmed by comparing the predict results with the actual experimental data from accelerated and natural exposed carbonation depths.

Keywords: Carbonation rate, environmental conditions, carbonation prediction model

* Corresponding Author

1. Introduction

The construction industry in Afghanistan is very different from Western countries and faces many challenges in maintaining good quality. Availability of materials and lack of equipment dictate most construction methods. Until 2004, no building codes existed for the concrete industry. Outside of major cities, building design is rarely considered, if ever existing, has historically had any consideration for earthquake force with no influence from modern building codes. Currently, ASC (Afghan Structural Code) has been established by ANSA (Afghanistan National Standard Authority).
Recently in Afghanistan, according to Afghanistan Building Code (ABC)/ Afghanistan Structural Code (ASC), the major concerns about the durability of concrete structures have been defined in terms of freezing/thawing, sulfate attack, and chloride-induced corrosion [1]. However, there is no defined exposure class for carbonation-induced corrosion.
Physical and chemical processes such as acid, sulfate, or alkali attacks can cause the concrete deterioration in service. The most serious failure mechanism is the corrosion of steel bars and one of the main factors of the corrosion is carbonation [2], carbonation reduces the alkalinity of concrete and break the passivity layer of steel bars [3]. carbonation rate is directly related to the concrete strength, type of curing, quality of concrete, mix-proportion, and environmental and climatic factor such as (temperature, relative humidity, and Carbon dioxide concentration).
Relative humidity in concrete is of great importance. Many researchers have stated that the carbonation is significant at a relative humidity between 50-70% [2-6]. Hence, proper design should be carried out to avoid degradation of concrete due to carbonation. Therefore, much research has been done; and many concrete carbonation models have been formulated by applying appropriate modifications using different parameters to Fick's second law of diffusion. However, typical carbonation models have the format of $Xc=A\sqrt{t}$ [8-9]; but some models overestimate the carbonation depth after a certain time period.

2. Materials and Methods

2.1 Materials and Mix proportion

In this study, OPC was used as a binder. Crushed stone with a maximum size of 20mm and washed sea sand were used as fine aggregate. In addition, tap water was used as mixing water for concrete. The physical properties of materials and the concrete mix proportion are described in Table 1 and Table 2, respectively.

Table 1: Physical Properties of Materials

Material	**Description**
Cement	OPC Density = 3.16 g/cm^3, Specific surface area (SSA)= 3330cm^2/g
Gravel	Crushed stone Density (SSD) = 2.88 g/cm^3, Maximum size aggregate (MSA)= 20 mm
Sand	Washed Sea sand Density (SSD) = 2.53 g/cm^3, Fine modulus (FM)=2.69

Table 2: Mix proportion and Fresh properties of the Concrete

Mixture	W/B %	Unit Content (kg/m^3)						Slump (cm)	Air %	Temp ºC
		W	C	Gravel	Sand	WR	AE (ml)			
N-60	60	165	275	1114	800	1031	1586	5.5	4.9	22

* W: Water, C: Cement, * WR: Water Reducer- 3.0 ml / 1 kg of cement

2.2 Methods

Concrete prism specimens of 75x75x75 mm were de-molded 24 hours after casting. Then specimens were then transferred to a temperature and humidity-controlled room. The specimens were kept for 28 days in air curing at a constant humidity of 60% and a temperature of 20 ^{0}C.

After 28 days of curing, samples were prepared to conduct exposure tests. For natural exposure, four distinct countries were selected; namely Japan, Afghanistan, Indonesia, and Malaysia. In addition, the specimens in the natural environment were exposed to normal conditions. Before starting the exposure test, four sides of the specimens were coated with epoxy, and two parallel sides were kept uncoated for CO2 diffusion (see photo 1). The detailed exposure plan is shown in Table 3 and the specimens in exposure site are shown in photo 2.

At 6 months and 1 year of age, the carbonation depths were measured in the laboratory, the specimens were split and cleaned, and 1% of phenolphthalein 90% ethyl alcohol solution was applied to the freshly cut surface. When the solution is sprayed onto broken concrete surface, the carbonated portion remains uncolored (concrete color) and the non-carbonated portion changes to dark purple. The average carbonation depths were measured at 10 points from each side and take the average carbonation depth at a certain age (see photos 3 and 4).

Photo 1: Specimens preparation photos.

Photo 2: Concrete specimens exposed in different regions.

Table 3: Detailed Exposure plan

Exposure Area	Mixture	Exposure Condition			
		Sheltered condition		Unsheltered condition	
		Age			
		6 Months	12 Months	6 Months	12 Months
Japan	N-60	☑	☑	☑	☑
Afghanistan		☑	☑	☑	☑
Indonesia		☑	☑	☑	☑
Malaysia		☑	☑	☑	☑

*N60- normal OPC concrete with 60 W/C ratio

* SH- sheltered condition, UnSH- unsheltered condition

3. Results and Discussions

3.1 Climate Conditions of Four Regions (exposure sites)

Exposure tests in the natural environment were conducted in four different regions, such as Kabul (Afghanistan), Fukuoka (Japan), Makassar (Indonesia), and Batu Pahat (Malaysia). Different regions have different climates and environmental conditions. The average relative humidity and maximum temperature data for four regions have been plotted in Figures 1 and 2, respectively. For Afghanistan, data were collected using hydrometer equipment and for the other three regions, the data are collected from internet sources [3], [11]–[15].

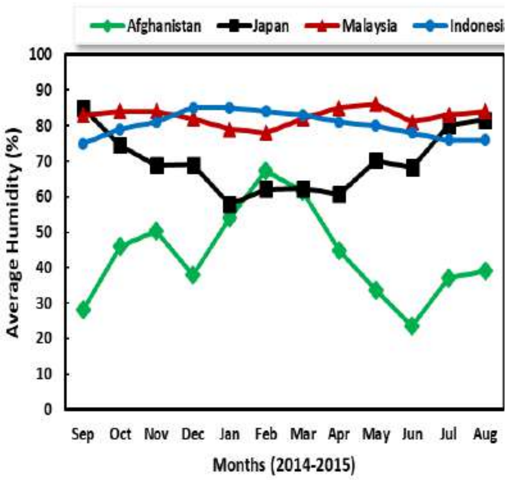

Fig. 1: Average Relative Humidity data

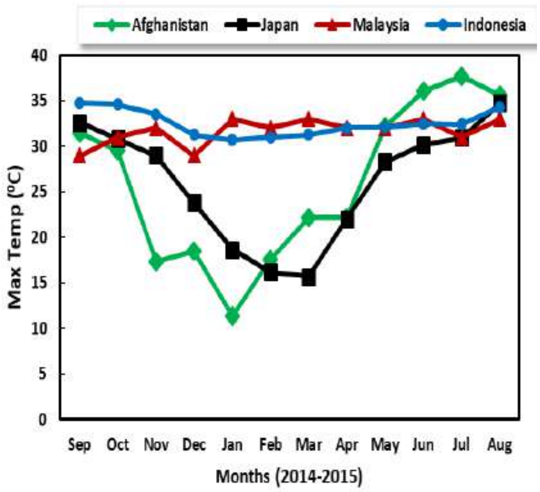

Fig. 2: Annual max temperature data

3.2 Carbonation Depth

Fig. 3 illustrates the carbonation progress for concrete exposed in four different regions with different climate conditions, it was observed that climatic and environmental conditions have influenced the carbonation progress. Higher carbonation has been observed in Afghanistan, the effect of sheltered and unsheltered conditions was insignificant compared to other regions due to the lower annual rainfall.

It was also observed that carbonation was significant in RH <50%; in the case of Afghanistan, the average annual relative humidity was recorded in the range of 45%. The average relative humidity and temperature in Fukuoka were recorded as 65-70% and 17 ^{0}C, respectively. While in Indonesia and Malaysia, the annual average annual relative humidity and temperature were (75-80%), and (28-30^{0}C), respectively. In the case of Japan, the carbonation progress was significant in sheltered conditions compared with two other regions such as Indonesia and Malaysia. This may be due to the effect of temperature. Lower carbonation with high humidity and high temperature.

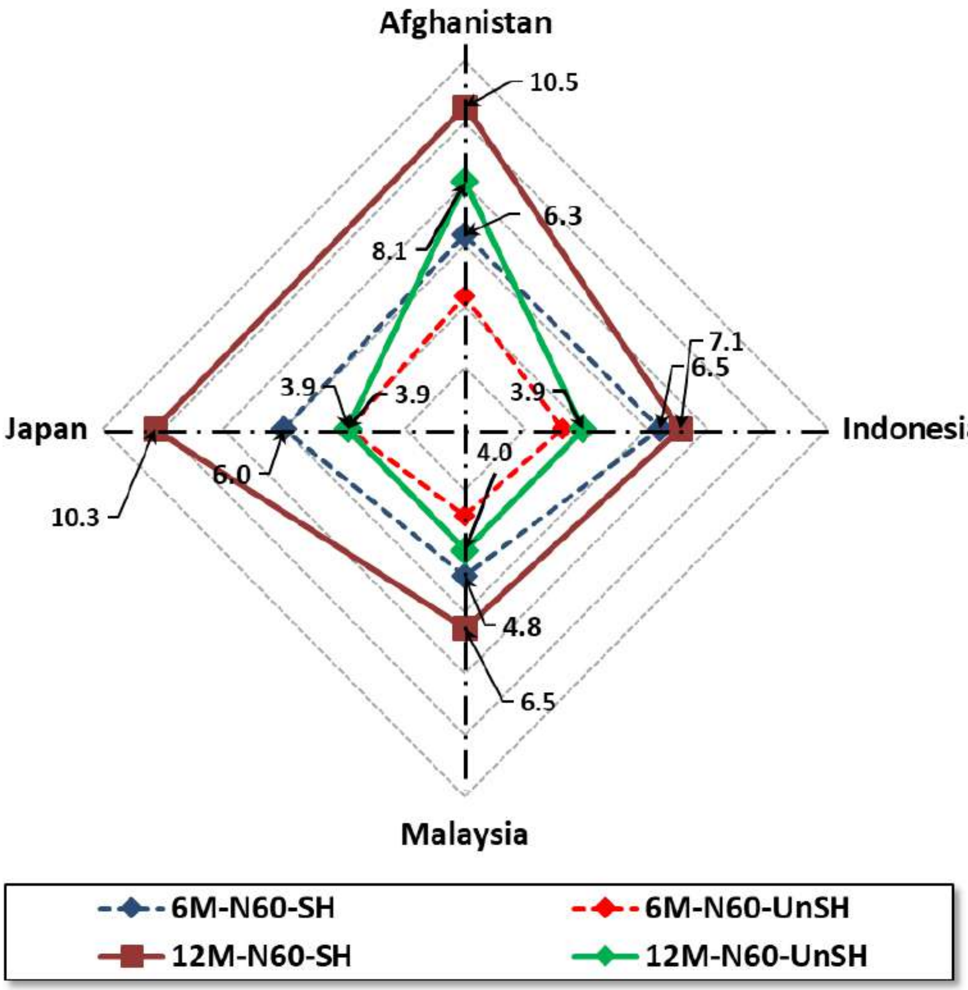

Fig. 3: The measured carbonation depths in four different regions

The climatic conditions of Indonesia are different from Afghanistan and Japan. The average annual temperature and humidity are high; According to research, carbonation is faster for warmer regions and sheltered conditions. Somewhat this statement holds for all exposure conditions at sheltered exposure sites, whereas it can be observed that although the annual temperature in Indonesia is higher than that of Afghanistan and Japan, the carbonation depth is lower than in other two regions, the reason may be the high relative humidity in Indonesia. Concrete faces higher carbonation in high temperatures unless the relative humidity is lower [6].

For the Malaysian environment, it was found that carbonation progress during the first six months was significant, while the increment was not significant until 1 year. The increment in the first six months of the year can be attributed to the dry weather conditions from January to March, and March to February which is usually the rainy season in Malaysia, which causes the carbonation increment less than the 6 months and the carbonation was not significant at high humidity. This means that the drying and wetting processes have a great influence on carbonation progress. The carbonation depth of concrete for four different regions are shown in Photo.3 and Photo 4, respectively.

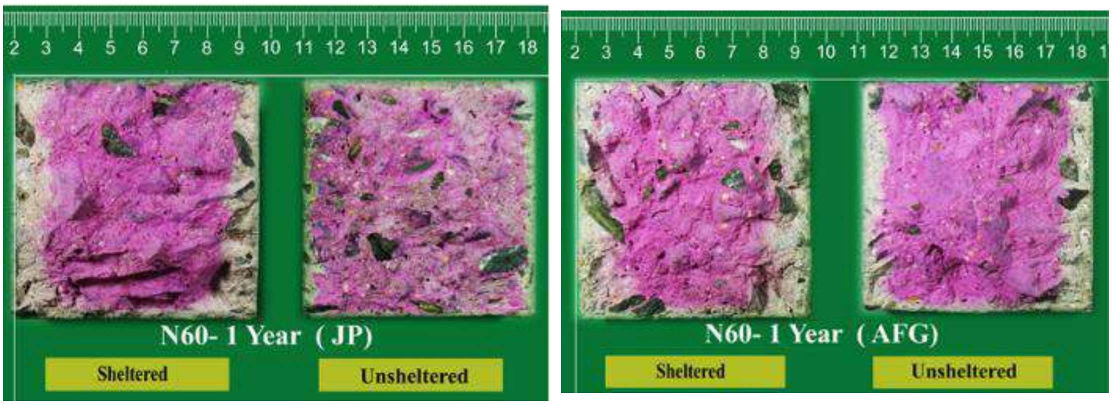

Photo 3: Graphical representation of carbonation depth of concrete for Afghanistan and Japan

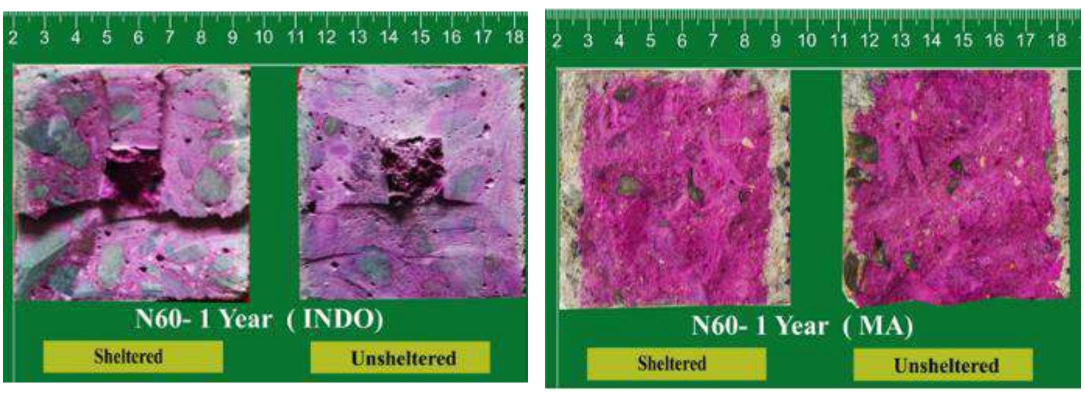

Photo 4: Graphical representation of carbonation depth of concrete for Indonesia and Malaysia

3.3 Carbonation Prediction model

The carbonation process is a complicated process, because it is a combination of the movement of gases and liquids through the pores of concrete. The carbonation of concrete is, in general, a diffusion process. The CO_2 diffusion rate mainly depends on the quality and exposure condition of concrete. Many concrete carbonation models have been formulated by applying suitable modification using different parameters to Fick's second law of diffusion. The models generally contain the parameter which relate to environmental factors involved in carbonation process and the others which describe the capacity of the cement past matrix to bind the CO_2, but typically, the carbonation models take the format of **Eq 1.1** (DuraCrete: Modelling of Degradation 1998).

$$X_{ca} = K_{ca} \cdot \sqrt{t} \qquad (1.1)$$

X_{ca}: is the carbonation depth at time t [mm];
k_{ca}- is the carbonation rate [(mm/year)$^{0.5}$];
t- Is the age of the concrete [years].

The carbonation prediction model used for estimation was developed by Papadakis [3]. Which takes into account the influence of concrete composition, climate parameters such as relative humidity and temperature, and environmental parameter such as the concentration of CO2 on the carbonation of concrete [10-11].

$$Xc = k_{con} \cdot k_{RH} \cdot k_{cur} \cdot k_{CO2} \cdot k_{temp} \cdot \sqrt{t} \qquad (1.2)$$

Where

k_{con}: is the concrete quality related coeffecient
k_{Cur}: is the curring related coeffecient
k_{T}: temprature related coeffecient.
k_{RH}: is the relative humidity related coeffecient
k_{CO2}: the squar root of CO_2 content (Here the concentration of CO_2 0.05%)

Papadakis has summarized the main composition parameters of concrete, which affect the carbonation process as the water-to-cement ratio and aggregate-to-cement ratio. The effects of concrete composition is shown in **Eq 1.2.1** [9][12].

$$K_{con} = 350\left(\frac{\rho_c}{\rho_w}\right)\frac{\left(\frac{w}{c} - 0.3\right)}{1 + \left(\frac{\rho_c}{\rho_w}\right) \cdot \frac{w}{c}} \cdot \sqrt{1 + \frac{\rho_c}{\rho_w} \cdot \frac{w}{c} + \frac{\rho_c}{\rho_a} \cdot \frac{a}{c}} \qquad (1.2.1)$$

Where

ρ_c – the mass density of the cement [kg/m^3],
ρ_w – the density of the water [kg/m^3],
ρ_a – the mass density of the aggregates [kg/m^3],
$\frac{w}{c}$ – the water-to-cement ratio, and
$\frac{a}{c}$ – the aggregate-to-cement ratio

The moisture content of the concrete is of great importance. As diffusion of CO_2 controls the carbonation process. It has been reported that the optimum mositure conditions for carbonation are 50% to 70% relative humidity. Papadakis et al. 1992 and Saetta et al. 1993 have indicated the effective diffusivity of CO_2 as a function of relative humidity in concrete as below [3], [18]:

$$D \propto (1 - RH)^n$$

Where in this part of research, the coefficient for expressing the effects of relative humidity is shown as below:

$$k_{RH} = \left(1 - \frac{RH}{100}\right)^n \qquad (1.2.2)$$

Where,

k_{RH} − is the relative humidity related coefficient
RH − is the relative humidity
n − is a humidity constant.

A group of researchers has suggested values of (n) values, ranging from 0.6 to 2.8 [13-21]. Meanwhile, De Ceukelair and Van Nieuwenburg proposed a relative humidity influence factor betwee 6064- 1.0288 [11] [20], while Papadakis et al. proposed 2.2 [3]. However, in this study, the influence factor was significantly different than that of Papadakis et al. The factor varies depending on the initial curing of concrete and exposure conditions (Sheltered and unsheltered). For W/C≥0.6 and RH<55%, the "n" and Kcur factors are between (21.-2.2) and (0.70-0.76); for W/C≥0.6 and RH>60%, the "n" and Kcur factors are between (1.6-1.9) and (0.65-0.76); for W/C≤0.55 and RH>60%, the coefficents "n" and Kcur factors are between (1.2-1.9) and (0. 5-0.70. Nevertheless, in this study, the initial curing conditions were the same for all concrete specimens, while the humidity levels were different based on the exposure area; these values enable the prediction to be close to actually measured carbonation depths.

The influence of ambient temperature of surrounding environment on the carbonation depth is shown as below:

$$k_t = EXP(\frac{Q}{R} * (\frac{1}{273 + T_0} - \frac{1}{273 + T})$$

Q- Is the diffusion active energy of the carbonation process (Q= 2.7 [kJ/mol]
R- Is the gas constant, R= 0.008314 [kJ/mol.K]
T_0- is the reference temperature, 25 ^{0}C
T- is the actual temperature of surrounding environment.

The influence factor of curing on carbonation of concrete is given in Duracrete (2000), as 1 and 0.76 for 7 and 28 days, respectively [9] . Although in this study, these values are valid only for air-curing specimens and do not take into count the influence of W/C, exposure conditions, and water curing. However, these values vary depending on the environmental conditions, strength level of concrete, and initial water curing.

The results from the four-exposure sites were compared with the predicted carbonation depths, as shown in Fig. 4. The actual carbonation depth well matches with the predictions. The coefficients were calculated as a function of the exposure conditions and are listed in Table 4. In addition, in Figure 4b, a strong correlation was found between actual and predicted carbonation. Therefore, the carbonation model is suitable for predicting the carbonation rate in both sheltered and unsheltered conditions.

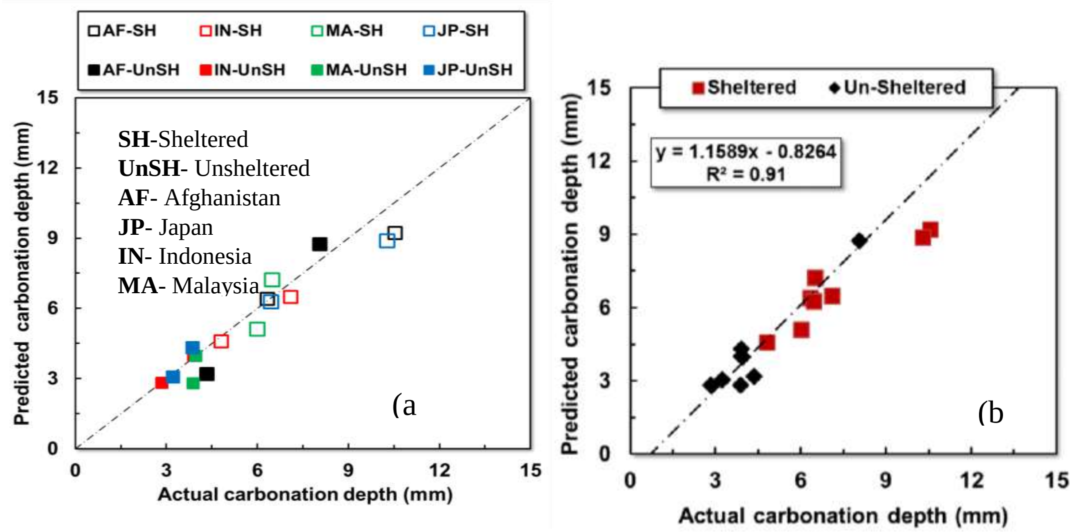

Fig. 4: actual carbonation depths vs. predicted carbonation depth (mm)

Fig. 5 depicts the carbonation prediction for long-term exposure at Fukuoka. The carbonation model is used to verify the long-term estimate of the carbonation depth; Here, the carbonation depth is estimated for over 15 years and compared with the actual data presented in a research paper published in the proceedings of the Trondheim Conference in 1989 [27]. The carbonation depths measured over 15 years are presented in Table 5. The model predictions are in good agreement with the actual data. Therefore, it can be concluded that the prediction of carbonation is significantly influenced by environmental and climatic conditions, concrete compositions, and initial curing parameters. Therefore, all the factors should be considered accordingly.

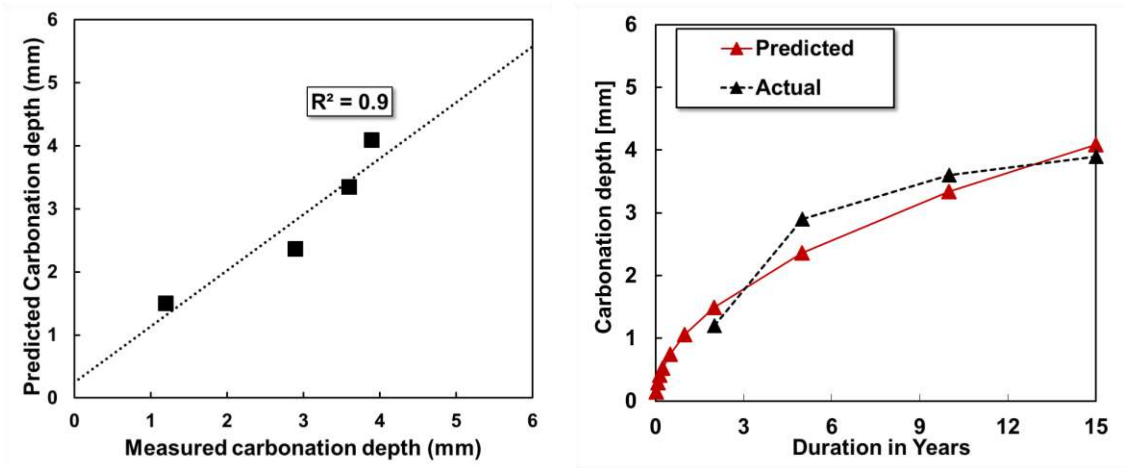

Fig 5: measured carbonation depth vs. model predictions for normal OPC concrete exposed for over 15 years at Fukuoka, Japan.

Table 4: Calculated coefficients for different exposure sites (regions).

Exposure area	Sheltered condition					X_c (1) year
	K_{con}	K_{RH}	K_{temp}	K_{cur}	Kco_2	
Japan	310	0.24	0.97	0.76	0.0224	8.9
Afghanistan		0.25	0.97			9.2
Indonesia		0.16	1.02			6.2
Malaysia		0.19	1.01			7.3
Exposure area	Unsheltered condition					X_c (1) year
	K_{con}	K_{RH}	K_{temp}	K_{cur}	Kco_2	
Japan	310	0.11	0.97	0.76	0.0224	4.1
Afghanistan		0.22	0.97			7.5
Indonesia		0.10	1.02			3.9
Malaysia		0.10	1.01			3.8

Table 5: Carbonation depth of concrete exposed in various regions. (Source: Proceedings of 1989 Trondheim Conference)

Exposure Area	Age (years)	Carbonation Depth (mm)			
		2	5	10	15
Hokkaido		2.0	3.5	3.8	3.3
Miyagi		0.7	2.4	2.6	3.3
Chiba		1.0	2.0	3.0	-
Tokyo		1.6	-	2.2	6.4
Kanagawa		2.2	3.8	3.9	5.5
Hyogo		1.2	2.9	2.3	5.2
Hiroshima		1.2	2.8	3.7	-
Fukuoka		1.2	2.9	3.6	3.9
Kanagawa (in seawater)		0.6	0.0	1.6	2.2

4. Conclusions

1. The carbonation rate of concrete exposed to natural exposure is significantly affected by climatic and environmental conditions; concrete exposed to a relatively dry environment and low annual rainfall indicates higher carbonation over the one-year exposure period. Therefore, it can be said that carbonation is still significant even when the relative humidity is less than 50% and proper durability design shall be carried out to resist the carbonation of concrete in Afghanistan.
2. The specimens under sheltered conditions showed a higher carbonation rate than those kept in unsheltered conditions, however, the carbonation was lower in the environment with high humidity and high-temperature, even when stored under sheltered conditions. The carbonation rate was lower for the specimens exposed with the possibility of rain subjection (non-sheltered) than that without rain subjection.
3. The carbonation model proposed by Papadakis(1992) is suitable for prediction. However, more attention is required to avoid overestimating a long-term estimate. The equation more accurately estimates the depth of carbonation by taking into account the coefficient of initial curing that strongly influences the carbonation process in concrete. Therefore, it can be concluded that the carbonation model considering the environmental and climatic conditions, concrete composition, and initial curing parameters can be an effective way to estimate the carbonation depth and make realistic prediction.

5. Acknowledgement

The authors would like to thank Kyushu university concrete engineering laboratory for providing research facilities in conducting experimental work.

6. Conflicts of Interest

On behalf of all authors, the corresponding author states that conflict of interest to disclose.

References

[1] S. ANSA, "Afghan Structural Code ASC," in *Afghan Structural Code ASC*, 2012, p. 212.

[2] Comite Euro-International du Beton, "Durability of Concrete Structures-State of the Art Report," Paris, 1982.

[3] V. G. Papadakis, M. N. Fardis, and C. G. Vayenas, "Effect of composition, environmental factors and cement-lime mortar coating on concrete carbonation," *Mater. Struct.*, vol. 25, no. 5, pp. 293–304, 1992, doi: 10.1007/BF02472670.

[4] P. A. M. Basheer, G. I. B. Rankin, A. E. Long, and D. Russell, "Effect of relative humidity and air permeability on prediction of the rate of carbonation of concrete," *Proc. ICE - Struct. Build.*, vol. 146, no. 3, pp. 319–326, 2001, doi: 10.1680/stbu.2001.146.3.319.

[5] Y. F. Houst, "The role of moisture in the carbonation of cementitious materials," *Int. J. Restor. Build. Monum.*, vol. 2, pp. 49–66, 1996.

[6] M. Koichi, K. Yoshinori, T. Masayuki, K. Matsuzawa, Y. Kitsutaka, and M. Tsukagoshi, "Effect of Humidity on Rate of Carbonation of Concrete Exposed to High-Temperature Environment," *Int. Symp. theAgeingManagement &Maintenance Nucl. Power Plants*, pp. 109–114, 2010.

[7] E. Marie-Victoire, E. Cailleux, and A. Texier, "Carbonation and historical buildings made of concrete," *J. Phys. IV*, vol. 136, pp. 305–318, Dec. 2006, doi: 10.1051/jp4:2006136031.

[8] S. K. Roy, K. B. Poh, and D. o. Northwood, "Durability of concrete—accelerated carbonation and weathering studies," *Build. Environ.*, vol. 34, no. 5, pp. 597–606, 1999, doi: 10.1016/S0360-1323(98)00042-0.

[9] C. Dura, "General guidelines for durability design and redesign," The European Union-BriteEuRarrdII, Project BE95-1347, Document BE95-1347.

[10] K. Y. Ann, S.-W. Pack, J.-P. Hwang, H.-W. Song, and S.-H. Kim, “Service life prediction of a concrete bridge structure subjected to carbonation,” *Constr. Build. Mater.*, vol. 24, no. 8, pp. 1494–1501, 2010, doi: 10.1016/j.conbuildmat.2010.01.023.
[11] “Climate - Indonesia - average, annual, temperature.” [Online]. Available: http://www.nationsencyclopedia.com/Asia-and-Oceania/Indonesia-CLIMATE.html#b. [Accessed: 14-Oct-2015].
[12]“Climate Data for Fukuoka.” [Online]. Available: http://www.data.jma.go.jp/gmd/risk/obsdl/index.php#. [Accessed: 14-Oct-2015].
[13] *Fukuoka, Japan*. Japan Meteorological Agency.
[14] “Weather of Indonesia - Indonesia Weather - Climate & Weather in Indonesia - Indonesia Weather Forecast.” [Online]. Available: http://www.indonesiapoint.com/weather-of-indonesia.html. [Accessed: 14-Oct-2015].
[15] “Average Weather For Makassar/Ujung Pandang, Indonesia - WeatherSpark.” [Online]. Available: https://weatherspark.com/averages/33999/Makassar-Ujung-Pandang-Sulawesi-Selatan-Indonesia. [Accessed: 14-Oct-2015].
[16] A. V Saetta, B. A. Schrefler, and R. V Vitaliani, “The carbonation of concrete and the mechanism of moisture,heat and carbon dioxide flow through porous materials.,” *Cem. Concr. Compos.*, vol. 23, pp. 761–772, 1993, doi: 10.1016/0008-8846(93)90030-D.
[17] A. Saetta, “Deterioration of Reinforced Concrete Structures due to Chemical–Physical Phenomena: Model-Based Simulation,” *J. Mater. Civ. Eng.*, vol. 17, no. 3, pp. 313–319, Jun. 2005, doi: 10.1061/(ASCE)0899-1561(2005)17:3(313).
[18] A. V Saetta, B. A. Schrefler, and R. V Vitaliani, “2-D model for carbonation and moisture/heat flow in porous materials,” *Cem. Concr. Res.*, vol. 25, no. 8, pp. 1703–1712, 1995, doi: 10.1016/0008-8846(95)00166-2.
[19] K. Van Balen and D. Van Gemert, “Modelling lime mortar carbonation,” *Mater. Struct.*, vol. 27, no. 7, pp. 393–398, 1994, doi: 10.1007/BF02473442.
[20] H.-W. Song, S.-J. Kwon, K.-J. Byun, and C.-K. Park, “Predicting carbonation in early-aged cracked concrete,” *Cem. Concr. Res.*, vol. 36, no. 5, pp. 979–989, 2006, doi: 10.1016/j.cemconres.2005.12.019.
[21] T. Rilem, C. Ingress, and C. Engineering, “Effect of Carbonation on Chloride,” no. September, 2002.
[22] V. Papadakis, C. Vayenas, and M. Fardis, “Physical and chemical characteristics affecting the durability of concrete,” *ACI Mater. J.*, vol. 8, no. 88, pp. 186–196, 1991.
[23] C. E. and T. A. Marie-Victoire E, “Carbonation and historical buildings made of concrete,” *J. Phys. IV Fr.*, vol. 136, pp. 305–318, 2006.

[24] T. Ishida and K. Maekawa, "Modeling of pH profile in pore water based on mass transport and chemical equilibrium theory," *Proceedings-Japan Soc. Civ. Eng.*, no. 648, pp. 203–216, 2000.
[25] L. De Ceukelaire and D. Van Nieuwenburg, "Accelerated carbonation of a blast-furnace cement concrete," *Cem. Concr. Res.*, vol. 23, no. 2, pp. 442–452, 1993, doi: 10.1016/0008-8846(93)90109-M.
[26] C.-F. Chang and J.-W. Chen, "The experimental investigation of concrete carbonation depth," *Cem. Concr. Res.*, vol. 36, no. 9, pp. 1760–1767, 2006, doi: 10.1016/j.cemconres.2004.07.025.
[27] M. K. and S. Nagataki, "Carbonation of Concrete with Fly Ash and Corrosion of Reinforcements in 20 Year Tests," *Spec. Publ.*, vol. 114, doi: 10.14359/2007.

Authors Profile

Inamullah Inam received the BSc. degree in Civil Engineering from Nangarhar University in 2012 and in 2016, he completed his MSc. degree in Civil and Structural Engineering from Kyushu University in Japan. Currently, He is working as teaching assistant in the Department of Civil Engineering, Laghman University, Mehtarlam, Afghanistan. His areas of research include durability of concrete materials.

Abadurahman Naser received the BSc. degree in Civil Engineering from Nangarhar University in 2013 and completed MSc Civil Engineering (Project Management) in 2019, from Istanbul Kultur University, Istanbul City, Turkiye. Currently, He is working as teaching assistant in the Department of Civil Engineering, Laghman University, Mehtarlam, Afghanistan. His areas of research include building construction materials and construction management.

Mirwais Sediqmal received the BSc. degree in department of Hydraulics and Hydraulic Structures from Kabul Polytechnic University in 2009 and completed the MSc. degree in the same department from Kabul Polytechnic University in 2016. Currently, He is working as teaching assistant in the Department of Civil Engineering, Laghman University, Mehtarlam, Afghanistan. His areas of research include hydraulics structures.

KPU International Journal of Engineering & Technology
Volume 3, Issue1, Sep. 2023
e-ISSN:2790-0819, p-ISSN:2790-0800

Date Received: 2023-04-11
Date Accepted: 2023-06-05
Date Published: 2023-09-15

Evaluation of Underground Water Contamination with Toxic Elements (Arsenic, Manganese, Fluoride and Magnesium) in Khost City

NAQIB AHMAD NAEEMI[1*], MOHAMMAD NOOR JAN AHMADI[2]

[1*]Senior Teaching Assistant, Civil Engineering Department, Engineering Faculty, Shaikh Zayed University, Khost, Afghanistan. Email: naeemi.naqib@gmail.com

[2]Senior Teaching Assistant, Head of Department, Civil Department, Engineering Faculty, Shaikh Zayed University, Khost, Afghanistan. Email: eng.ahmadi786@gmail.com

Abstract

Water is considered one of the most important and basic materials of life, but for drinking, there must be such water that does not have bad effect on health. For this purpose, a lot of research has been done at the international level, in these researches the chemical composition of water has been determined that is suitable for health. Since mostly the people of Khost use the underground water for drinking purpose, so we considered it necessary to check the toxic elements (arsenic, manganese, fluoride and magnesium) in the underground water composition at Khost city, that more or less quantity of these elements has a very bad effect on health. The purpose of this research is to determine the toxic (arsenic, fluoride and magnesium) composition of underground water in Khost city and compare it with international standards and to know that can we use the underground water for drinking propose. This research, which was carried out at three places of underground water in the center of Khost province, found that the underground water at Khost city does not contain arsenic, the amount of manganese is below the permissible level, the amount of fluoride is within the permissible limit and the amount of magnesium is 0.28 mg/l which is less than the permissible level.

Keywords: Underground Water, Toxic Elements, Water Quality for Drinking, Arsenic, Manganese, Fluoride, Magnesium, Water Contamination.

* Corresponding Author

1. Introduction

Water is life. This vital fluid is the basis of life, health development and well-being. In developing countries during the last few decades, with the increase of population and industrial activities, on the one hand, the chances of contamination of water resources has increased, on the other hand, the demand for good quality water is increasing day by day. Among them, underground water resources are considered as a reliable source of natural filtration, because underground water plays an important role in the circle of human life. [6]

Water is an irreplaceable substance as a component and vital substance of the living environment, which plays an important role in ensuring health and avoiding of producing diseases. The importance of water in the lives of humans and other living beings has such a clear role that it does not need any reasons. Water is responsible for the transportation of substances to the body that form vital parts of the body. 65-75 percent of human body weight consists of water. Rapid growth of population, community development, agricultural and urban water needs, industrial and electrical needs have led to the scarcity of healthy drinking water. [20]

Groundwater is assessable both in terms of quality and quantity. All the attention in the developed and third world is to find suitable underground water reservoirs for irrigation, agriculture and industry. Meanwhile, very little attention is paid to underground water reservoirs. [4,19] The results of Fao studies have shown that water is unsustainable in 93 countries of the world, which means that the use of underground water is much higher than its renewal. [15] In order to protect public health, water that is available to consumers must comply with national and international standards. Studies have shown that dirty water causes various diseases, such as nitrite-contaminated water, low hemoglobin, and high nitrite water causes cancer in children. Nitrite pollution is considered to be a very serious problem at the international level. [26,27]

Fluoride is very important for humans, the appropriate amount of fluoride is used to prevent the attack of microbes on the teeth, especially in children. But long-term excess use of fluoride causes chronic fluorosis of the teeth and bones, neurological problems and Alzheimer's. [13,18] This problem exists in many parts of the world. While 250 million people in 25 countries are at risk from high fluoride concentrations in underground water. [1, 14]

A lot of research has been done around the world, as a result, the amount of water compounds has been determined in such a way that there is no harm to humans, animals and plants. These fixed amounts of compounds in water are accepted by health institutions and the available water around the world is compared to these and then decided about the purity and impurity of the water. [17] In this research, four type toxic elements i. e. arsenic, manganese, fluoride and magnesium toxic substances are studied, and we will discuss about them as below:

1. Arsenic: Arsenic is an element with the symbol As. This element does not found pure in nature, but it founds together with other elements such as gold, copper and zinc. This heavy element is very poisonous, it exists in soil and water. Arsenic-containing insecticides, when it used for killing insects, so increase the arsenic in the environment,

in result, this toxic elements enter the food cycle of humans and endanger human health, for example, the liver disease that occurred in fishermen in Japan was caused by fish contaminated with arsenic. [24]
Researches have shown that there is a problem of arsenic in major underground water bodies in the world, the concentration of arsenic in this water is more than 50µg/l. According to the guidelines of the World Health Organization, the amount of arsenic in drinking water should be no more than 0.01mg/l. In the beginning, the amount of arsenic was accepted 0.2 mg per liter (200 µg/l). In 1363, there was a revision in the section of drinking water, which reduced the amount of arsenic to 0.05 mg per liter (50µg/l). Later, in 1993 and 2011, the World Health Organization determined that the amount of arsenic in drinking water to be less than 0.01 mg per liter (10µg/l) because mineral arsenic was proven to cause cancer. Also, the World Health Organization has set the maximum amount of arsenic at 10 µg/l. [30]
When groundwater passes through rocks that have arsenic, so arsenic mixes with the water. Other sources of arsenic include the presence of arsenic in the earth's crust, the dissolution of minerals and industrial wastes in water, and the burning of fossil materials. [24] Large amount of arsenic is highly poisonous and can cause serious health problems, including death in some cases. The effect of arsenic is not immediately apparent in the case of small amounts, but continuous entrance of arsenic into the body has various effects on health and increases the risk of contracting chronic diseases. These diseases include: various types of cancer, narrowing of blood vessels, high blood pressure, heart disease and type 2 diabetes. Arsenic is a toxin that affects nerve cells and affects a person's actions. [22]
2. Manganese: Manganese is abundant in the earth's crust. It occurs in various forms such as Mn-II in the environments where air does not exist. Another form of manganese is Mn-IV which exists in the presence of oxygen. Mn-IV is in the form of an insoluble black sedimentary matter, while Mn-II is completely soluble in the form of Mn^{+2}. Surface water contains less than 0.1mg/l of manganese, but underground airless or vacuum water contains more manganese up to 1mg/l. Soluble manganese often coexists together iron, which is also soluble under anaerobic conditions.
Manganese is very important for humans, but studies have shown that if the amount of this element in drinking water increases, it can cause adverse neurological effects. Because of the potential health risks, the WHO has set a manganese content of 0.4 mg/l. It is not recommended for consumers to use the water containing more than this amount of manganese because the taste of the water deteriorates due to the presence of this metal. In addition, cases have been recorded in which the people are using water that have more amount of Manganese than the WHO amount such as Bangladesh. Manganese levels of 0.05-0.1 mg/l are acceptable to users, but sometimes lead to the deposition of black sediments on pipes. [25]
3. Fluoride: A concern of the medical community, especially dentists, is the presence of fluoride in drinking water. Fluoride is an element that exist in large quantities on the surface of the earth. Fluoride form three percent of the Earth's crust. Fluoride is found in small quantities in surface water reservoirs and in higher quantities in underground water reservoirs. The amount of fluoride in raw water is 0.1 to 1.5 mg/l. But in the composition

of underground water, this amount can exist up to 15 mg/l. Fluoride plays an important role in dental health. Fluoride prevents tooth enamel from dissolving and tooth decay in acidic conditions. Fluoride is an element that is useful in low quantity but harmful in high quantity. The main source of fluoride is drinking water, but small amounts are found in tea, salmon and sardine types of fish. One milligram of fluoride per day is required for adults and children. Fluoride should not exceed 3 mg because it is a toxic element. Increasing the amount of fluoride in the body causes dental and bone fluorosis and intestine diseases. That is, if the amount of fluoride exceeds 1.5 ppm and reaches 2-2.5 ppm, fluoresce starts in the teeth, and in this case, the beauty of the teeth is lost and the general appearance is affected. And besides, the transparency of the teeth also disappears. If the fluoride concentration reaches 4-8 ppm, it causes skeletal fluorosis, and drinking such water reduces bone growth in children. [11]

4. Magnesium: The important mineral cations in drinking water include: calcium, magnesium, sodium and potassium. Although iron ions are present in drinking water in low quantity, they have a greater impact on the quality of water because it causes corrosion of iron pipes and, as a result, spoils the smell and taste of water. Magnesium is the fourth most important cation that is essential for human life and is present in all cells and living tissues. Magnesium is abundantly found in vegetables. It exists in the porphyrin group of vegetable chlorophyll. It is also found in the tissues of many animals. Other important sources of magnesium include whole grains, beans, green vegetables, potatoes, almonds and dairy products such as cheese. Magnesium plays a significant role in activating the activity of many enzymes. Presence in the combination of bones and teeth, which contains 70% of magnesium in the enamel of the teeth and bones. Magnesium induces temporary and permanent hardness in water. An excess of magnesium in the water can be a laxative. Magnesium deficiency causes nervous disorders, chronic fatigue, back pain, muscle weakness, loss of appetite, insomnia, and irregular heartbeat. The maximum level of magnesium in drinking water is 100mg/l and the desired quantity is 30mg/l. [5]

2. Literature Review

A lot of research has been done in this area, some of which are mentioned here.

According to the report of the World Health Organization, one out of three people in developing countries do not have access to clean water. Also, 80 percent of diseases are caused by water.

A study was conducted in Taiwan that found that water contaminated with arsenic caused the development of arsenicosis. [28]

Geen and colleagues in Bangladesh in 2003 investigated 6,000 wells and the depth of drilling necessary to reach these low-As arsenic aquifers ranges from 30 to 120 m depth within the study area. [8]

A study conducted by Boyan and colleagues in 2010 near the coal mine in northwest Bangladesh revealed that the groundwater was 50% contaminated with heavy metals. [2]

In 2010, drinking water was analyzed by Yashbir in Sanganer, India. It was found that the water quality is not good and the amount of fluoride and nitrate in this water has increased due to artificial and natural sources. [12]
Hafiza Hamidi, a professor at the University, conducted an investigation on the water of Kabul, after which it was found that 56% of samples had less quantity of fluoride than the permissible level, 42% of samples had the quantity of fluoride within permissible level, and 2% of samples had more quantity of fluoride than the permissible level. 86% of samples had very hard water due to magnesium, 4% of samples had hard water and there was no sample that did not have hard water. Arsenic quantity in water for all areas were below the permissible limit of the international standards. [9]
Ali Akbar Mohammadi and colleagues conducted a research on the physical and chemical analysis of underground water in the Babol region of Iran, in result, it was found that the amount of nitrite, sulfate, chloride, sodium, electrical conductivity and pH are in standard condition. But the water turbidity, total hardness and iron were more than the permissible limit. And it was found that the amount of fluoride in 87.2 percent of the samples was less than the permissible level and 12.8 percent of the samples were within the permissible level. [16]

3. Research Methodology

For research, samples were taken from three points of Khost city in accordance with the rules, and then these samples were taken to a standard laboratory and analyzed according to international standards, in result all compounds have been identified. Those three are:

1. Near the ring road (University Road) of Khost city, there is an underground water source on the left side of Haji Mirnawaz Khan Plaza. This borehole is 80 meters deep and 14 inches in diameter. The GPS coordinates of this borehole are($33°20'35''N\ \ 69°55'27''E$).
2. The second sample was taken from an underground water source next to the Khost city project bridge near the main road of Khost Kabul. The depth of this borehole is 90 meters and its diameter is 14 inches. The GPS coordinates are ($33°20'8''N\ \ 69°54'28''E$).
3. The third sample was taken near Mujahid Square in Khost city. The depth of this borehole is 85 meters and its diameter is 14 inches. The GPS coordinates are($33°20'10''N\ \ 69°55'7''E$).

Due to the non-availability of an equipped laboratory in Khost city, the water samples was transferred to Kabul and tests were performed there at the laboratory of Shawal Construction and Geotechnical Company. The address of this laboratory is Daburi, 3rd zone, 3rd Street, next to Behzad Private School, Kabul-Afghanistan.
After obtaining the results of the tests, these results are compared with international standards and the final results are mentioned.

4. Results and Discussion

Firstly, as a result of many studies, international standards for water were found and then compared with laboratory results.

Table 1 Quantities of Toxic Elements in Various International Standard in mg/l [29],[21],[23],[7][10][3]

No	Parameters	Chemical Symbol	WHO (2011)	SASO (1994)	US EPA (2018)	FDA (2008)	IBWA (2008)	BIS (2012)
1	Arsenic	As	0.01	0.05	0.01	0.05	0.01	0.05
2	Manganese	Mn	0.5	0.05	0.05	0.05	0.05	0.3
3	Fluoride	F	1.5	0.6-1.0	4	0.8-2.4	0.8-2.4	1.5
4	Magnesium	Mg	150	30-150	30-60	-	-	100

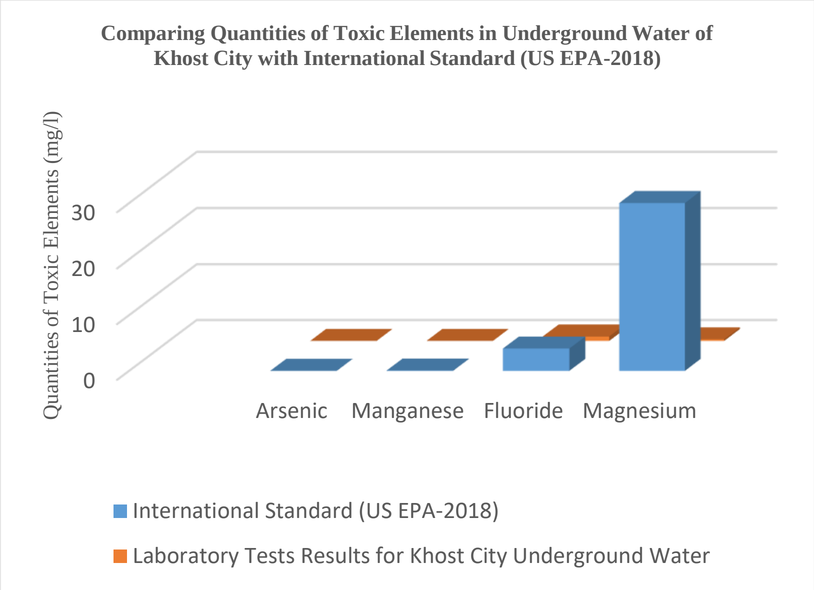

Fig. 1 Comparing Quantities of Toxic Elements in Underground Water of Khost City with International Standard (US EPA-2018)

Table 2 Arsenic, lead, fluoride and magnesium quantities (mg/l) for three centers after laboratory tests

No	Parameters	Center 1	Center 2	Center 3
1	Arsenic	0	0	0
2	Manganese	0.001	0.001	0.001
3	Fluoride	0.79	0.79	0.79
4	Magnesium	0.28	0.28	0.28

Since Khost city is not very wide, the results of all the centers are the same.

From the Fig. 1 above, it is observed that the amount of arsenic in the water is zero, so it can be said that the water of Khost city is not contaminated with arsenic. The quantity of manganese in the water composition is 0.001 mg/l, according to the all standards, this quantity is less than the standard amount. So it does not cause the water to taste bad. The quantity of fluoride in the composition of this water is within the permissible limits according to all standards and does not cause any problems. The amount of magnesium in the composition water is very low and it can cause some diseases.

5. Conclusion

In this research, the toxic elements (arsenic, manganese, fluoride and magnesium) in the underground water composition at Khost city have been studied, because more or less quantity of these elements has a very bad effect on health. The research was carried out at three points of underground water in the center of Khost province. The results of the research are concluded as following:

- From this study, it was found that the underground water of Khost city does not contain arsenic, and there is no problem for consumers.
- The quantity of manganese is not too high to cause the taste of water to deteriorate.
- The quantity of fluoride in this water is within the permissible limit and this water does not cause any problem due to fluoride.
- From the research, it was found that the amount of magnesium in this water is very low, which can cause some diseases, and a solution should be found as much as possible.
- In general the quality of underground water is good for drinking propose.

References

[1] Ayoob S, Gupta, AK. (2006) Fluoride in drinking water: A review on the status and stress effects. Crit Rev Environ Sci and Tech.;36(6):433-87.

[2] Bhuiyan et al. (2010). Preliminary assessment of heavy metals in water and sediment of Karnaphuli River, Bangladesh (Vol. 5). Elsevier B.V, 205, 212-218.

[3] Bureau of Indian Standards (BIS) (2012). Specification for Drinking Water; Indian Standards Institution: New Delhi, India, pp. 1–5. Available online: https://law.resource.org/pub/in/bis/S06/is.10500.2012.pdf (accessed on 22 May 2021).

[4] Datta PS, Deb DL, Tyagi SK. (.1997) Assessment of ground- water contamination from fertilizers in the Delhi area based on 180, N03− and K+ composition. J Contam Hydrol;27(3-4):249-62.

[5] EPA. (2003). EPA National Primary Drinking Water Standards. Washington, USA: Environmental Protection Agency, 76 (11).

[6] Faithful J, Finlayson W. (2005) Water quality assessment for sustainable agriculture in the Wet Tropics-A community assisted approach. Mar Pollut Bull.;51(1-4):99-112.

[7] FDA. (2008) Bottled Water Everywhere: Keeping it Safe. Available online: http://www.fda.gov/consumer/updates/bottledwater08250 8.html (accessed on 26 August 2008).

[8] Geen et al. (2003). Spatial variability of arsenic in 6000 tube wells in 25km2 area in Bangaladesh. Water Resources Res, 6-8.

[9] Hamidi, H. (2018). Investigating the contamination of arsenic, fluoride and magnesium in drinking water. in some areas of Kabul city. Kabul: Kabul University.

[10] International Bottled Water Association. (2008) Bottled Water Code of Practice; IBWA: Alexandria, VA, USA, 2008; Available online: http://bottledwater.org/public/modelmain.htm (accessed on 5 May 2021).

[11] J.Fawell et al . (2006). Fluoride in Drinking Water. Geneva, : WHO, 315-325.
[12] Kumar M, Singh Y. (2010) Interpretation of Water Quality Parameters for Villages Sanganer Tehsil, by Using Multi- Variate Statistical Analysis. Water Resource and Protection, 860-3.
[13] Mahvi AH, Zazoli MA, Younecian M, Nicpour B, Babapour A. (2006) Survey of fluoride concentration in drinking water sources and prevalence of DMFT in the 12 years old students in Behshahr city. J Med Sci. 658-61.
[14] Majumdar KK. (2011). Health impact of supplying safe drinking water containing fluoride below permissible level on flouro- sis patients in a fluoride-endemic rural area of West Bengal. Indian J Public Health303-8.
[15] Moradinezhad A, Agha Razi HA. (2002) Evaluation of drought in Markazi province by analysis of rainfall data. J Water &Wastewater. 20-5. [Persian].
[16] Muhammad, A., & Amoui, A. (2015). Physical and chemical analysis of potable underground water resources in rural areas of Babylon. Journal of Neyshabur University of Medical Sciences, 61-68. [Persian].
[17] Naeemi, N. (2019). Comparison of Khost city groundwater hardness and dissolved solids with international standards. Sheikh Zayed University Academic Journal.
[18] Narbutaite J, Vehkalahti MM, Milciuviene S. (2007) Dental fluorosis and dental caries among 12-yr-old children from high-and low-fluoride areas in Lithuania. Eur J Oral Sci.137-42.
[19] Robertson WD, Russel BM, Cherry JA. (1996) Attenuation of nitrate acquitted sediments of southern Ontario. Hydro. 267-81.
[20] Sary, I. A. (2001). Futures, health and standards in the environment. Tahran: Naqsh Mohar.
[21] Saudi Arabian Standards Organization.(1994), Bottled and Unbottled Drinking Water. Standard No. 409, Saudi Arabia. Available online: http://www.saso-gov.com/index.php?rzmb.html (accessed on 19 May 2021).
[22] Shrivastava R, Kanugo VK. (2013). Physico-Chemical Analysis of Pond Water of Surguja District, Chhattishgrah.India. International journal of Herbal Medicine, P35-43.
[23] The United States Environmental Protection Agency, US EPA.(2018), Edition of the Drinking Water Standards and Health Advisories Tables; Environmental Protection Agency: Washing, DC, USA,Available online: https://www.epa.gov/sites/production/files/20 18 03/documents/dwtable2018.pdf (accessed on 21 May 2021).
[24] U.S Agency. (2007). Toxicological Profile for Arsenic. Washington: U.S Agency for Toxic Substances and Disease Registry, Department of Health and Human Services, 113-118.
[25] United Nations Children's Fund (2008). UNICEF HANDBOOK ON WATER QUALITY. New York: UNICEF.

[26] Van Busse CGJ, Schroeder JP, Sven Wuertz S, Carsten S. (2012) The chronic effect of nitrate on production perfor- mance and health status of juvenile turbot (psetta maxima). Aquaculture.163-7.
[27] Wen Y, Chen Y, Zheng N, Yang D, Zhou Q. (2010) Effect of plant biomass on nitrate removal and transformation of car- bon subsurface-flow constructed wetland. Bioresour Tech-nol.7286-92.
[28] WHO/UNICEF. (2000). Global Water Supply and Sanitation Assessment 2000 Report. Geneva and New York: WHO and UNICEF.
[29] WHO. (2011). Hardness in Drinking-water, Guidelines for Drinking Water Quality (4th ed.). Available online: https://apps.who.int/iris/bitstream/handle/10665/44584/9789241548151_eng.pdf?sequence=1 (accessed on 17 May 2021).
[30] World Bank/WSP. (2005). Arsenic Contamination of Groundwater in South and East Asia.

Authors Profile

Naqib Ahmad Naeemi received a B. Eng. degree in Civil Engineering from Shaikh Zayed University, Khost Afghanistan in 2013, and he completed his MSc. degree Civil and Industrial Engineering from Kabul Polytechnic University, Kabul Afghanistan in 2018. Currently, he is working as Senior Teaching Assistant in the Department of Civil engineering of the Construction Faculty of Shaikh Zayed University. His area of research includes Civil Engineering.

Mohammad Noor Jan Ahmadi is from Khost Afghanistan. He received the B. Sc. degree in Civil Engineering from Shaikh Zayed University in 2010, Khost Afghanistan, and he got M. E. degree in Civil (Structural Engineering) from Gujarat Technological University (GTU) in 2017, Ahmedabad, Gujarat, India. Currently, he is working as Senior Teaching Assistant in the Department of Civil Engineering at shaikh Zayed University, Khost, Afghanistan. His areas of research includes Civil Engineering.

KPU International Journal of Engineering & Technology
Volume 3, Issue1, Sep. 2023
e-ISSN:2790-0819, p-ISSN:2790-0800

Date Received: 2023-05-07
Date Accepted: 2023-06-25
Date Published: 2023-09-15

Copper mineral exploration and metamorphic rock investigation using remote sensing: A case study in the Shaida Copper Mine, Herat, Afghanistan

ABDULKHALIL KHALIL[1], FARID AHMAD MOHAMMADI[2*],
SAYED SHABUDDIN SADAT[3]

[1]Department of Mining Engineering, Balkh University, Balkh, Afghanistan, Email: akhalil.mmm@gmail.com

[2*]Department of Mining Engineering, Faculty of Mining and Environment Engineering, Balkh University, Balkh, Afghanistan, Email: faridahmad.mh@gmail.com, amfarid@graduate.utm.my,

[3]Department of Chemical Technology, Engineering Faculty, Balkh University, Balkh, Afghanistan, Email:sayedshahabuddinsadat786@gmail.com

Abstract

The Shaida copper mine is located on the Herat fault to Badakhshan and the old alpine zone of Harirud, and in terms of geological age, it belongs to the Mesozoic (Cretaceous) to Cenozoic era. There are many copper mines in Afghanistan which are still unknown. The main purpose of this research is to explore and predict the nature and type of copper mines in Afghanistan, which uses remote sensing and multispectral ASTER and Landsat (OLI) images to explore and investigate the metamorphic rocks of the Shaida Herat copper mine in western Afghanistan. Necessary corrections were applied to satellite images. To explore and investigate the transformation parameters, different satellite image processing algorithms, including principal component analysis (PCA) and inter-band ratios (BR) and spectral angle mapping (SAM), and the most spectral similarity (MLC) are used. Principal component analysis in bands PC1, PC2, and PC7 shows the maximum absorption range for providing copper mineralization. The inter-band ratio was used to examine stones and minerals (calcite, alunite, and kaolinite and to examine mafic rocks and carbonates). The algorithm of the most spectral similarity is used in the investigation of metamorphic rocks and to evaluate the performance of the algorithms, the spectra of the reference library provided by the United States Geological Survey (USGS) have been used. The evaluation and validation of alteration zones in the Shaida copper mining area provide the most spectral similarity algorithm with an accuracy of 0.61%, and the evaluation and validation of exploration in the Shaida copper mining area provide the spectral angle mapping algorithm with an accuracy of 0.68%. According to this research, the conditions of the formation of copper mines are oxide and sulfide mania. It is predicted that the reserve of the Shaida copper mine will increase over time as a result of detailed exploration and more detailed studies, and the increase in oxide and sulfide minerals of copper is economically important.

Keywords: Copper mineral, mining, metamorphic rocks, remote sensing

*Corresponding Author

1. Introduction

Remote Sensing (RS) is the science of information acquisition, processing, and interpretation of data and satellite images obtained from sensors that record the interaction between matter and electromagnetic energy [1]. Due to the use of satellite images, remote sensing is one of the important sources of information in many "geological" applications, such as mining exploration at local, regional, and global scales, monitoring exploration operations and mining, use of land cover, and environmental studies [2]. Over the last few years remote sensing science has been the best method in terms of time, resource, and cost [3]. Use of RS and GIS technology in the exploration of mines and investigation of metamorphic rocks and investigating geological structures are the basic goals of this technology [4].

In terms of geological research of Russian scientist Silavin from the years 1976 to the early 1800s the area of Afghanistan is extremely complicated in terms of geology. The development of rocks and geological structures in the territory of Afghanistan reaches the tectonic stages before Baikal [5]. The geology of Afghanistan's minerals was also presented by a team of Russian and Afghan engineers who prepared the geological map of Afghanistan in Moscow in 1980. Only in Afghanistan, the amount of copper reserves is estimated more than 68,500 million tons (Figure 1) [6]. This research and subsequent research aim to explore and predict the nature of copper mines in Afghanistan. In this research, the exploration of copper minerals and the investigation of metamorphic rocks in the Shaida copper mine of Herat, which is one of the platform areas in Afghanistan, have been discussed. Aerial photos and satellite images can be used to analyze the changes in the extent of sight according to the period [7]. Based on the studies conducted by many researchers, it is possible to detect metamorphic minerals and rocks using optical satellite image information [8] which in this research - multi-spectral satellite Landsat (OLI) is used.

ASTER sensor has 14 bands, three of which are in the visible and near-infrared VNIR with a resolution of 15 meters and six bands in the short infrared SWIR which has a spatial resolution of 30 meters. It has five TIR thermal bands with a resolution of 90 meters. (OLI) Landsat sensor has 11 bands, 8 spectral bands, one panchromatic band with a spatial resolution of 15 meters, and 2 thermal bands with a spatial resolution of 90 meters [9].

Principal component analysis (PCA), Spectral angle mapping (SAM), and Interbrand ratio (BR) were used to explore copper minerals and to check the metamorphic rocks in the period from 2013 to 2021, the algorithm of the most spectral similarity (MLC) was used. The result of this research shows that the evaluation and validation of changes in the Shaida copper mining area show the most spectral similarity algorithm, with 0.61% accuracy. The evaluation and validation of the spectral angle mapping algorithm in the Shaida copper mining area provide an accuracy of 0.68%.

In this research, based on the studies of Russian and Afghan engineers in 1980, the Shaida copper mine has conditions for oxide and sulfide formation. It is predicted that copper minerals will increase over time based on tectonic developments and movements (Herat fracture to Badakhshan) [10] and that these movements cause an increase in copper minerals in the Shaida copper mine. From an economic point of view, copper oxide and sulfide minerals are very important.

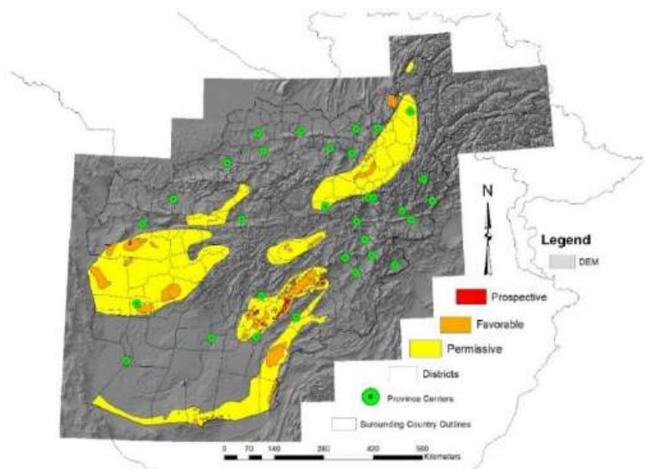

Figure 1: Location map of Afghanistan's copper mines. Red borders for Prospective limits, orange borders for Favorable limits, yellow color Permissive, and green color State center (www.USGS.Gov2004).

Study area

The Shaida copper mine in Herat is located in the common area between Pashtun Zarghoon and Adraskan at 33°47′24″N and 61°49′30″E (figure 2). The Shaida copper mine with 1.1% of pure material, 4 meters wide and 150 meters long, 2.4–8 meters thick, 2400 meters area is situated 65 km from Herat province. The copper reserves of this mine are 5 million tons, which were specified in the joint survey of Russia and Afghanistan in 2018. The Shaida copper mine is related to the tectonic zone of Farah and Qala-e-Naw, which is in the Turkmen segment of Iran and Harirud fault, and the subsidence of Herat as a position (Figure 3) [11]. In this region, the rocks are young, and in terms of geological age, they reach the Mesozoic (Perm, Cretaceous) to Cenozoic eras (Figure 4). In terms of folding, it is related to the old Alp and Harirud zone [12].

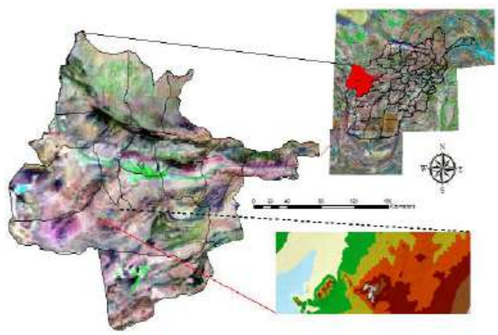

Figure 2: A) DEM map of Afghanistan, B) Map of Landsat ETM+ satellite zone, C) Location map of Shaida copper mine (Jorris et al. 2002).

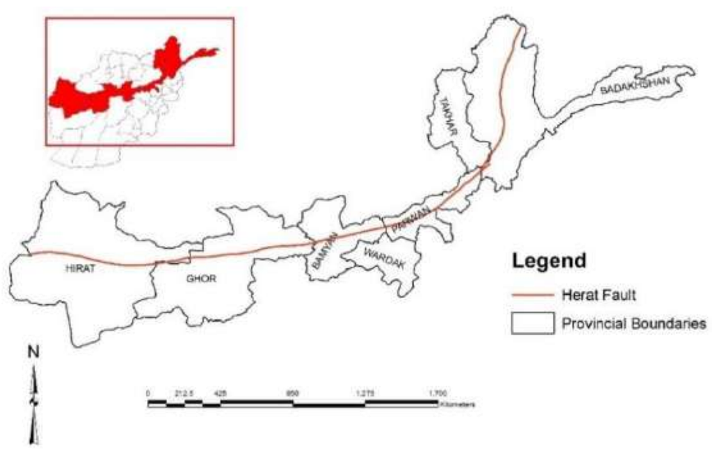

Figure 3: Map of Harirud fracture (Desi, A., 1975)

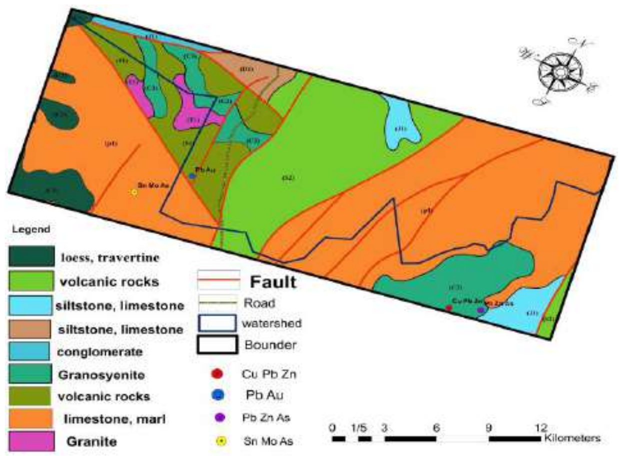

Figure 4: Geological map of Shaida copper mine in Herat (Afghan Geological Map 2005)

2. Data preprocessing

Materials and Methods

In this research, to explore and investigate the metamorphic rocks multi-spectral ASTER and Landsat (OLI) satellite images were used which includes data preparation, processing of satellite images, and preparation of a mineralogical map and preparation of metamorphic rock map of the Shaida copper mine. For atmospheric correction of Shaida, VNIR, and SWIR bands of ASTER and R, G, and B bands of Landsat (OLI) (Quick Atmospheric correction) algorithm and for correction of TIR band ASTER will use (Thermal atmospheric correction). Image geometric correction operations of ASTER and ground referencing them using crosstalk correction (Crosstalk) on the ASTER images were done. The general research processes are shown in (Figure 5).

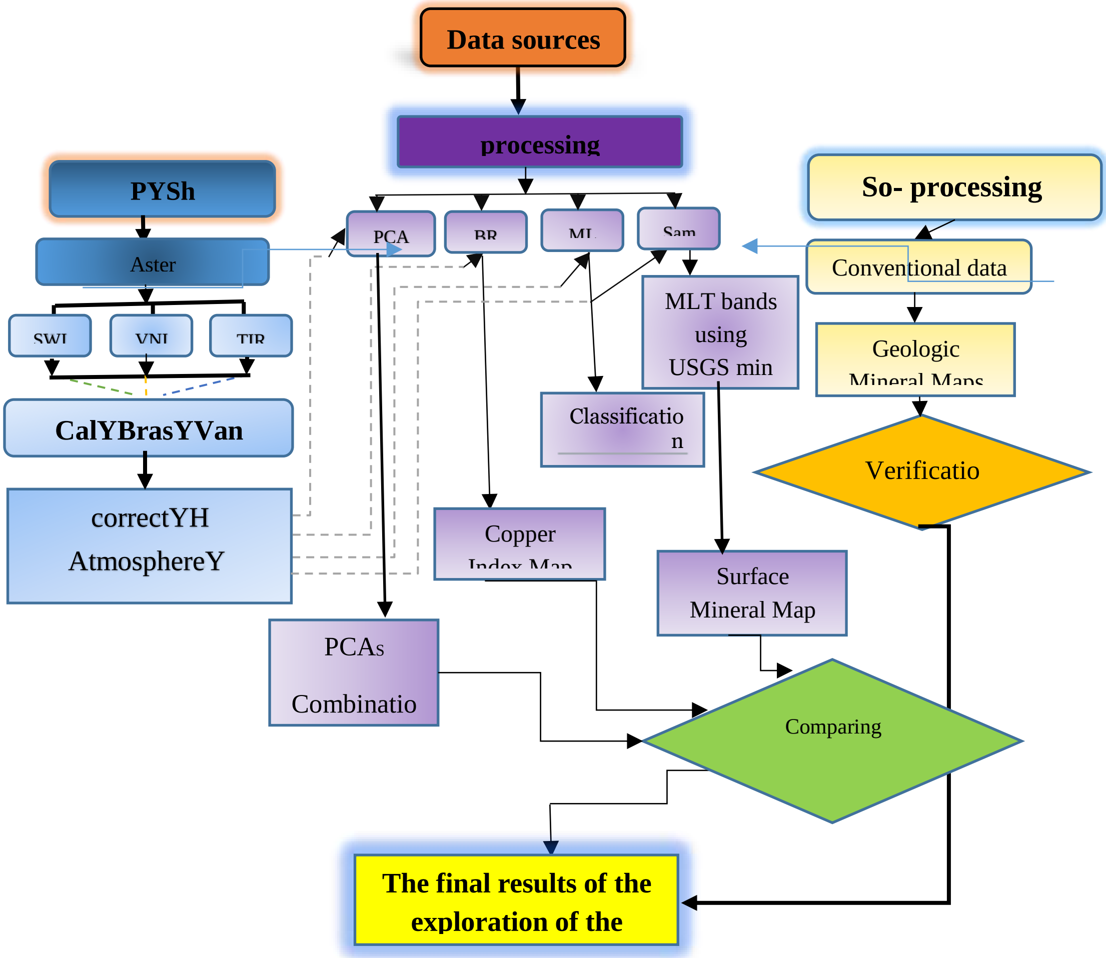

Figure 5: The general research process

Satellite data processing

Principal component analysis (PCA)

PCA is used to reduce the interference effect of materials, especially vegetation, and also extensively for metamorphic mapping [13]. This vector algorithm of a matrix and variance-covariance or one correlation matrix can be computed [14]. This method is into two modes of standard (use of all bands) and suitable bands (here bands containing absorption and reflection characteristics of the desired minerals) is used with the lowest correlation (Figure 5).

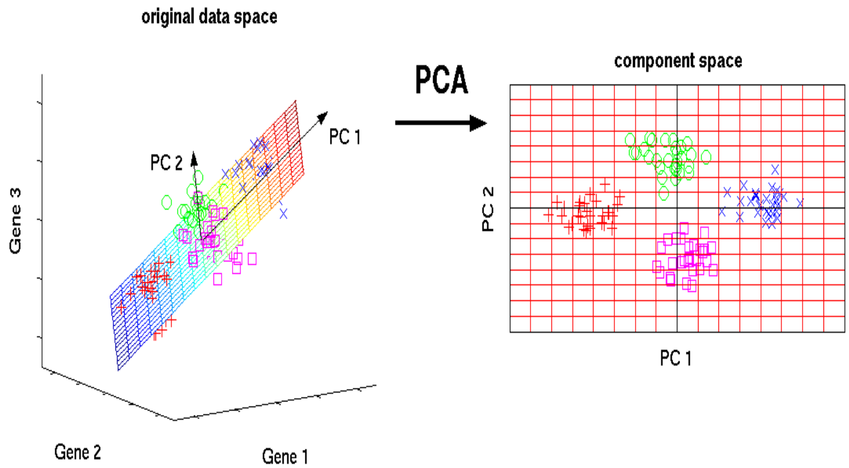

Figure 6: The structure of the principal component analysis algorithm in two general modes of standard component analysis and appropriate component analysis.

In the method of principal component analysis or reduction of input bands, while avoiding the interference effect of certain spectra (such as plants), the discussion of highlighting the desired minerals should be increased [15].

The principal component analysis distinguishes copper minerals from other phenomena where characteristic values are shown. In the bands PC1-PC2-PC7 which has suitable values for highlighting, characteristics of copper minerals have been provided based on the RGB. The red colors inside the ellipses show the copper minerals in this area, and the green color shows the areas where other minerals such as quartz or minerals that are in the composition of copper sulfide and minerals with prominent oxide exist. Blue and purple colors show areas where non-mineral materials are highlighted (Figure 7).

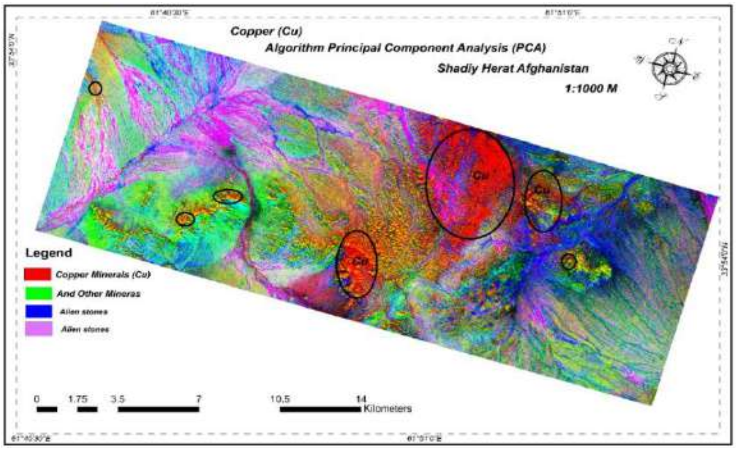

Figure 7: RGB map from the method of principal component analysis with R:7, B:2, and G:1 copper mineral using ASTER satellite images. Elliptical shapes with red pixels show copper minerals. The green pixels show other minerals in the copper mineral limit, and the blue and pink pixels indicate soil and other natural materials around the mine environment.

Spectral angle mapping (SAM)

This type of mapping (has been widely used by researchers in recent years to identify minerals. This algorithm was presented by a researcher named Boardman as part of a spectral angel mapping image processing system [16]. SAM is used as part of a diagram in the scattered space drawn by the values of the pixels in the bands of an image. In this diagram, pixel spectra are presented against target spectra which calculate each of the sampled points. A smaller angle between the pixel spectrum and the reference spectrum indicates a higher similarity (Figure 8). The spectral angle is relatively insensitive to changes in pixel brightness, as the direction of the vector remains constant, and only the size changes [17].

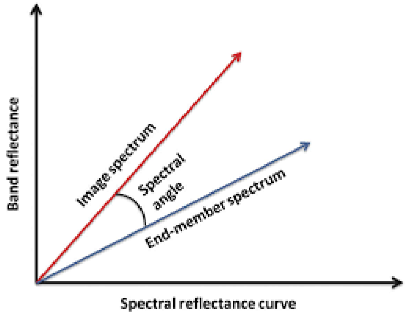

Figure 8: The structure of the implementation of the spectral angle mapping algorithm.

$$a = cos^{-1}[\frac{\sum_{j=1}^{nb} b_i r_i}{[\sum_{j=1}^{nb} E_J^2]^{\frac{1}{2}} \sum_{j=1}^{nb} r^2]^{\frac{1}{2}}} \quad 1$$

- Here n_b indicates Band numbers, b_i laboratory spectrum, and r_i reference spectrum [18].

In this research, for copper minerals classification Spectral angle mapping algorithm was used based on the standard of the ASTER spectrometer library and the USGS website.
To identify copper minerals, using SAM classification systems and spectral libraries of the USGS geological site and based on spectral behaviors, copper minerals have been identified (Figure 9).
In this research, copper minerals including Chalcopyrite, Malachite, Azurite, Quartz, Bornite, and chalcocite are classified (Figure 9). The SAM method displays the areas related to copper minerals. Here the yellow pixels show chalcopyrite minerals, the green pixels show Bornite minerals, the orange pixels show quartz minerals, the pink pixels show malachite minerals, the red pixels show azurite minerals and the blue pixels show chalcocite minerals. The spectral behavior of copper minerals extracted from ASTER sensor images is presented in (Figure 10).

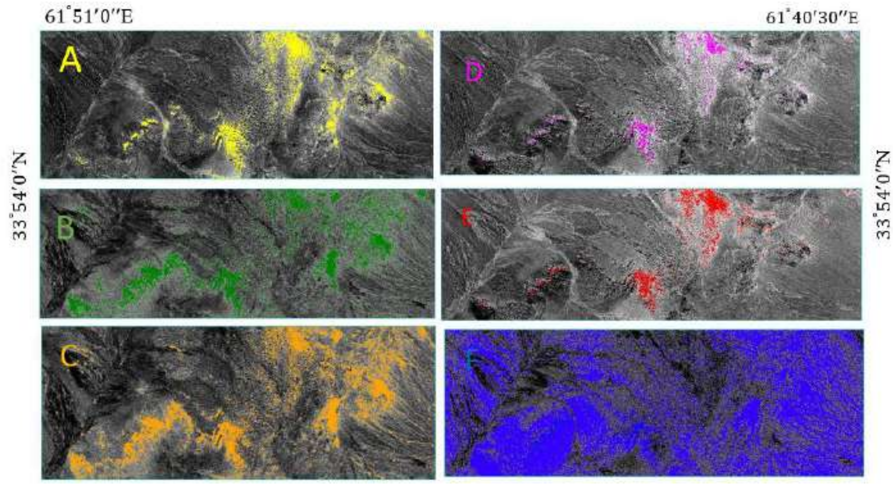

Figure 9: Output map of copper mineral identification by SAM spectral angle analysis method. Here it shows A- chalcopyrite, B- bornite, C- quartz mineral, D- malachite, E- azurite mineral, and chalcocite mineral.

.

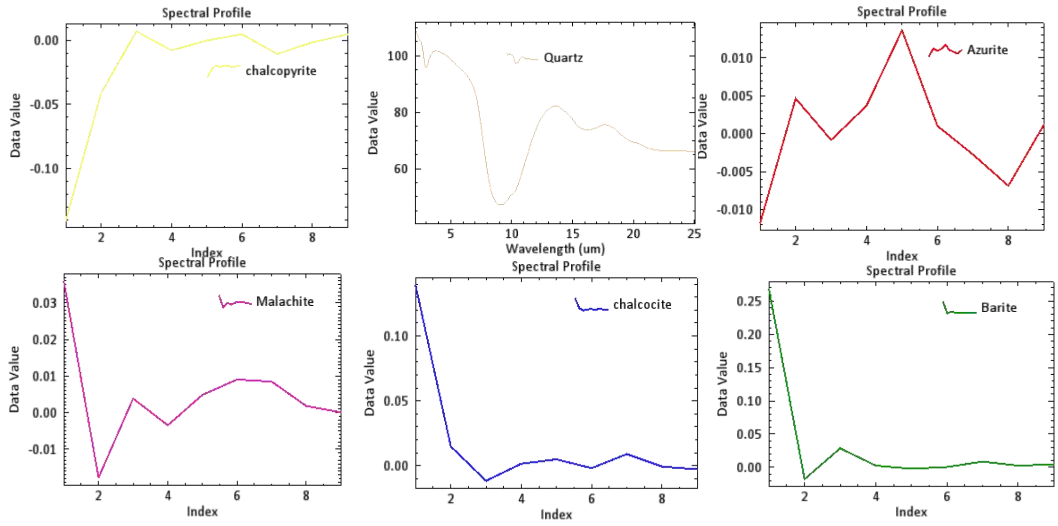

Figure 10: Spectral behavior of copper minerals extracted from ASTER sensor images

Algorithm of band ratio (BR)

This is the algorithm that by knowing the characteristics of maximum absorption and maximum reflection of different minerals, can highlight different phenomena [19]. The result of dividing the pixel identification degree values in one spectral band by another spectral band is called band ratio [20]. This method makes the difference between brightness levels more obvious and makes the border between effects clearer. Technically, band ratio is a certain number of band values divided by the DN number of another band value [21].

The band ratio (BR) for the absorption feature is the sum of the number of bands that represent the values and the band denominator. which is located in the closest absorption feature (Figure 14) [22]. The basis of this algorithm is based on the band ratios of four mathematical operations. In this research, the band ratios method is used to check mafic rocks (Figures 11 and 12).

$$OH\ bearing\ altered\ minerals\ Index(OHI) = \left[\frac{band7}{band6}\right]\left[\frac{\mathrm{band4}}{\mathrm{band6}}\right] \quad 2$$

$$\mathrm{Kaolinite\ Index(KLI)} = \left[\frac{\mathrm{band4}}{\mathrm{band5}}\right]\left[\frac{\mathrm{band8}}{\mathrm{band6}}\right] \quad 3$$

$$\mathrm{Alunite\ Index\ (ALI)} = \left[\frac{\mathrm{band7}}{\mathrm{band5}}\right]\left[\frac{\mathrm{band7}}{\mathrm{band8}}\right] \quad 4$$

$$\text{Calcite Index(CLI)} = \left[\frac{band6}{band8}\right]\left[\frac{band9}{band8}\right] \quad 5$$

$$Carbonate\ Index(Cl) = \left[\frac{band13}{band14}\right] \quad 6$$

$$Mafic\ Index(MI) = \left[\frac{band12}{band13}\right] \quad 7$$

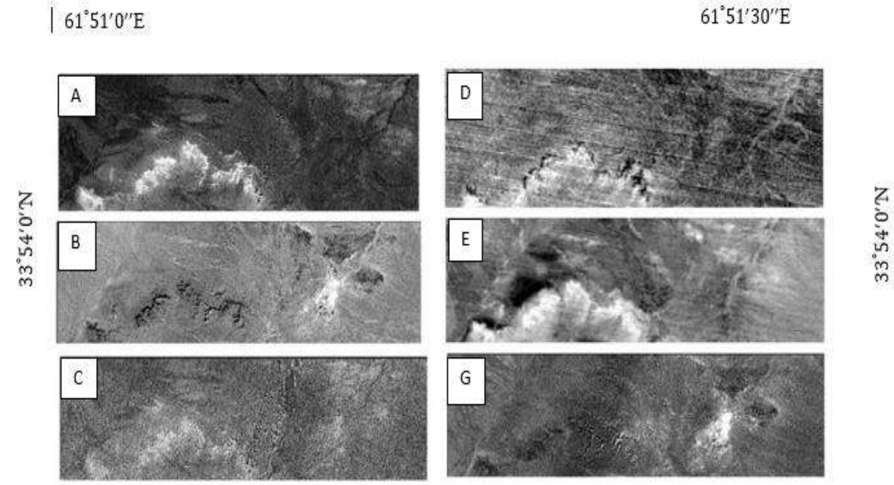

Figure 11: Output map of the band ratio algorithm A - band ratio (b6/b8+b8/6) of bright pixels representing minerals (calcite) B-band ratio (b4/b5+b8/b6) of bright pixels representing minerals (kaolinite) - ratio C Band (b7/b5+b7/b8) bright pixels of minerals (alunite) D-band ratio (b13/b14) of bright pixels of minerals (carbonates) E- band ratio (b12/b13) of bright pixels of mafic stones G- The band ratio (b7/b6+b6/b4) of the bright pixels of the alteration rocks.

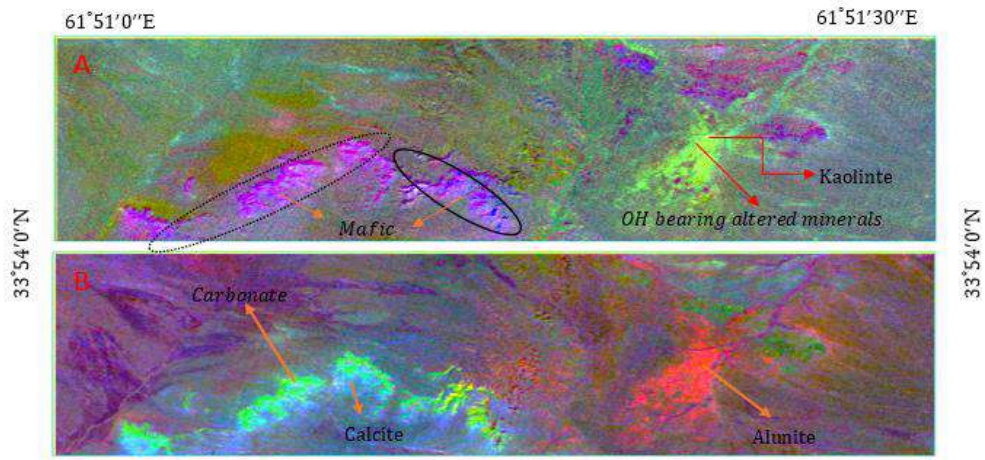

Figure 12: A) RGB image of band ratio R:7/6+4/6, G:4/5+8/6, B:12/13; B) RGB image of band ratio R:7/5+7/8, G:6 /8+9/8, B:13/14.

In the output of image, A, green and light yellow pixels represent rocks (alteration) and minerals (kaolinite), and pink to red pixels represent rocks (mafic).
In the output of image B, green and turquoise pixels represent mineral (carbonate) and mineral (calcite), and red to reddish pixels represent mineral (alunite).

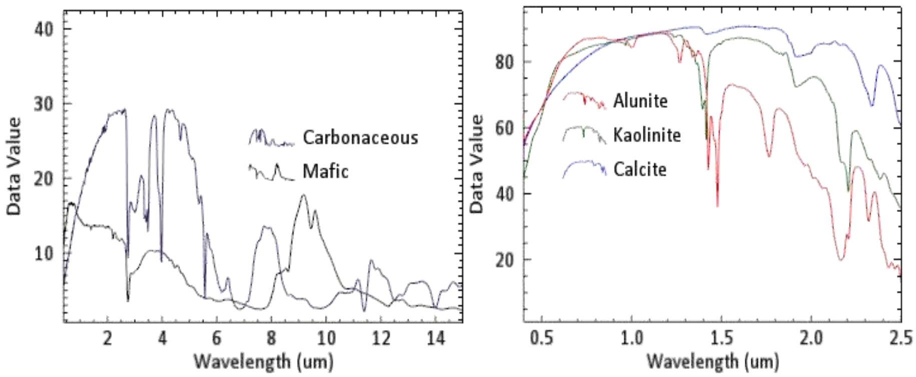

Figure 13: Spectral behaviors of minerals and carbonate rocks, mafic, calcite, Alunite, and Kaolinite using the spectral behavior of the ASTER sensor library.

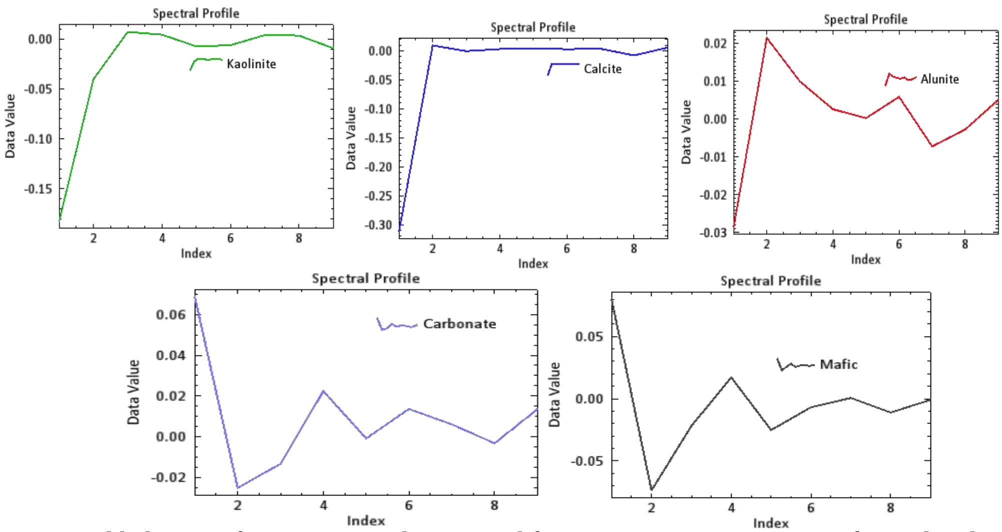

Figure 14: Spectral behavior of copper minerals extracted from ASTER sensor images of inter-band ratio algorithm.

The most spectral similarity algorithm MLC

This algorithm is one of the most famous statistical algorithms for classification, which is among pixel-based methods [23]. In the classification of the most similarity, the class is assigned to the pixel that has the highest probability of belonging to that class [24].

In this research, Landsat satellite images (OLI) have been presented in the Shaida copper mine to investigate the changes in metamorphic rocks in the period from 2013 to 2021 (Figures 15 and 16).

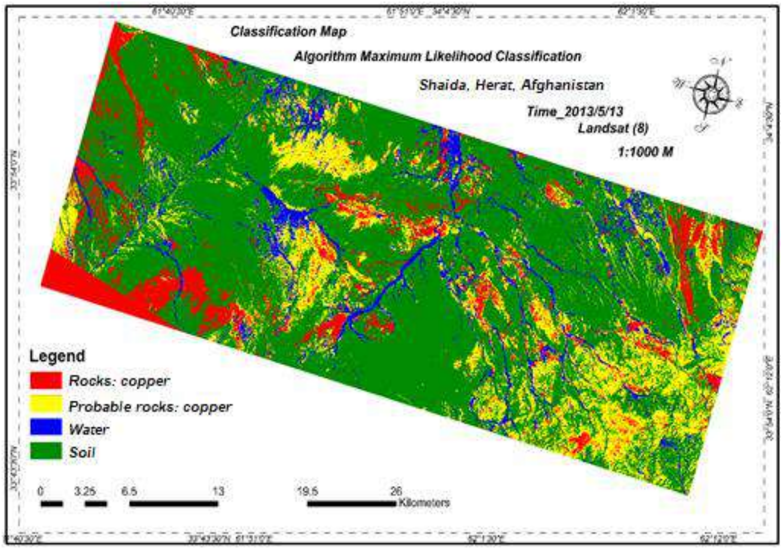

Figure 15: Classification map of alteration stones with MLC algorithm in 2013. Red colors show the rocks that contain copper minerals. Yellow colors are areas where there is a possibility of copper minerals among mafic rocks. The blue colors are the amount of water in the Shaida region. The green colors are the amount of soil, sand, etc. available in the area.

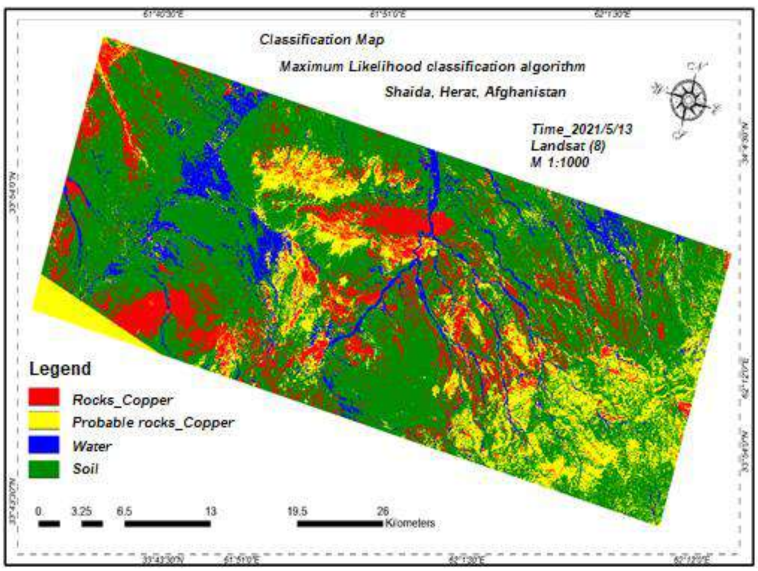

Figure 16: The classification map of alteration rocks with the MLC algorithm for 2021. Red colors show rocks that contain copper minerals, the yellow colors are the areas where there is a possibility of the presence of copper minerals among the mafic rocks. Blue colors are the amount of water that exists in the Shaida region. The green colors are the amount of soil, sand, etc. available in the area.

.

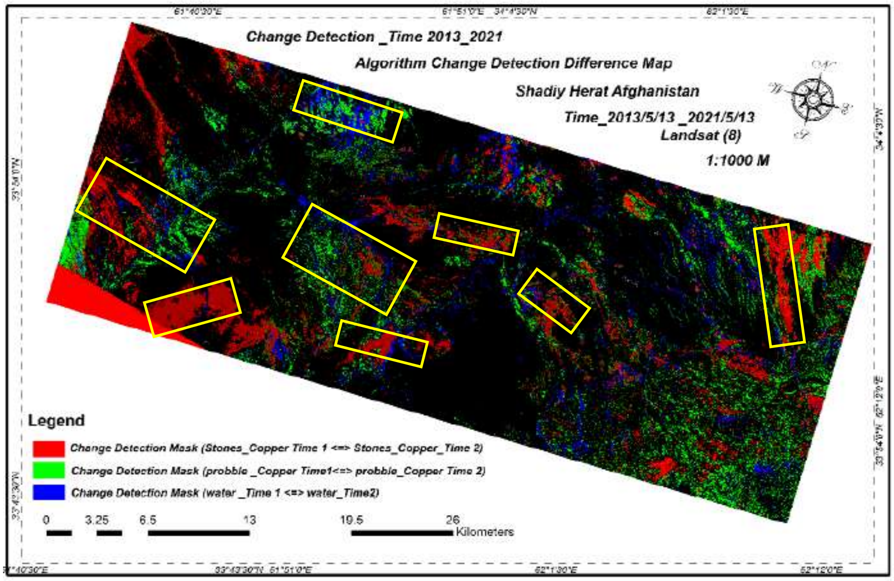

Figure 17: The map of the number of changes from the first time to the second time based on the classification of the most spectral similarity. The yellow rectangles show the areas where copper minerals have changed from the first period to the second period. Red colors show the number of rock changes in which copper mineral compounds are more. The green colors show the minerals and materials including soil and rocks, in which the changes have occurred from the first time to the second time, and the blue colors show the amount of water changes.

Investigating the formation conditions of copper minerals and predicting the nature of copper in the Shaida copper mine

Copper is a periodic table element with the chemical symbol of Cu. Copper is a metallic element with high electrical and thermal conductivity whose main feature is malleability. Copper minerals are classified into different types in terms of formation conditions [25] which include all kinds of oxides, sulfides, silicates, chlorides, and hydroxides. The types of copper deposits include porphyry copper deposits along with skarn and vein deposits and magmatic copper deposits. Volcanogenic massive sulfide-type copper deposits [26].

The results of this research are obtained in the prediction section of this result which the copper minerals exist in the Shaida mineral deposit. In this area, minerals are oxide and sulfide types. The amount of copper minerals in oxide minerals is more in the earth's crust. Natural interactions cause the transformation of sulfide rocks into oxide rocks. Copper oxide rocks are mostly formed from sulfates, carbonates, and sometimes silicates. Sulfide rocks, unlike oxidized rocks, are located lower and deeper than the earth's crust. Most of the copper ores are sulfur rocks. Sometimes in nature, copper is found in free form. This copper is found in the form of small grains inside the conglomerate, although larger pieces have also been found [27]. In terms of studies and research conducted from 1976 to the early 18th century by V. A. Slavin and Wolfat Witkin in 1980 on the tectonics and geology of Afghanistan Shaida copper mine has oxide and sulfide formation conditions and in terms of stratigraphy and paleontology, Herat province and Shaida copper mine includes the Mesozoic era (Cretaceous) to the Cenozoic era [28].

Based on the founding of this research most of the copper minerals in the Shaida copper mine are azurite, chalcopyrite, malachite, chalcocite, and bornite.

3. Discussion

Considering that in this study two goals such as the preparation of an exploratory map and examination of alteration rocks exist, therefore these two issues are discussed separately.

A- Preparation of exploratory map: - In this study, to better determine the exploratory map and mineralogy of the Shaida copper mine, principal component analysis and inter-band ratio and spectral angle classification methods have been used. According to the fact that each method has advantages and disadvantages, there are three maps such as PCA, BR, and SAM to check how well each method works in characterizing copper minerals.

B- Preparing a map of alteration rocks: -Maximum spectral similarity maps are the most rejection-tolerant category of methods and in the method of maximum spectral similarity, it is assumed that the distribution of educational data of each class is normal. In the method of maximum spectral similarity after data collection, n is the total number of reference points, ni is the number of pixels that are actually in the category of points, ni+ is the number of reference pixels in the class and n+i is the number of pixels placed in the class according to the detection method. The overall accuracy is also obtained by dividing the sum of correctly segmented pixels by the total number of reference data. The accuracy and detection of each image are done by the parameters of the overall accuracy of the Kappa coefficient of the calculated confusion matrix and the confusion matrix resulting from two classification methods, MLC is shown in Table 1, and the Kappa coefficient and overall accuracy are calculated using the equations 8 and 9 respectively.

$$k = \frac{n\sum_{i=1}^{k} n_{ii} - \sum_{i=1}^{k} n_i + n + i}{n^2 - \sum_{i=1}^{k} n_i + n + i} \quad 8$$

$$Overall\ accuracy = \frac{correctiy\ classified\ totals}{Reference\ data\ totals} \quad 9$$

Accuracy (70+39+60+80)/346= (249/346) = 0.71% 0.71*100=71% MLC

Kappa Coefficient = 0.61% = 0.61*100 = 61%

Accuracy = 173/282 = 0.61% SAM

Kappa coefficient = 0.47%

Table 1: Maximum likelihood ambiguity matrix classification

Collection	Water	Soil	Possible copper mineral	copper mineral	Class
94	16	8	0	70	copper mineral
40	1	0	39	0	Possible copper mineral
100	13	60	2	25	Soil
112	80	10	10	12	Water
346	107	78	51	110	Collection

4. Conclusion

Preparation of an exploratory map and alteration map of the studied area using satellite images is a fast and reliable method. ASTER, Landsat (OLI) satellite data of the exploratory region is used to investigate the metamorphism of the Shaida copper mine and processing methods such as principal component analysis (PCA), inter-band ratio (IBR), spectral angle mapping (SAM) and maximum spectral similarity (MLC) were also used. In this research, by applying the mentioned processing methods, the minerals azurite, malachite, quartz, chalcopyrite, chalcocite, bornite, calcite, alunite, and kaolinite were identified in the exploration area of the Shaida copper mine. According to the geological studies of the Shaida copper mining area, most of the copper alteration rocks are present, which are related to the conditions of oxide and sulfide formation. However, in the Shaida area, porphyry copper rocks are less available, and if they are available, they are in the depths of the deposit layers. The obtained results and images show that these methods have acceptable results in determining and separating the copper and metamorphic extents in the exploration area of the Shaida copper mine. Also, the optimal method for determining regional alterations is the MLC spectral similarity method and the effective method for mineral exploration is the SAM (spectral angle mapping) method. From the results of this research on the formation of copper minerals and the prediction of copper-rich areas, it can be seen that in addition to the Shaida copper mine, there are copper oxide and sulfide mines in other parts of the country, which can be investigated and explored in the future using remote sensing methods which are used in this research.

Reference

[1] Dr. Ankara Rajendran, Dr. Subhi Nasir, Mapping of manganese potential areas using ASTER satellite data in parts of Sultanate of Oman, May 2013International Journal of Geosciences and Geomatics ISSN: 2052-5591

[2] Dry Jian Yang, Prof. Dr. Le Yu (April 30, 2020). Special Issue. Applications of RS and GIS Integration in Natural Resources and Environmental Science: Remote (ISSN 2072-4292). This special issue belongs to the section Environmental.

[3] Guha. Himanshu. Evaluation of ASTER TIR data-based lithological indices in Malanjkhand Copper Mines of Madhya Pradesh, India. 03 Nov 2019.https://doi.org/10.1080/25726838.2019.1684018

[4] Alshaya, MS, Alshaya, MS, Mohammed, AM, Javed, A., & Alba root, MA Manual and Automatic Extraction of Lineaments From Multispectral Image in Part Manual and Automatic Extraction of Lineaments From Multispectral Image is Part of Al-Rawdah, Shabwah, Yemen by Using Remote Sensing and GIS Technology. International Journal of New Technology and Research (IJNTR). ISSN: 2454-4116, Volume-3, Issue-2, February 2017 Pages 67-73.

[5] Sahel, A., 2015, Structural setting and evolution of the Afghan orogenic segment – A review, in Brunet, MF, McCann, T., and Sobel, RR, eds., Geological Evolution of Central Asian Basins and the Western Tien Shan Range, London: The geological society of London, p. 427.

[6] Abdullah, S. & Chmyriov, VM (eds). 2008. Geology and Mineral Resources of Afghanistan. 2 Volumes. British Geological Survey, Occasional Publications, 15. http://www.bgs.ac.uk/downloads/browse. cfm? sec=7&cat=83.

[7] De Oliveira Andrade's Filo C. De FáTima Rossetti D. Effectiveness of SRTM and ALOS-PALSAR data for identifying morpho-structural lineaments in northeastern Brazil, Pages 1058-1077, Nov 2010, https://doi.org/10.1080/01431161.2010.549852

[8] A. Gasman. C. Gomez, H. Zohar, A. Masse, D. Doctor. PCA and SVM as geo-computational methods for geological mapping in the south of Tunisia, using ASTER remote sensing data set.Arabian J. Geosocial., 9 (20) (2016), pp. 1-12,10.1007/s12517-016-2791-1

[9] Ibtissame Bentahar.Mohammed RajiComparison of Landsat OLI, ASTER, and Sentinel 2A data in lithological mapping: A Case study of Rich area (Central High Atlas, Morocco). Volume 67, Issue 3, 1 February 2021, Pages 945-963. https://doi.org/10.1016/j.asr.2020.10.037

[10] John Ford Schroder, Naima Eqrarb, Hamidullah Waizyc, Hemayatullah Ahmadi c and Brandon J. Weihs. Review of the Geology of Afghanistan and its water resources. 13. May 2021. http://orcid.org/0000-0002-8995-0234

[11] Abdullah, Sh., Chmyriov, VM, Stazhilo-Alekseev, KF, Dronov, VI, Gannan, PJ, Rossovskiy, LN, Kafarskiy, A.Kh., and Malyarov, EP, 1977, Mineral resources of Afghanistan (2nd edition): Kabul, Afghanistan, Republic of Afghanistan Geological and Mineral Survey, 419 p.

[12] Aghanabati, A. & Ghorbani, M. 2011. Metallogenetic Map of the Middle East, 1:5 000 000. Geological Survey of Iran, Commission for the Geological Map of the World (CGMW/CCGM), Paris.

[13] GJ Orris, JD BlissMine and mineral occurrences of AfghanistanOpen-File Report 2002-110, https://doi.org/10.3133/ofr02110

[14] Desio, A., 1975, Geology of central Badakhshan (North-East Afghanistan) and surrounding countries, Italian expeditions to the Karakoram and Hindu Kush, scientific reports III, geology-petrology: Leiden, EJ Brill, p. 628.

[15] Geologic Map of Quadrangle 3264, Nawzad-Musa-Qala (423) and Dehrawat (424) Quadrangles, Afghanistan. US Geological Survey Open-File Report 2005-1115-A, compiled by Robert G. Bohannon and Charles R. Lindsay.

[16] Kaufmann, H., 1988- Mineral Exploration along the Aquila-Levant Structure by Use of TM Data, Concepts, Processing, and Results. International Journal of Remote Sensing, 9, 1639-1658. doi 10.1080/01431168808954966.

[17] Ibtissame Bentahar.Mohammed RajiComparison of Landsat OLI, ASTER, and Sentinel 2A data in lithological mapping: A Case study of Rich area (Central High Atlas, Morocco). Volume 67, Issue 3, 1 February 2021, Pages 945-963. https://doi.org/10.1016/j.asr.2020.10.037

[18] Freak D. van der Meer, Harald MA van der Warf, Frank JA van Ruitenbeek, Chris A. Hecker, Wim H. Bakker, Marleen F. Noomen, Mark van der Meijde, E. John M. Carranza,J. Boudewijn de Smeth, Tsehaie Woldai, 2012- Multi- and hyperspectral geological remote sensing: A review. Volume 14, Issue 1, February 2012, Pages 112-128. https://doi.org/10.1016/j.jag.2011.08.002

[19] Golchin Hajibapir, Mohammad Lotfi, Afshar Zia Zarifi, Nima Nezafati1 Application of Different Image Processing Techniques on Aster and ETM+ Images for Exploration of Hydrothermal Alteration Associated with Copper Mineralizations Mapping Kehdolan Area (Eastern Azarbaijan Province-Iran), Open Journal of Geology, 2014, 4, 582-597, http://dx.doi.org/10.4236/ojg.2014.411043

[20] Honarmand, M., Ranjbar, H. and Shahabpour, J. (2012) Application of Principal Component Analysis and Spectral Angle Mapper in the Mapping of Hydrothermal Alteration in the Jebal-Barez Area, Southeastern Iran. Resource Geology, 62, 119-139 .http://dx.doi.org/10.1111/j.1751-3928.2012.00184.x

[21] Girouard, G., Bannari, A., El Harti, A., & Durocher's, A. (2004, July). Validated spectral angle mapper algorithm for geological mapping: a comparative study between Quick Bird and Landsat. In Ext ISPRS Congress, Geo-Imagery Bridging Continents, Istanbul, Turkey (pp. 12-23). Grainger, JH, Ratkoski, AJ, & Hoke, ML (2004, August). The sequential maximum angle convex cone (SMACC) endmember model. In Defense and Security (pp. 1-14). International Society for Optics and Photonics

[22] Gopinathan Pa, Parthian Sb, Magnetron Tc, Ayad M. Faddily Al-Quashed, Ashok K. Singe, Pradeep K. Singe, Mapping of ferric (Fe3þ) and ferrous (Fe2þ) iron oxides distribution using band ratio techniques with ASTER data and geochemistry of Kanjamalai and Godumalai, Tamil Nadu, south India. Remote Sensing Application: Society and Endearment 18(2020)100306:http://www.elsevier.com/locate/rsase

[23] Mamadou Traorea, Jonas Didero Takodjou Wambob, Cyrille Prosper Ndepetec, Senem Tekinea, Amin Beiranvand Pourd Aidy M Muslimd, Lithological and Alteration Mineral Mapping for Alluvial Gold Exploration in the South East of Birao area, Central African Republic Using Landsat-8 Operational Land Imager (OLI) Data 9 June 2020, doi:https://doi.org/10.1016/j.jafrearsci.2020.103933.

[24] Hashim M, Park Y, Hong JK. 2017. Mapping alteration mineral zones and lithological units in Antarctic regions using spectral bands of ASTER remote sensing data. Geocarto Int. doi:10.1080/10106049.2017.1347207

[25] Qi Chen1, & Zhifang Zhao, Qigang Jiang, Shucheng Tan, Yinggui Tian, Identification of metamorphic rocks in Wuliangshan Mountains (Southwest China) using ASTER data 29 May 2018 Arabian Journal of Geosciences (2018) 11:311, https://doi.org/10.1007/s12517-018-3635-y

[26] Rowan.LC, Mars.JC, 2003, Lithologic mapping in the Mountain Pass, California area using Advanced Spaceborne Thermal Emission and Reflection Radiometer (ASTER) data, Journal of Remote Sensing of Environment, Vol: 84, p: 250-266.

[27] Azizi.H., Tarverdi.MA, Akbarpour.A., 2010, Extraction of hydrothermal alterations from ASTER SWIR data from east Zanjan, northern Iran, Journal of Adv Space Res, Vol: 46, p: 99–109.

[28] Donald G. Barceloux,Dr. Donald Barceloux, Copper 06 Aug 1999 https://doi.org/10.1081/CLT-100102421

Authors Profile

Abdul Khalil Khalil son of Mullah Mohiuddin was born in 1968 in Darzab district of Jawzjan province. In 1990, he started his undergraduate studies in the Department of Geology and Mining, Faculty of Engineering, Balkh University, and successfully graduated in 1996. Since 1996, he has been working as a professor in the mining engineering department of the Faculty of Mining and Environmental Engineering and the supervisor of this faculty. He entered the National University of Tajikistan in 2015 to continue his master's studies and successfully graduated in 2017 and is currently teaching at Balkh University.

Farid Ahmad Mohammadi son of Hassan Reza, was born in 1991 in a religious and cultured family in Kabul city. He successfully graduated from Balkh University's Faculty of Engineering in 2013, with excellent grades. In 2013, he was recruited as a scientific staff in the Department of Mining Engineering, Faculty of Mining and Environmental Engineering. He successfully completed his Master's degree in 2020 in the field of Geomatics Engineering, University Technology Malaysia (UTM). He is currently a member of the scientific staff of the Mining Engineering department, Faculty of Mining and Environmental Engineering, Balkh University.

Sayed Shahabuddin Sadat was born in Mazar-e-Sharif city in 1972. He enrolled scientific staff membership in the chemical technology department of Engineering faculty at Balkh University in 2002. He graduated from the field of Products Management from the Polytechnic University of Tajikistan in 2016. From 2016 up to now he works as a lecture at Balkh University.

KPU International Journal of Engineering & Technology
Volume 3, Issue1, Sep. 2023
e-ISSN:2790-0819, p-ISSN:2790-0800

Date Received: 2023-04-15
Date Accepted: 2023-06-25
Date Published: 2023-09-15

The Contribution of Coal Resources to Electrical Energy Production in Afghanistan

M. SHAHAB SHARIFI[1*], M. SHUAIB MOHSINI[2], ALYAS ASLAMI[3], M. ARIF NOORI[4], M. HAMED PATMAL[5]

[1*]Energy Engineering from Kabul University's faculty of Engineering. Founder and lead organizer of TEDxKabulUniversity, an international platform of events amid promoting ideas worth spreading globally. Cooperated with several national and international organizations and had remarkable contributions on making youth empowerment programs happen. Email: Shahabsharrifi7@gmail.com

[2]Mechanical Engineering from Kabul University, Afghanistan. Completed master's degree from the National Institute of Technology Warangal, India, 2016 in Environmental Engineering and currently Assistant Professor at Kabul University, Engineering Faculty. Email: Shuaib.mohsini@gmail.com

[3]Active senior student of energy engineering of Kabul University. Accomplished leadership, management and Rhetorical programs at Kabul University. Assisted several missions of HDDO organization over the course of one year. Email: elyasaslami08@gmail.com

[4]Perusing bachelor in Energy engineering, faculty of Engineering at Kabul University. Participated at Elimination of Violence against Women and Reduce Administrative Corruption Activities Supported by Center for Peace and Development Initiatives (CPDI) Afghanistan and at Environmental Care and Greenery Activities supported by Green Forest Organization. Email: Noorimohammadaref98@gmail.com

[5]Electrical and Electronics Engineering from Kabul University, Afghanistan. Completed master's degree from Waseda University, Japan, 2019 in Electrical Engineering and currently Assistant Professor at Kabul University and PhD student at Southwest Jiaotong University, China. Email: mhpatmal@ku.edu.af

Abstract

This study investigates the impact of coal reserves in Afghanistan on the country's electricity generation. To conduct this study, the secondary data collected by reliable sources was used. For the analysis of data, a quantitative approach with descriptive methods is used. The analysis showed a massive impact of electricity-from-coal with a 4.94 times increase in generation making 93% of the overall energy consumption of the country. It has been concluded that sustainable usage of coal in electricity production could reduce the annual imports to zero making the country self-sufficient. However, there are several limitations in the data collected including fewer data for the types and quality of the coal in the country and no previous research in the field.

Keywords: Energy, Electricity, Coal, Afghanistan

* Corresponding Author

1. Introduction

Afghanistan, is a country rich in mineral mines and energy resources especially fossil fuels like coal, natural gas, and oil. Afghanistan's minerals mines are estimated to be worth over $1 trillion. Due to everlasting political and economic crisis, not enough research have been conducted in the area of energy resources to find the potential capacity of each source for electricity production. [1]

A large percentage of electricity production in Afghanistan is of non-renewable energy resources, renewable resources makes small percentages. [2] [3] While the country has total electricity production capacity of 5.55 billion kWh, yet consumes most of its electricity from imported power mainly from Tajikistan and Uzbekistan. [4]

With high capacity of electrical energy production from fossil fuels in Afghanistan, unfortunately it has only oil power plants currently active in several locations of the country and zero coal and gas power plants. [5]

Coal plays a significant role in energy production in most countries and is the largest single resource for electricity production making 36% of total electrical energy produced as of 2019 in the world. It may be an efficient energy source in Afghanistan due to the large reservoirs that the country possesses. [6]

Initial researches estimated the total amount of coal to be 100-400 million tons. However, recent studies by the United States Geological Survey showed that the amount of proven and economic available coal reservoirs in Afghanistan seems to be less than that is mainly located in the north and south areas of the country. [7]

Annual coal production and consumption in the country is equal. Making Afghanistan 45th for production in world rankings and 61st for consumption in rankings. Either all the coal, which is being produced annually, is consumed for domestic use or as a thermal energy source in factories and a portion of it is being exported to foreign countries. [8] [2]

In this study, with the data collected about the coal status in Afghanistan and using Quantitative approach and data analysis methods, this study aims to estimate the contribution of coal resources in electrical power generation in the country.

2. Literature review

Afghanistan is one of the countries that uses non-refined materials such as wood, animal excrement and waste materials in the winter season for heating homes. This causes various diseases mainly due to the lack of electricity and its high prices. In general, in the winter season, the household energy consumption in this country is 40% from wood, 40% from coal, 10% from natural gas and 10% from electricity. [9]

Energy is an important necessity for humankind. Hence, the level of progress and development of a country is directly related to its energy consumption. Coal, which is the primary cause of the industrial revolution in the world, with the reduction of oil and gas reserves, it is one of the main alternatives to meet the world's energy needs. [10]

Global coal production in 2018 showed an increase of 4.3%, which was much higher than the 10-year average of 1.3%. China accounted for half of this global growth and Indonesia had an increase of 51 million tons. Coal consumption in 2018 shows an increase of 1.4%, which is the fastest growth since 2013. Globally, coal still accounts for 38.0% of electricity production, which is the continuation of the trend of the past two decades. Coal is still mainly used for 66.5% of commercial electricity and heat generation. The above statistics show the value of coal in electricity production. [11]

Despite the advances in renewable energy, the role of fossil resources in electricity production is still unshakable. Coal makes up about 40% of electricity production in the world and the reason is its cheapness and availability. [11]

The distribution of coal is much fairer than other fossil energy sources such as oil and natural gas, which is concentrated in the Middle East, for example, Turkey, which does not have much capacity in terms of other fossil energy sources, but in terms of coal, it has 2% of all coal in the world. After 1973 with the energy crisis in the world, it turned to using coal resources inside the country for electricity production. [10]

In order to achieve the purpose of the research, the data were collected and filtered outliers out according to our needs. The results of this study are presented below.

2.1. Electricity production, consumption, and import

Table below shows the data provided by the US Energy Information Administration about the energy generation, consumption and import in 2019. [4] [12]

Table 1 Total amount of electrical energy consumption, production and import of Afghanistan in 2019

Electricity	Total	per capita
Own consumption	5.9 bn kWh	138.72 kWh
Production	1.1 bn kWh	30.40 kWh
Import	4.9 bn kWh	110.45 kWh

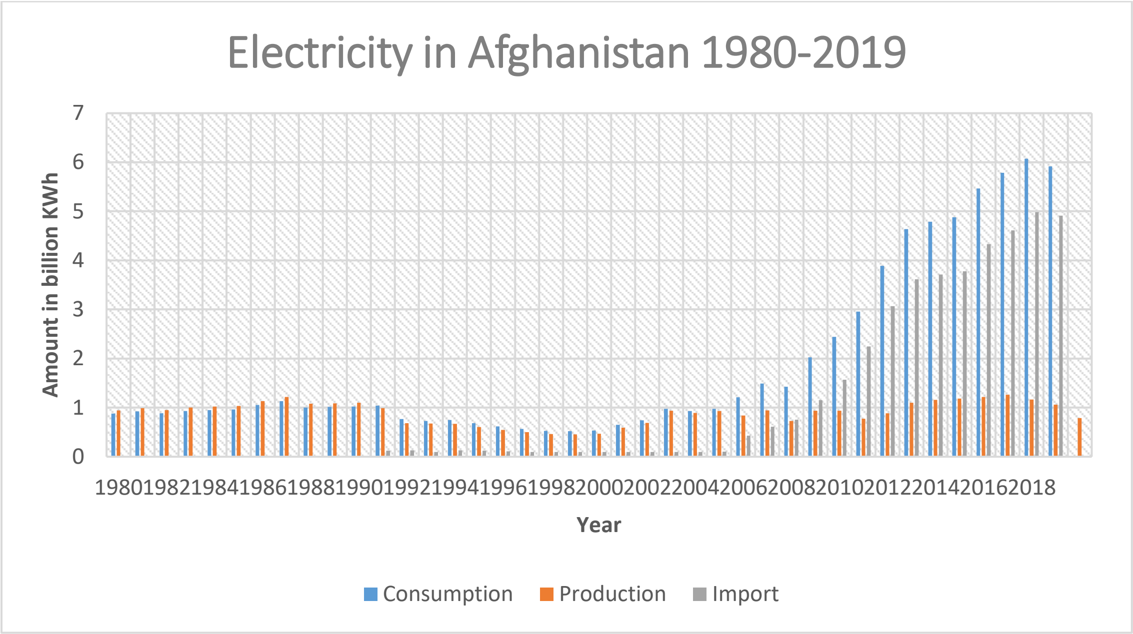

Figure 1 Electricity generation, consumption and import level of Afghanistan between the years 1980-2019(Source: US Energy Information Administration)

According to the United Nations Statistical Division total household electrical consumption in the year of 2020 is estimated to be 3.4 GWh. [13]

2.2. Potential electricity generation capacity by source

Table below shows the potential capacity of electricity generation by source. The theoretical value of the production capacities for electric energy is only possible under ideal conditions. They are measuring the amount of energy that would be generated if permanent and full use of all capacities of all power plants. In practice, this is not possible, because e.g. solar collectors are less efficient under clouds. In addition, wind- and water-power plants are not always operating under full load. All these values are only useful in relation to other energy sources or countries. [4] according to McGinely of UK, From each tone of coal in average 0.00246 GWh (that is equal to 2.46 MWh) electrical energy could be generated. [14]

Table 2 Source based electricity generation potential of Afghanistan

Energy source	Total	Percentage	per capita
Fossil fuels	2.50 bn kWh	45.0 %	62.75 kWh
Nuclear power	0.00 kWh	0.0 %	0.00 kWh
Water power	2.89 bn kWh	52.0 %	72.51 kWh
Renewable energy	222.19 m kWh	4.0 %	5.58 kWh
Total production capacity	5.55 bn kWh	-	139.44 kWh
Actual total production	1.21 bn kWh	21.8 %	30.40 kWh

2.3. Share of renewable and non-renewable sources in electricity generation

Table below shows data of renewable and non-renewable share of electricity generation in Afghanistan according to a research conducted by International Renewable Energy Agency (IRENA) in 2020. [15]

Table 3 Current domestic electricity generation by source in Afghanistan 2020

Generation in 2020	GWh	%
Non-renewable	135	12
Renewable	995	88
Hydro and marine	933	83
Solar	63	6
Wind	0	0
Bioenergy	0	0
Geothermal	0	0
Total	1128	100

2.4. Coal reserves and annual production

According to a report from ministry of mines and industry of Afghanistan in 2002, coalmines estimated to be 440 million tons with annual production rate of 150000 ton in which only 40000 tons of it was from governmental controlled mines. [8]

Recent studies with developed mechanism showed the proven coal reserves in Afghanistan to be about 73 million tones. Bituminous and Anthracite are the two types making the majority of reserves in the country. [16] Figure below shows the production rate of coal from the year 1980 to 2021 in Afghanistan:

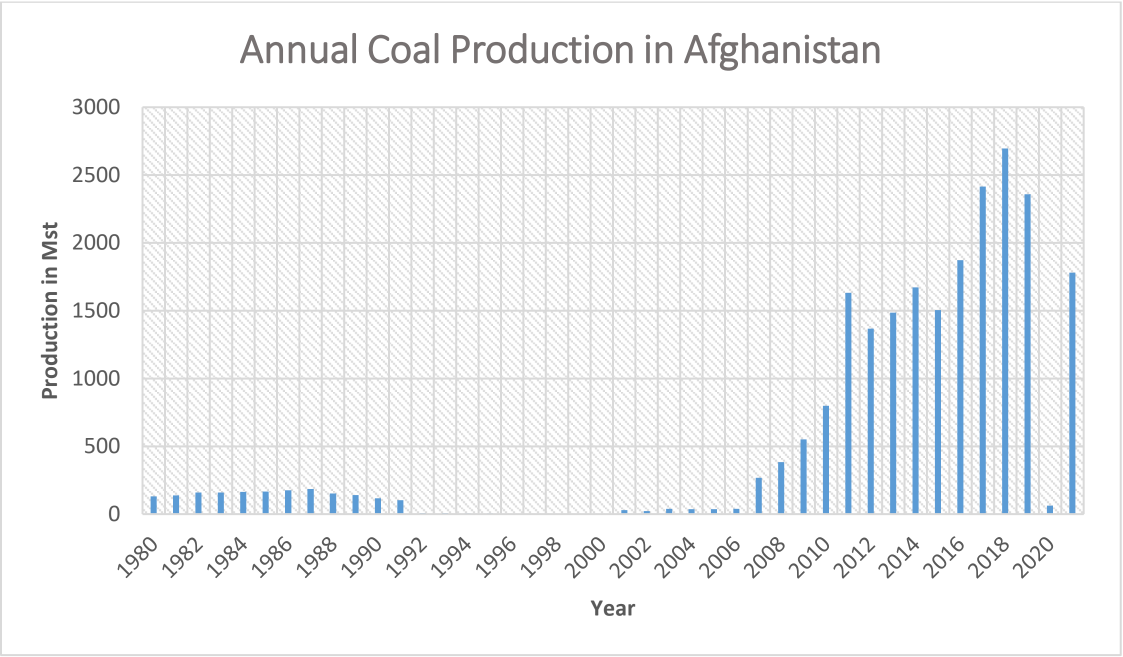

Figure 2 Annual Coal production in Afghanistan from years 1980 to 2021(Source: US EIA)

Coal plants require enormous amounts of coal. Shockingly: a 1000 MWe coal plant uses 9000 tons of coal per day, equivalent to an entire trainload (90 cars with 100 tons in each!). [17]

3. Methodology

Through this study, the electricity generation capacity of coal in kWh was analyzed and compared with other sources currently used in Afghanistan and the amount of electricity imported from foreign countries.

The data used were primarily collected through laboratory tests, field investigations, surveys and interviews conducted by various national and international organizations. The data used in this research is secondary data collected and compiled from reliable sources. With deep literature review of other researches, the amount of coal and it's types were determined. Then from laboratory experiments of international energy laboratories, the potential electrical capacity of each ton of coal in GWh was found. Furthermore, the data for total electricity consumption for that last decade collected and its sources was determined to be further compared with coal power.

To carry out this research, quantitative methods are used to analyze and evaluate the collected data and present the results and calculations with the help of formulas and tables. To complete this review paper, descriptive analysis is used to organize and categorize data collected from sources with the help of Microsoft Excel. In addition, inheritance analysis will be used to interpret and analyze the data of the results to achieve the purpose of this study.

4. Results and analysis

4.1. Potential electricity generation capacity of coal reserves

From each tone of coal in average 0.00266 GWh (that is equal to 2.66 MWh) electrical energy could be generated. With the amount of coal exist in Afghanistan (73 Million tons), about 194,180 GWh electricity could be generated in total. By considering the electricity consumption in Afghanistan, which is shown in Figure below, the country could achieve it's electricity demand for 43.7 years with only using electricity generated from coal reserves.

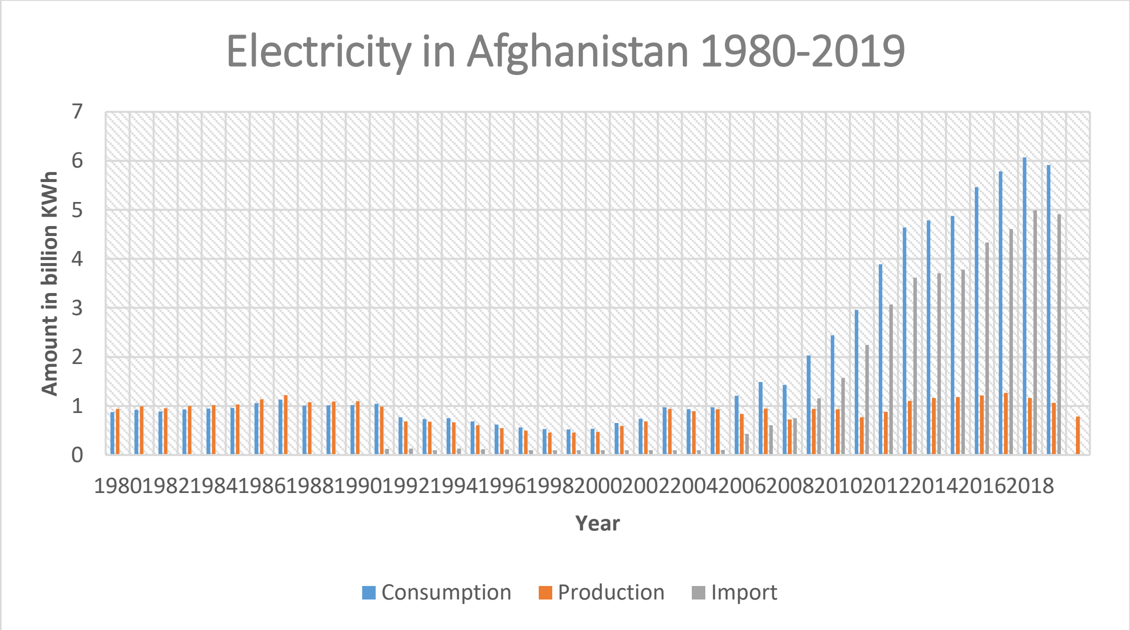

Figure 3 Electricity generation, consumption and import level of Afghanistan between the years 1980-2019

Calculations:

Potential Electricity Generation Capacity= (Conversion factor GWh/metric tone)(total reserves in tone)

Potential Electricity Generation Capacity= 0.00226GWh/tone x 73 Mt= 194,180 GWh

Total Years for a single source to meet the annual electricity demand = (Electrical capacity of the source)/(Annual Energy Consumption)= (194,180 GWh/year) /(4442 GWh)=43.7 years

4.2. Contribution of coal generated electricity to electricity consumption and generation

Based on our calculations we found that the average annual production of coal in last decade (2011-2021) is 1713.004 Mst (thousand short tons). This is equivalent to 1.5 Million tones (1,554,011 tones). By considering the assumption of using annual coal production to generate electricity, there will be 4133.669 GWh electrical energy generation per year.

Using descriptive analysis, we can find that the average electricity production in the past decade (2010-2020) is 1.047 bn kWh that is equivalent to 1047 GWh. With addition of the amount energy generated from coal, annual electricity generation of the country will become 5180.669 GWh, which shows 4.94 times increase in total electrical energy generation from interior sources.

Analysis shows that with annual production rate and annual potential electricity generation capacity of coal, it secures 93% of total electricity consumption per year. Since with the help of descriptive analysis, the average electricity consumption of the country is 4442 GWh from 2009 to 2019.

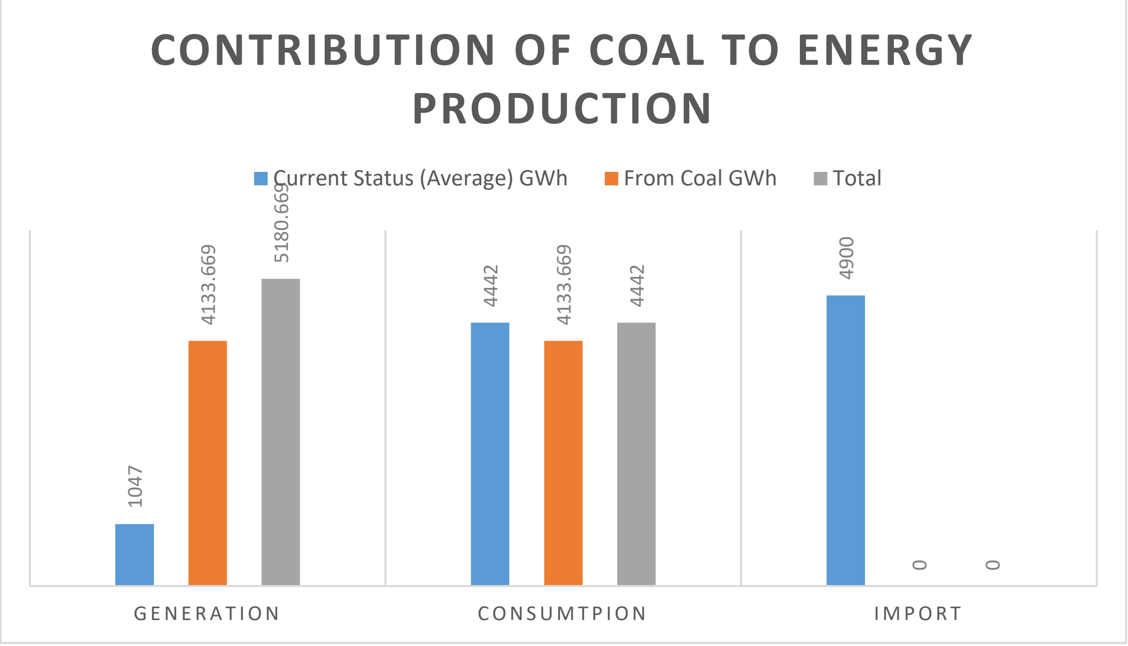

Figure 4 The contribution of coal reservoirs to Electrical energy production in Afghanistan

5. Conclusion

Because electricity is such an essential part of everyone's life, especially in the age of technology and computers, it is important to understand the potential of every available resource. Coal, the world's main source of energy, is plentiful in Afghanistan with vast amounts. The country is still not using its coal reserves for electricity generation and there is no coal-fired power plant. It is crucial to understand the overall electrical energy potential capacity of these reserves and its impact on all aspects of energy production, consumption and imports. With the results presented, the use of coal as an energy source could be very effective in reducing imports and saving the country's financial resources.

A total of 194,180 GWh electricity could be produced in coal-burning power plants. This amount of electricity will increase Afghanistan's energy production by 4.94 times, making the country self-sufficient in the energy sector and reducing foreign energy imports to zero. Annual electricity produced from coal accounts for 93 percent of the country's total electricity consumption, leaving little room for the use of other sources. The total generated electrical power could meet the electricity demand of country for up to 43 years. However, calculating how a hybrid system can improve its life cycle is a remarkable feat.

In the future, studies can be conducted on financial difficulties and technical obstacles that may prevent the realization of the results of this study. It is also the duty of researchers to investigate methods aiming to establish a national sustainable energy production plan for sustainable utilization and life cycle extension of energy resources.

6. Discussion

The study demonstrates a correlation between the electrical energy that could be generated from coal reserves in Afghanistan and its impact on total electricity generation and import. However, due to the lack of data on types of reserves in Afghanistan with their respective percentages, the results may not fit well with implications in practice. Investment costs of building power plants, Carbon Dioxide emissions and relevant limitations in conversion processes should be also taken into consideration. Avenues for future research include accurate investigations to find percentage and qualitative values for each type of coal available and its impact on sustainable energy and economic development.

References

[1] Agnieszka, "Why is Afghanistan unable to extract its vast mineral wealth?," Aljazeera, [Online]. Available: https://www.aljazeera.com/features/2019/5/28/why-is-afghanistan-unable-to-extract-its-vast-mineral-wealth. [Accessed 13 Septermber 2022].

[2] BP, "Statistical Review of World Energy," [Online]. Available: https://www.bp.com/en/global/corporate/energyeconomics/.

[3] "EIA," [Online]. Available: https://www.eia.gov/.

[4] E. Lars, "Energy Statistic of Afghanistan," World Data, 6 March 2021. [Online]. Available: https://www.worlddata.info/asia/afghanistan/energy-consumption.php. [Accessed 28 September 2022].

[5] 'estments and trades | Afghanistan Energy Resources," Embassy of Afghanistan in Jnited Kingdom, 2020. [Online]. Available: ://afghanistanembassy.org.uk/english/business-investment/energy-sector/. cessed 20 September 2022].

[6] "Reports- Coal Rserves in Afghanistan," [Online]. Available: https://www.iea.org/reports/global-energy-review-2019/coal#:~:text=Coal%20continues%20to%20be%20the,produced%20more%20electricity%20than%20coal.. [Accessed 1 October 2022].

[7] USGS, "Assessment of Coal in Afghanistan," United States Geological survey USGS.

[8] G. M. Malikyar, "The State of Environment in Afghanistan 2011-1017," *ResearchGste*, 2017.

[9] M. A. Rasuli and S. Torii, "The Environmental Implications of Coal Usage as an Energy Resource for," *The International journal of analytical and experimental modal analysis* , July 2022.

[10] A. O. Yılmaz and T. Uslu, "The role of coal in energy production—Consumption and," *Department of Mining Engineering, Karadeniz Technical University, 61080 Trabzon, Turkey,* 17 April 2006.

[11] M. Hafner and G. Luciani, The Palgrave Handbook of International, 2022.

[12] "Afghanistan | Electricity | International - U.S. Energy Information Administration (EIA)," [Online]. Available: https://www.eia.gov/international/data/country/AFG/electricity/electricity-

consumption?pd=2&p=00000020000020000000007vo70400bvu2&u=0&f=A&v=mapbubble&a=-&i=none&vo=value&vb=33&t=C&g=none&l=249--1&s=315532800000&e=1609459200000&ev=true. [Accessed 5 October 2022].

[13] "UNdata | record view | Afghanistan total electricity," Untied Nations, 8 January 2021. [Online]. Available: http://data.un.org/Data.aspx?d=EDATA&f=cmID%3AEL%3BtrID%3A1231. [Accessed 10 October 2022].

[14] McGinley, "News | How Much of Each Energy Source Does It Take to Power Your Home?," 29 9 2017. [Online]. Available: https://www.mcginley.co.uk/news/how-much-of-each-energy-source-does-it-take-to-power-your-home/bp254/. [Accessed 10 September 2022].

[15] "Afghanistan Energy Profile," Internation Renewable Energy agency, Masdra City, 2022.

[16] "International - U.S. Energy Information Administration (EIA) | International | Afghanistan | coal reserves," International - U.S. Energy Information Administration (EIA), 2020. [Online]. Available: https://www.eia.gov/international/data/country/AFG/coal-and-coke/coal-reserves?pd=1&p=3i000000000000000000000000000000000187nm2g00000000n&u=0&f=A&v=column&a=-&i=none&vo=value&vb=260&t=C&g=none&l=249--1&s=315532800000&e=1609459200000&ev=true. [Accessed 10 October 2022].

[17] R. A. Hinrichs and M. Kleinbach, "Electricity: Circuits+ superconductors," in *Energy: Its use and the environment*, Toronto, Ontorio: Thomson Brooks/Cole , 2006, p. 320.

[18] "Afghanistan Energy Profile," International Renewable Energy Agency IREA, [Online]. Available: https://www.irena.org/IRENADocuments/Statistical_Profiles/Asia/Afghanistan_Asia_RE_SP.pdf. [Accessed 1 October 2022].

Authors Profile

Shahab Sharifi is a senior Energy Engineering student at Kabul University's faculty of Engineering. He is founder and lead organizer of TEDxKabulUniversity, an international platform of events amid promoting ideas worth spreading globally. He has cooperated with several national and international organizations and had remarkable contributions on making youth empowerment conferences and events happen. He also delivered a clever business idea, which won On-campus round of competitions and was pitched in regional level in south east of Asia at international platform of HultPrize.

Mohammad Shuaib Mohsini Mechanical Engineering from Kabul University, Afghanistan. Completed master's degree from the National Institute of Technology Warangal, India, 2016 in Environmental Engineering and currently Assistant Professor at Kabul University, Engineering Faculty.

Alyas Aslami is from Kabul, Afghanistan. He is currently active senior student of energy engineering of Kabul University. He accomplished leadership, management and Rhetorical programs at Kabul University. He have assisted several missions of HDDO organization over the course of one year.

Mohammad Arif Noori is perusing his bachelor in Energy engineering, faculty of Engineering at Kabul University. He has participated at Elimination of Violence against Women and Reduce Administrative Corruption Activities. Supported by Center for Peace and Development Initiatives (CPDI) Afghanistan and at Environmental Care and Greenery Activities supported by Green Forest Organization.

Mohammad Hamed Patmal Electrical and Electronics Engineering from Kabul University, Afghanistan. Completed master's degree from Waseda University, Japan, 2019 in Electrical Engineering and currently Assistant Professor at Kabul University and PhD student at Southwest Jiaotong University, China.

KPU International Journal of Engineering & Technology
Volume 3, Issue1, Sep. 2023
e-ISSN:2790-0819, p-ISSN:2790-0800

Date Received: 2022-08-07
Date Accepted: 2023-07-29
Date Published: 2023-09-15

Avalanche Susceptibility Mapping Using GIS-based Multi-Criteria Decision Analysis: The Case of Shighnan District

AHMAD SHEKIB IQBAL[1*], ABDULLAH NASER[2]

[1*]Assistant Professor, Department of Geographical Information Systems, Kabul Polytechnic University, KPU campus, 5th District, Kabul, Afghanistan. Email: shekibiqbal.si@kpu.edu.af

[2]Professor, Department of Engineering Geodesy, Kabul Polytechnic University, KPU campus, 5th District, Kabul, Afghanistan. Email: abdullah848032@gmail.com

Abstract

Avalanche is one of the most dangerous natural disaster phenomena, which causes heavy damage to properties and fatalities in most mountainous and inaccessible regions across the globe. In the present study, avalanche susceptibility map of the Shighnan district is prepared by applying GIS-based multi-criteria decision analysis-analytic hierarchy process method. The prominent avalanche occurrence terrain factors such as slope, elevation, aspect, curvature, and land cover are used in this method. Shuttle Radar Topography Mission (SRTM) digital elevation model (DEM) and Corine Land Cover data are used to generate considered terrain factors. The pairwise comparison matrix is used to calculate the weight values of terrain factors. Then, the weight values of each avalanche occurrence terrain factor are utilized in the AHP model to produce the avalanche susceptibility map. The results are classified into five zones of very high, high, moderate, low, and very low, which covers 13%, 35%, 28%, 23%, and 1% of the total area respectively. This avalanche susceptibility map will assist decision-makers in better planning and taking precaution while moving across the region.

Keywords: Snow avalanche, GIS, Remote Sensing, AHP model, MCDA

[*]Corresponding Author

1. Introduction

Avalanches are one of the most hazardous natural disaster incidents in Afghanistan, which are very destructive and unpreventable. Avalanche is a rapid, downward movement of a large mass of snow, ice, and rocks. An avalanche occurs when accumulated snowpack moves downside of a mountain under the influence of gravity. The flow speed of an avalanche may accelerate up to 200 km/h and put pressure up to 50 T/m^2 [1]. Due to high flow speed and pressure, the avalanches tend to destroy forests, human, property, road networks, and communication lines [1]. An avalanche is highly uncertain and hard to predict. Hence, it threatens the life of those who live in mountainous regions [2].

Normally, there are two main types of avalanches: loose avalanches and slab avalanches [1]. Loose avalanches initiate from a point or a single area and tend to collect masses of snow as it continues downside. Typically, this avalanche occurs due to poor connection between snow crystals and flow down a sloping surface in a triangular pattern [3]. In contrast, slab avalanches occurs due to failure in snow depth which take off from a large surface and hold more layers of organized snow [3]. This type of avalanche is more dangerous and cause most casualties and property damage [1]. In slab avalanches, the shear displacement depends on the slope angle and snow type. When the slope angel ranges between 25-90 degree, almost 90% of the total deformation is in shear displacement [3]. In slab avalanches the shear deformation will become more dominant when the density of snow increases. The chances of slab avalanches become rare when the slope angel reaches lower than 25 degrees. By increasing the slope angel, the frequency of slab avalanches also increase due to the higher shear stresses and deformation [3].

The occurrence of avalanches are affected by several factors such as topographical, metrological, snowpack structure, natural triggers, social activities, land cover, etc. [4], [5]. For avalanche susceptibility mapping of a region, it's difficult to consider all effective factors because, there are many contributing factors, and they are not homogenous. Indeed, there are two main types of factors, static terrain factors and dynamic metrological factors [6].

Prediction of avalanches are very difficult and challenging tasks as it involves dynamic meteorological factors i.e., snowfall, temperature, water content, wind speed, precipitation, rain fall and static terrain factors such as slope, aspect, elevation, curvature, and ground cover [6], [7]. Thus, an avalanche susceptibility map is an essential step for the evaluation of high-risk areas and very helpful to plan, manage and travel safely across the snow covered regions [6].

Various studies have been conducted to generate avalanche susceptibility maps using GIS, Remote Sensing, and multi-criteria decision analysis (MCDA) approaches. Several studies applied GIS-based AHP methods [5]–[8], Kumar et al. (2019), while producing avalanche susceptibility map, used probabilistic occurrence ratio (PRO). Many studies applied static factors such as slope, elevation, curvature, aspect, land cover, vegetation cover, and terrain roughness to generate susceptibility maps, since static factors are constant and can be used effectively for avalanche susceptibility mapping for long duration [1], [4], [5], [7]. Singh et al. (2019) integrated the static and dynamic factors to produce avalanche susceptibility map. Dynamic factors like meteorological parameters and snowpack structures are changing in different times related to the weather conditions [7].

The present study attempted to produce an avalanche susceptibility map considering terrain and land cover parameters in Shignan district of Badakhshan province of Afghanistan by using GIS-based multi-criteria decision analysis Analytic Hierarchy Process (AHP) model that suggested by Saaty [10]. The key advantage of GIS in the assessment of natural hazard is its ability to integrate large heterogenous datasets, their management and analysis [6]. An important reason while using the AHP model is that it's easy to understand and has the strong capability in solving the complex decision problems [11] and this model can be implemented in GIS effortlessly.

2. Study area and dataset used

2.1 Study area

The study area is Shignan district of Badakhshan province, which is located in the mountainous northeast region of Afghanistan. It is bordered by Tajikistan in the east and northeast (Figure 1). Geographically, the study area lies between latitudes 37°15′22″ to 38°03′49″ N and longitude 70°44′41″ to 71°35′54″ E. The altitude of the study area extends from 1720 to 5150 m. The study area covers the area of 4486 km^2. Shighnan district has a relatively hot, dry, and short summers and cold and long winters. The region has a humid continental climate which is cold and temperate. The winters are rainier than the summers with an average annual precipitation of about 867mm. January is the coldest month with the average daily temperature of -3.3°C, and -17.5°C is the recorded lowest temperature. At the end of June, summer starts and ends in September. The average high temperature is 11.8 °C, and the highest recorded temperature is 16.6 °C has ever measured (Climate-data.org). Due to the high mountains, this district is very difficult to navigate, especially during the snowy winter where almost all the roads in this district are blocked, causing mobility difficulties for the inhabitants. The study area is characterized by cold temperatures, slight precipitation, and heavy snowfall that has led to an escalation of incidents including floods, avalanches, and landslides.

Fig. 1: Geographical position of the study area.

2.2 Dataset used

In the present study, the avalanche occurrence related factors are obtained from SRTM DEM and Copernicus. The avalanche occurrence terrain related factors, including slope, elevation, aspect, curvature, and land cover are considered as significant factors for generating avalanche susceptibility mapping [12]. The slope, elevation, aspect, and curvature are generated from SRTM DEM which was downloaded with a spatial resolution of 30m from USGS Earth Explored website (https://earthexplorer.usgs.gov/). The land cover data downloaded from Copernicus Global Land Service Portal (https://land.copernicus.eu/global/index.html). Each of them was considered a prominent avalanche occurrence factor and utilized for avalanche susceptibility mapping.

3. Methodology

The methodology adopted to generate the avalanche susceptibility map is illustrated in Fig. 2. and explained in the subsequent sections. The first part of the methodology was to collect the datasets used and proceeded to generate, analyze, rank, and reclassify the most significant avalanche occurrence terrain factors to acquire thematic layers. The next part was to generate pairwise comparison matrix between all terrain factors and calculate the weight values of thematic layers by applying analytic hierarchy process (AHP) method.

The final part was to integrate these thematic layers using a GIS-based AHP model to generate an avalanche susceptibility map. The methodology workflow is as follows:

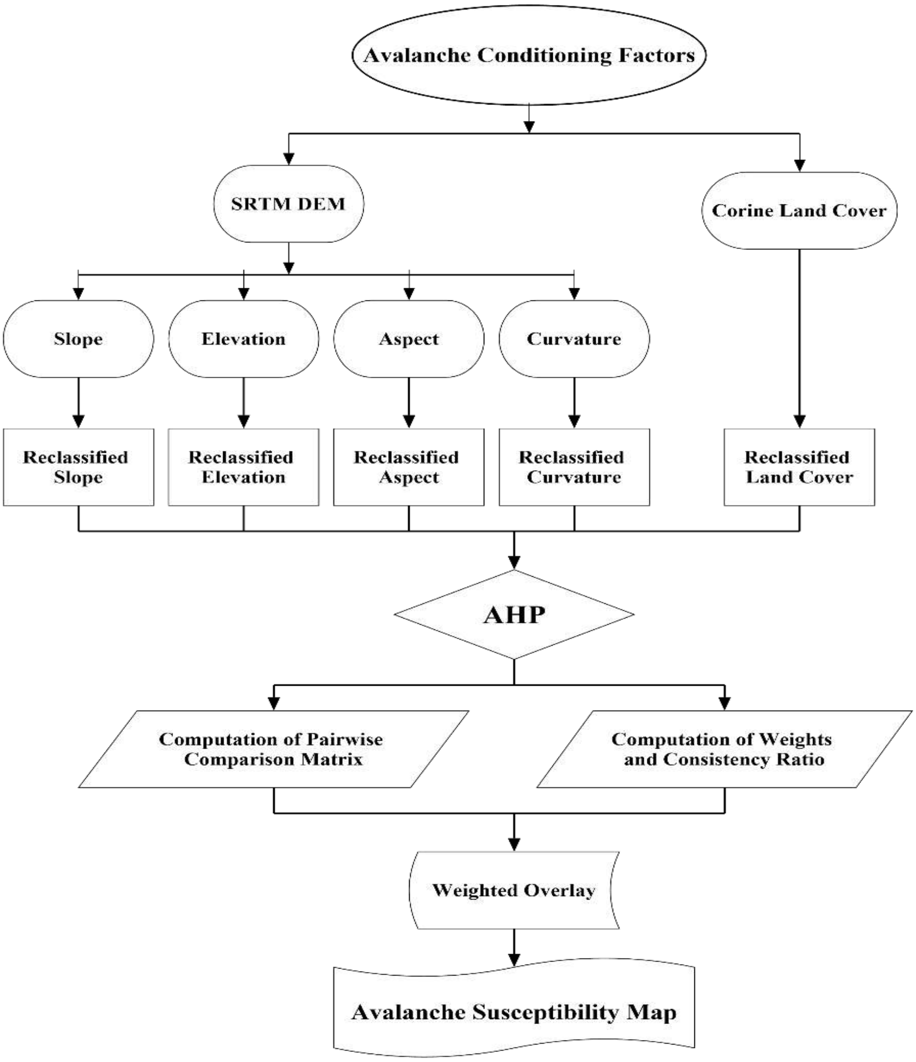

Fig. 2: Flowchart of the avalanche susceptibility mapping methodology.

3.1 Analysis of the factors and generation of thematic layers

The assessment of avalanche susceptibility mapping is a difficult and challenging task because there are several factors influencing an avalanche. Some factors that contribute to an avalanche susceptibility mapping are meteorological, snowpack structure, topographic characteristics, social activities, and natural triggers. The meteorological parameters incorporated in mapping avalanches are snowfall, wind speed, wind direction, precipitation, temperature, etc. Under meteorological conditions the snowpack structure rely upon successive snowfalls. The avalanches happen when the snowpack loses its stability and becomes so weak or dislocated by natural triggers or social activities. The meteorological parameters and snowpack structure change continuously because they depend on weather conditions. Nevertheless, the topographical or terrain factors such as slope, elevation, aspect, curvature, and land cover are the constant factors for avalanche susceptibility mapping. Due to inadequate information about meteorological factors and short-term validity, the present study only considered the terrain factors. The details of each factor are summarized in the following subsections.

3.1.1 Slope

The slope is considered as a significant terrain factor for avalanche susceptibility mapping [7]. According to statistics, it is reported that most avalanche accidents occur where the slope angle is greater than 30° and less avalanches start on slope angle less than 25° [7], [12]. Though, the avalanches release from slope angle less than 25° when the snow has higher water content. Generally on such slopes, the shear stress is not large enough to initiate an avalanche [13]. Majority of avalanches release from slope angles between 28° and 45° [4], [6], [7], [14]. On steep slopes between 45°–55° very small avalanches can occur because the amount of snow deposition is limited. In the present study, the slope values were obtained from SRTM DEM and categorized into five classes (Figure 3).

3.1.2 Elevation

Elevation does not directly impact the initiation of avalanches. Nevertheless, meteorological factors such as snowfall, temperature, wind speed, and snow depth are directly connected to elevation, which in turn directly influence the occurrence of avalanches [7], [12]. Generally, at low elevations the chance of an avalanche occurring is low due to warm air. Likewise, snow that falls on lower elevation regions often melt and may change to rain when it reaches the ground. In the higher elevation regions, the snow can remain available for avalanche for a longer duration due to low temperatures [4], [6] . The present study area has the lowest elevation of 1719m and the highest elevation of 5148m, and most of the avalanches occur near regions with the highest elevations. The elevation ranges of the study area were categorized into six classes (Figure 3).

3.1.3 Aspect

Aspect is considered as a significant factor in evaluation of avalanche high risk zones [12]. Aspect does not directly influence the risk of avalanches; it is directly influenced by the sun radiation. The sun facing aspects receive more radiation from the sun with the snowpack structures becoming more stable than the shaded slopes. In addition, the windward slopes get stabilized due to less amount of snow while the leeward slopes increase the risk of avalanches because of extra snow loads [7]. According to Austrian and Swiss statistics report, 50% of all avalanches happen in the northern part (NW-N-NE) of the aspect [15]. Aspect map produced from SRTM DEM and categorized into 9 classes as illustrated in (Figure 3).

3.1.4 Curvature

Curvature is one of the significant parameter influencing avalanche susceptibility mapping [16]. Generally, avalanches happen on convex surfaces because of snowpack instability compared to concave and flat surfaces that support stabilization [17]. Curvature map generated from SRTM DEM is categorized into 3 classes such as convex, concave, and flat, which are illustrated in (Figure 3).

3.1.5 Land cover

Land cover is also considered as a significant avalanche contributory factor. The land cover map provides information about the snow/ice, vegetation, build area, bare ground, and water body classes. Generally, dense vegetation cover such as forest has significant influence on avalanche activities. Dense vegetation cover is a greater shield against the avalanches which holds and reduces the amount of snow available for avalanche initiation [8], [18]. Snowpack structures are more stable in the forestry areas than the snow/ice and bare ground areas. Therefore, snow/ice cover and bare ground slopes are considered more susceptible to avalanches [16]. The land cover map of the study area is shown in Fig. 3.

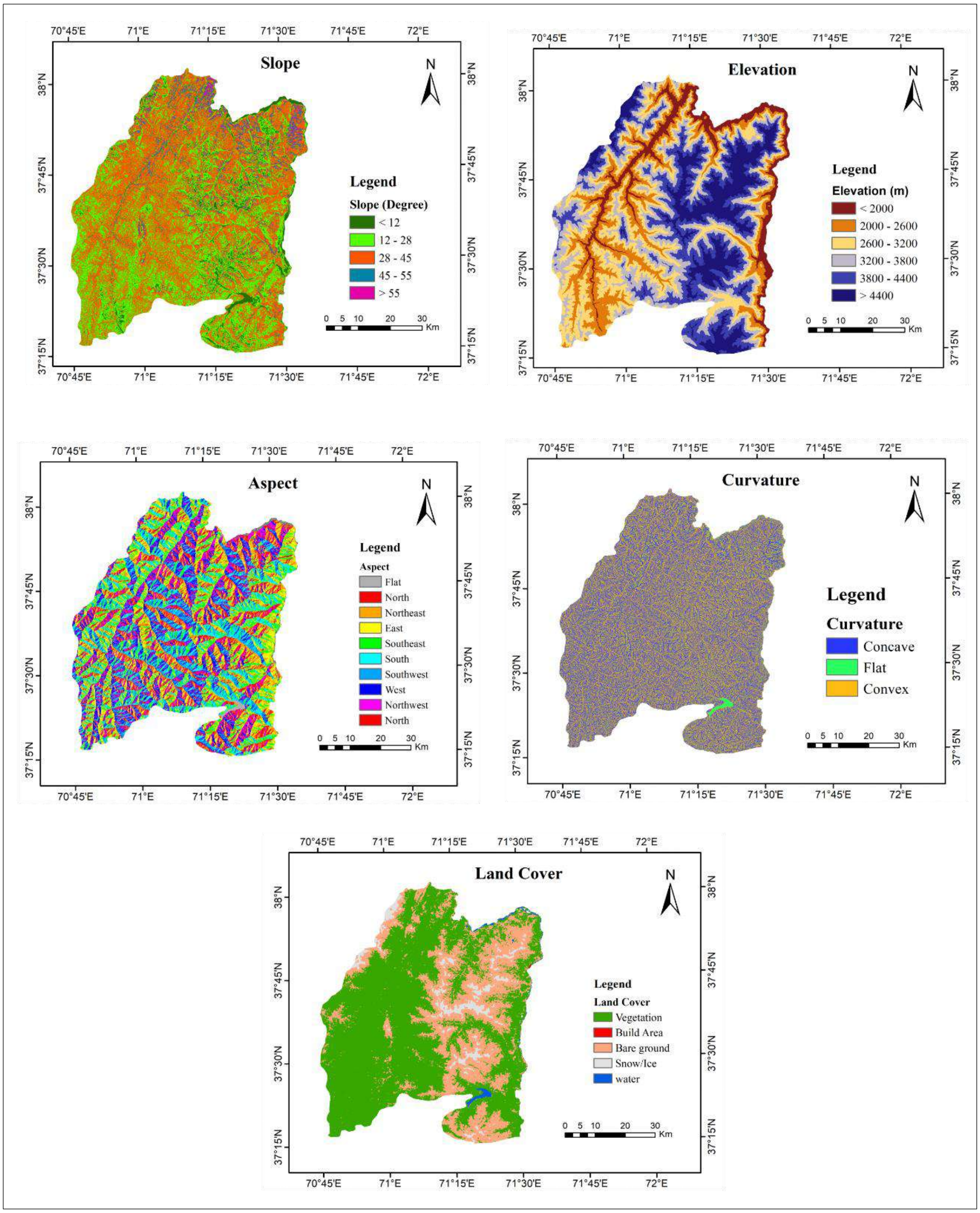

Fig. 3: GIS layers generated for avalanche susceptibility mapping.

3.2 Avalanche Susceptibility Mapping Using AHP Model

3.2.1 MCDA-AHP model

AHP is one of the Multi-Criteria-Decision-Making models that is broadly used in GIS-based decision-making problems. The concept of AHP was first proposed by Saaty [19]. AHP's wide use is because of its simplicity and does not need complex mathematics. In addition, it's possible to formulate the problems and consider qualitative and quantitative data simultaneously [19]. AHP model is widely and successfully used in various natural hazard studies such as avalanches [5], [7], [12], [18]. This technique is based on three main principles: decomposition of the problem, pair to pair comparison, and obtaining hierarchy of the priorities [19]. The principle of AHP is based on pairwise comparisons, which makes judgment easy and solve complex problems accurately. In the AHP technique, the problem is broken down into a hierarchical structure which makes the decision-makers to take the best decision. The judgment of this model is based on expert knowledge and the key concern is to create a hierarchy structure which splitting down the problem into a hierarchy of goal, criteria, and sub-criteria. In this study, the avalanche susceptibility mapping is the goal and the terrain factors which are described in section 3.1 are used as criteria.

The procedure for calculating the weights of parameters using AHP model can be summarized in the following steps [20]:

I. Generating pair to pair comparison matrix

In this step, we perform pair to pair comparison for each occurrence parameter. Each parameter must be at the same level, Saaty's importance value scale from 1 to 9 based on their relative importance (Table 1) were assigned and generated the pairwise comparison matrix for occurrence parameters which can be presented in Table 2.

Table 1: The importance value scale [19].

Importance	*Defining the relative importance*
1	Equally important
3	Moderately important
5	Strongly important
7	Very strongly important
9	Extremely important
2,4,6,8	Intermediate judgement

Table 2: Pairwise comparison matrix and weight values of parameters.

Criteria / Criteria	Slope	Elevation	Aspect	Curvature	Land Cover	Weight Value
Slope	1	2	4	5	7	0.45
Elevation	1/2	1	3	4	5	0.29
Aspect	1/5	1/3	1	2	3	0.12
Curvature	1/5	1/4	1/2	1	3	0.09
Land cover	1/7	1/5	1/3	1/3	1	0.05

II. Calculation of weights

In this phase, at first the sum of each column is calculated in the pairwise comparison matrix. Afterward, each sum is divided into the matrix by summation of its column and the result demonstrates the normalized pairwise comparison matrix. The average of weights is estimated in each row of the normalized matrix and the results provide weight of each criterion (Table 2) [10].

III. Evaluation of consistency ratio

In this step, the consistency ratio (CR) of the n^{th} element is calculated. The CR calculation is used to check whether the pairwise comparison matrix is consistent or not. The following formula calculates CR:

$$CR = \frac{CI}{RI} \quad (1)$$

In the above formula, CI is a consistency index and RI represent the random index which is acquired from Table 3 based on the number of variables (n).

Table 3: Values of Random Index proposed by saaty [10].

n	1	2	3	4	5	6	7	8	9	10
RI	0	0	0.58	0.9	1.12	1.24	1.32	1.41	1.45	1.49

The consistency index is derived using the following formula:

$$CI = \frac{\lambda_{max} - n}{n-1} \quad (2)$$

In the equation (2), λ_{max} is the maximum eigenvalue of the pairwise comparison matrix, and n is the number of criteria. The concept of the CR is designed in such a way that if the CR is less than 0.1 or 10% the matrix expresses inconsistency and requires reconsideration of pairwise comparison. If the CR is more than 0.1 or 10% the matrix expresses a validation of consistency [10]. The computed CI, λ max, RI, and CR of the matrix are illustrated in Table 4.

Table 4: Estimated consistency ratio and its variables.

CI	λ max	RI	CR
0.04	5.14	1.12	0.03

The weights of parameters have been computed based on their relative importance. The relative importance values were chosen based on avalanche-related published studies [5]–[9], [12], [18], [21], [22]. According to these studies, the relative importance of each criterion is carefully evaluated, and suitable relative importance values were assigned.

3.2.2 Avalanche Susceptibility Mapping

Th MCDA-AHP model is applied in GIS to produce an avalanche susceptibility map of the Shignan district. The avalanche occurrence terrain factors are reclassified as shown in Figure 3 and the ratings are assigned to each class using a scale range from 1 to 5 (Table 5). The reclassified avalanche terrain factors and the calculated weight values of corresponding terrain factors are used in equation 3 to produce an avalanche susceptibility map.

$$ASI = \sum_{i=1}^{n} (R_i \times W_i) \quad (3)$$

In the equation, *ASI* is avalanche susceptibility index, R_i is the rating value of reclassified class of the factors and W_i is the weight values for each avalanche terrain factor obtained from AHP technique.

The ASI map of the study area was then subdivided into the following five susceptible areas: very low, low, moderate, high, and very high susceptibility as illustrated in Fig. 4.

Table 5: Rating assignment to each factor.

Factors	*Categories (classes)*	*Ratings*
Slope	< 12°	0
	12° – 28°	1
	28° – 45°	5
	45° – 55°	3
	> 55°	1
Elevation	< 2000	1
	2000 – 2600	2
	2600 – 3200	3
	3200 – 3800	4
	3800 – 4400	4
	> 4400	5
Aspect	Flat	0
	North	5
	North-East	5
	East	2
	South-East	1
	South	1
	South-West	1
	West	2
	North-West	4
Curvature	Concave	1
	Flat	0
	Convex	5
Land cover	Vegetation	2
	Build Area	0
	Bare ground	4
	Snow/Ice	5
	Water	1

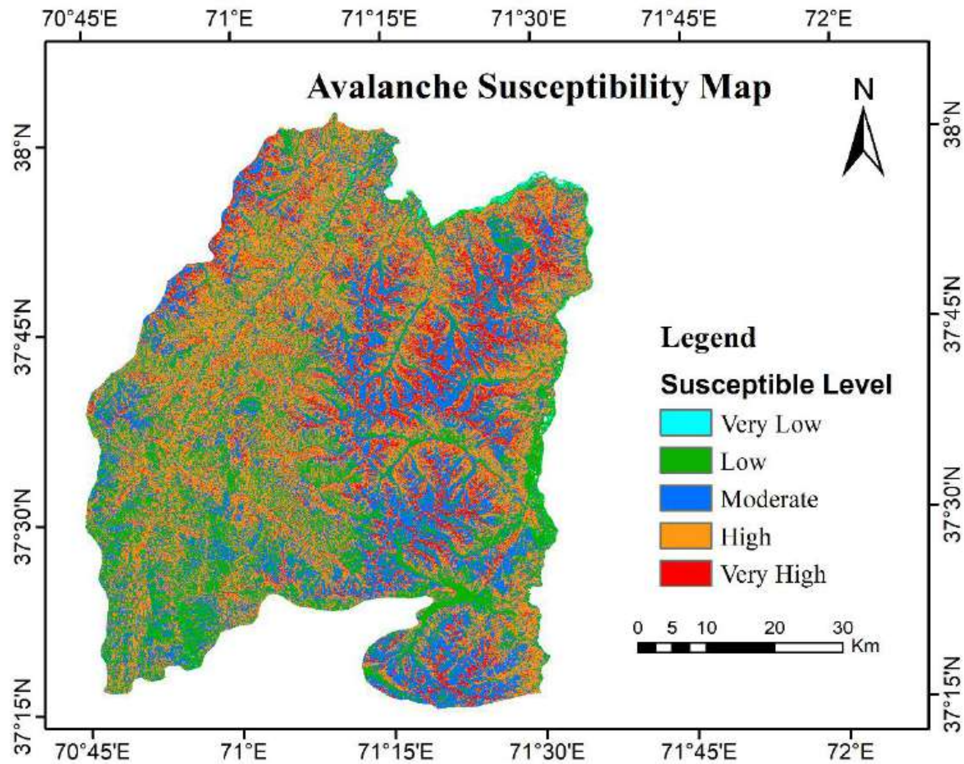

Fig. 4: Avalanche susceptibility map of the study area.

4. Results and discussion

Avalanches are one of the natural disaster incidents occurring due to terrain and meteorological factors. In this study, only terrain factors were applied to produce an avalanche susceptibility mapping due to their reliability, easy availability, and high dependency with avalanches. Avalanche occurrences are influenced by several factors such as slope, elevation, aspect, curvature, and land cover. For avalanche susceptibility mapping of Shighnan district, these factors were derived from the SRTM DEM and Copernicus portal. The slope was considered the most significant avalanche occurrence terrain factor. The slope layer was classified into five classes such as <12°, 12–28°, 28–45°, 45–55° and >55°. Those slope classes were rated, and maximum rating was assigned to the class ranges from 28–45° because this class was found to be the most prominent (Table 5).

The elevation layer was considered the second predominate terrain factor, which was classified into six classes such as <2000, 2000–2600, 2600–3200, 3200–3800, 3800–4400 and >4400. The maximum ratings were given to the elevation class of 3800–4400 and >4400 because of snow depth and heavy snowfall in these elevations (Table 5). Aspect layer was classified into nine classes; aspect classes of North, Northeast, and Northwest were assigned the maximum ratings because the snowpack is unstable in these zones (Table 5).

Curvature values were classified into concave, flat, and convex classes. The convex curvature values were considered more prone to avalanches than flat and concave. Thus, the maximum rating was given to the convex curvature values (Table 5). The land cover was generated from Copernicus and classified into five classes such as snow/ice, vegetation, bare ground, build area, and water. The maximum rating was assigned to snow/ice cover regions due to snowpack instability and susceptible to avalanche formation and minimum rating was assigned to water and build areas (Table 5).

Pairwise comparison matrix was used to calculate the weight values of each avalanche occurrence factor. The comparison matrix is given in Table 2. The slope factor was given the highest weight value in the pairwise comparison matrix than other factors. The degree of importance for each factor was specified based on the 1 to 9 scale (Saaty, 1980) and is presented in Table 1. After generating pairwise comparison matrix, the weight values of avalanche occurrence factors were computed. The weight values of slope, elevation, aspect, curvature, and land cover were assigned as 0.45, 0.29, 0.12, 0.09, and 0.05, respectively (Table 2). Therefore, the highest weight value is given to slope and lowest for land cover. The consistency ratio is computed as 0.03. The weight values of factor and given score to each class of the factors were integrated with GIS using Equation 3 to acquire the ASI.

The resulting avalanche susceptibility map for Shighnan district was divided into five zones as: very low, low, moderate, high, and very high (Figure 4). According to the results, high and very high susceptible regions cover 35% (1595.19 km^2) and 13% (586.25 km^2) of the study area, while moderate, low, and very low susceptible regions contribute 28% (1249.38 km^2), 23% (1018.44 km^2), and 1% (22.37 km^2) of the study area respectively (Table 6).

Table 6: Regional distribution of avalanche susceptibility map.

Avalanche Susceptibility	*Area (km^2)*	*Percentage %*
Very low	22.37	1
Low	1018.44	23
Moderate	1249.38	28
High	1595.19	35
Very high	586.25	13

5. Conclusion

Avalanches are one of the most dangerous natural phenomena occurring every year and tend to destroy properties, homes, livestock, and causes loss of lives. Hence, avalanche susceptibility mapping is a vital step in identifying the risky zones. The Shighnan district is a very complex mountainous area, and harsh climatic conditions. Therefore, avalanche susceptibility mapping of such an area is a very challenging task. The GIS and remote sensing technology integrated with MCDA-AHP model are applied to generate the avalanche susceptibility map of the Shighnas district. AHP model is being applied for solving many problems and widely used for solving natural hazard problems. This model can integrate large number of dataset and easily acquire the weight values of various numbers of criteria.

In the present study, five avalanche terrain factors such as slope, elevation, aspect, curvature, and land cover were used as an input to produce the avalanche susceptibility mapping of the study area. The procedure involved various steps such as creating and analyzing the avalanche occurrence terrain factors, generating pairwise comparison matrix, calculating weight values of terrain factors, and producing susceptibility mapping. The avalanche susceptibility map was divided into five susceptibility regions. The results demonstrate that 1% of the area is in very low susceptibility region and 13% of the area is in very high susceptibility region. The results show that GIS-based MCDA-AHP technique is suitable for detecting and locating the avalanche risky zones. This avalanche susceptibility map can help decision-makers and engineers in better planning of infrastructure development, taking precaution while moving across the region, and useful for authorities in disaster management. Considering the dynamic meteorological factors will be beneficial for more accurate and precise avalanche susceptibility mapping of the region.

6. Disclosure statement

The authors declare that there is no potential conflict of interests.

References

[1] S. Kumar, P. K. Srivastava, Snehmani, and S. Bhatiya, “Geospatial probabilistic modelling for release area mapping of snow avalanches,” *Cold Reg. Sci. Technol.*, vol. 165, p. 102813, 2019, doi: 10.1016/j.coldregions.2019.102813.

[2] I. McCammon and P. Hägeli, “An evaluation of rule-based decision tools for travel in avalanche terrain,” *cold Reg. Sci. Technol.*, vol. 47, no. 1–2, pp. 193–206, 2007, doi: 10.1016/j.coldregions.2006.08.007.

[3] D. . McClung and P. Schaerer, *The avalanche handbook*, 3rd ed. Seattle, WA, USA: The Mountaineers Books, 2006.

[4] V. Singh, P. K. Thakur, V. Garg, and S. P. Aggarwal, “ASSESSMENT OF SNOW AVALANCHE SUSCEPTIBILITY OF ROAD NETWORK - A CASE STUDY OF ALAKNANDA BASIN,” *Int. Arch. Photogramm. Remote Sens. Spat. Inf. Sci.*, no. December, 2018, doi: 10.5194/isprs-archives-XLII-5-461-2018.

[5] S. Nasery and K. Kalkan, “Snow avalanche risk mapping using GIS-based multi-criteria decision analysis: the case of Van, Turkey,” *Arab. J. Geosci.*, vol. 14, no. 9, 2021, doi: 10.1007/s12517-021-07112-4.

[6] R. Parshad, P. K. Srivastva, S. Ganguly, S. Kumar, and A. Ganju, “Snow Avalanche Susceptibility Mapping using Remote Sensing and GIS in Nubra-Shyok Basin, Himalaya, India,” *Indian J. Sci. Technol.*, vol. 10(31), no. August, pp. 1–19, 2017, doi: 10.17485/ijst/2017/v10i31/105647.

[7] S. Kumar, P. Kumar, S. Snehmani, L. Oli, and Á. A. Gdem, “Geospatial Modelling and Mapping of Snow Avalanche Susceptibility,” *J. Indian Soc. Remote Sens.*, vol. 46, no. 1, pp. 109–119, 2018, doi: 10.1007/s12524-017-0672-z.

[8] S. Kumar, P. K. Srivastava, and Snehmani, “GIS-based MCDA–AHP modelling

for avalanche susceptibility mapping of Nubra valley region, Indian Himalaya," *Geocarto Int.*, vol. 6049, pp. 1–14, 2017, doi: 10.1080/10106049.2016.1206626.
[9] D. K. Singh, V. Dutta, M. Hemendra, S. Gusain, and N. Gupta, "Geo-spatial Modeling for Automated Demarcation of Snow Avalanche Hazard Areas Using Landsat-8 Satellite Images and In Situ Data," *J. Indian Soc. Remote Sens.*, vol. 47, no. 3, pp. 513–526, 2019, doi: 10.1007/s12524-018-00936-w.
[10] T. L. Saaty and L. G. Vargas, "HIERARCHICAL ANALYSIS OF BEHAVIOR IN COMPETITION: PREDICTION IN CHESS," *Behav. Sci.*, vol. 25, pp. 180–191, 1980.
[11] J. Malczewski, "GIS-based multicriteria decision analysis: A survey of the literature," *Int. J. Geogr. Inf. Sci.*, vol. 20, no. 7, pp. 703–726, 2006, doi: 10.1080/13658810600661508.
[12] L. Selçuk, "An avalanche hazard model for Bitlis Province , Turkey , using GIS based multicriteria decision analysis," *Turkish J. Earth Sci.*, vol. 22(4), pp. 523–535, 2013, doi: 10.3906/yer-1201-10.
[13] C. Ancey, "Snow Avalanches," in *B. Schrefler, P. Delage (Eds.), Environmental Geomechanics*, New York, 2013.
[14] T. Arumugam, S. K. Dewali, and A. Ganju, "Integration of terrain and AVHRR-derived multi-temporal snow cover data for statistical assessment of avalanches : case study of a part of NW Himalaya," *Arab. J. Geosci.*, 2019.
[15] J. Benedikt, "Risk Assessment of Avalanches - a Fuzzy Gis Application," in *Proceedings of 5th international FLINS conference*, 2002, pp. 395–402, doi: 10.1142/9789812777102_0048.
[16] A. Snehmani, A. Bhardwaj, A. Pendit, and A. Ganju, "Demarcation of potential avalanche sites using remote sensing and ground observations : a case study of Gangotri glacier," *Geocarto Int.*, vol. 29, no. 5, pp. 520–535, 2014, doi: 10.1080/10106049.2013.807304.
[17] R. Nagarajan, G. Venkataraman, and Snehmani, "Rule based classification of potential snow avalanche areas," *Nat. Resour. Conserv.*, vol. 2, no. 2, pp. 11–24, 2014.
[18] A. A. Mohammed, H. R. Naqvi, and Z. Firdouse, "An Assessment and Identification of Avalanche Hazard Sites in Uri Sector and its Surroundin on Himalayan Mountain," *J. Mt. Sci*, vol. 12, no. 2, pp. 1499–1510, 2015.
[19] T. Saaty, "The analytic hierarchy process," *New York: McGraw-Hill*. 1980.
[20] T. Saaty, "Decision making with the analytic hierarchy process," *Int J Serv Sci*, no. 1, pp. 83–98, 2008.
[21] D. K. Singh, H. S. Gusain, V. Mishra, N. Gupta, and R. K. Das, "Automated mapping of snow / ice surface temperature using Landsat-8 data in Beas River basin , India , and validation with wireless sensor network data," *Arab. J. Geosci.*, 2018, doi: 10.1007/s12517-018-3497-3.
[22] J. Schweizer, B. Jamieson, and M. Schneebeli, "Snow avalanche formation," *Rev. Geophys.*, 2003, doi: 10.1029/2002RG000123.

Authors Profile

Ahmad Shekib Iqbal received the B.S. degree in Engineering Geodesy from Kabul Polytechnic University in 2015 and M.Sc. degree in Geomatics Engineering, Geodesy and Geographic Information Technologies Program from Gebze Technical University, Turkey in 2020. Currently, he is working as an Assist. Professor in the Department of Geographical Information System, Kabul Polytechnic University, Kabul Afghanistan. His research interests are Geographic Information Systems/Technologies (GIS), Remote Sensing, GIS-Transportation and Surveying Engineering.

Abdullah Naser received an M.Sc. degree in Engineering Geodesy from Moscow Institute of Geodesy, Aerial Surveying and Cartography in 1987. Currently, he is working as a HOD and Professor in the Department of Engineering Geodesy, Kabul Polytechnic University, Kabul Afghanistan. His research interests are Surveying Engineering, Cartography, GPS, and Spherical Geodesy.

KPU International Journal of Engineering & Technology
Volume 3, Issue1, Sep. 2023
e-ISSN:2790-0819, p-ISSN:2790-0800

Date Received: 2023-06-06
Date Accepted: 2023-08-09
Date Published: 2023-09-15

Comparing the Elongation and Tensile capacity of Khan steel Reinforcement bar with the Esfahan and Tashkent companies

AHMAD ZAKER MUDASER[1*], MATIULLAH WAHEDI[2]

[1*]Assistant Professor, Department of Civil Engineering, Al - Beroni University, 1st District, Kapisa, Afghanistan. Email: ahmad.zaker333@gmail.com

[2]Assistant Professor, Department of Theoretical and Applied Mechanics, Kabul Polytechnic University, 5th District, Kabul, Afghanistan. Email: Matiullah.wahedi@kpu.edu.af

Abstract

The present work studies and compares the tensile capacity of reinforcement bar, yield stress, ultimate stress, and elongation of reinforcement bar from different manufacturing companies (Khan Steel, Esfahan and Tashkent). The aims of this investigating is the yield and ultimate stress, tensile capacity, and elongation of steel bars under tensile stress used according to the standard in the members of reinforced concrete buildings. The laboratory test of yield, ultimate stress, and elongation on of reinforcement bar has been performed according to the (ASTM, A615) standard, the obtained result has been compered and the shows the tensile strength does not have a direct effect on the elongation, but in the other hand, tensile capacity, tensile strength and elongation of reinforcement bar considering the (ASTM, A615) standard is acceptable.

Keywords: Elongation, Reinforcement bar, Tensile capacity, Ultimate Stress, Yield Stress.

[*] Corresponding Author

1. Introduction

Reinforcement bar (rebar) is a steel product in the form of rod or cable, which is used to strengthen tensile strength of concrete members. [7].

Steel rebar is a material with high tensile strength, the characteristics of steel rebar make it the best option to combine with concrete and strengthen its tensile strength; for this reason the use of suitable steel rebar in concrete buildings is very important for the stability of the building [7].

Tensile capacity and elongation of steel rebar is called the ability to change longitudinal shape under tensile axial loads, because if additional loads are applied to the buildings, the rebar will significantly change shape, and in this way, they control the way of spreading cracks in concrete[9].

On the other hand, the amount of elongation for the rebar is related to the nominal diameter and tensile capacity.

Investigations about the tensile capacity and elongation which mentioned tool as reinforcement bar show that the same grade of rebar, but produced by different companies, have different capacity and elongations that should be checked before using them in the building structure.

Since the beginning of using rebar in the structure of buildings, various tests have been conducted on reinforcement bar to select the best rebar.

In this research, in order to support the domestic products of Afghanistan and introduce the quality of domestic products to those who use reinforcement bar, a comparison has been made between the tensile capacity and elongation of Khan Steel with Esfahan and Tashkent rebar's.

The results of the tests show that Khan Steel rebar have met the American (ASTM, A615) standard and can be a good alternative, for use in the structure of buildings instead of the aforementioned imported steel rebar's.

2. Experimental Work

2.1. Methods

To test steel rebar, there are different methods in different standards, the most important standards in the world for testing steel rebar are listed below.

- American standard (ASTM).
- German standard (DIN).
- Russian standard (GOST).

In this research, the American standard (ASTM, A615) is used.

2.2. Materials

The reinforcement bar used in the structure members of reinforcement concrete buildings is a steel product that is artificially produced in the factory, the composition of steel reinforcement bar according to (ASTM, A33) standard is 95% to 99% iron along with other chemical elements mentioned in table (1)[3].

Table 1**.** Chemical composition of steel reinforcement bar

Elements	*Minimum amount %*	*Maximum amount %*
Carbon	0.42	0.50
Silicon	---	0.40
Manganese	0.50	0.80
Phosphorus	---	0.03
Sulfur	---	0.035

Chemical elements are used in steel with a specific purpose, the quality and grade of steel reinforcement bar depends on the composition of these elements. As stated below each of the mentioned elements has a specific effect on the formation of steel reinforcement bar[3].

Manganese (MN): this element reduces hardness and increases strength in steel and increases wear resistance[3].

Carbon (c): this element is one of the most important constituents of steel and increases tensile strength, hardness and wear resistance, but reduces ductility in steel[1].

Phosphorus (P): this element increases strength and hardness and improves ductility, yet adds a certain brittleness to the steel.

Silicone (Si): this element increases tensile strength, yield strength of steel[3].

Sulfur (S): this element improves ductility, but without sufficient manganese it causes brittleness in steel[3].

The steel reinforcement bars that have been subjected to this research and their tensile capacity and elongation have been tested are grade 60 in different diameters of 25 mm, 22 mm, 18 mm, 14 mm, 12 mm, and 10 mm, which belong to three production companies (Khan steel, Esfahan and Tashkent).

2.3. Experimental procedure & Model tests

In order to obtain information about the characteristics of steel reinforcement bar and to answer the questions of whether the manufactured steel reinforcement bar meet the desired standard specifications or not, it is necessary to test the characteristics of reinforcement bar, mentioned below[4]:

- Tensile test
- Bending test
- Fatigue test
- Testing in terms of geometric characteristics
- Testing in terms of chemical composition

All the experimental model tests in this research were done in the Sky Geotechnical Material Laboratories. Kabul Afghanistan.

Testing the tensile capacity and elongation of steel reinforcement bar is one of the most important and main tests that must be done for the reinforcement bar [5].

For this purpose, the test of tensile capacity and elongation of steel reinforcement bar was carried out according to (ASTM, A615) standard, according to mentioned standard, 40 cm of steel reinforcement bar were prepared from each sample that was tested and in a laboratory experimental device as shown in figure (1). It is shown to be placed, which is 10 cm from the reinforcement the top knot and 10 cm in the bottom knot of the device and 20 cm in the middle are left free; after that, the device pulls the inserted reinforcement bar with a certain force until it breaks. And this force, which causes tearing, determines the tensile capacity of the tested steel reinforcement bar section.
Later, the tensile capacity determined by the machine for the tested samples for grade 60 reinforcement bar, we compared the results of the tests, with the values mentioned in (ASTM, A615) standard, it was found that all the reinforcement bars that were tested are acceptable to the standard[1].

Figure 1. Steel reinforcement bar tensile experimental machine

3. Result and Discussion

3.1. Laboratory modal tests result

The results of the test conducted on the tested reinforcement bar of three manufacturing companies are shown in figures 2, 3 and 4.

The test result show important things, which include:

- Effective diameter of the reinforcement bar
- Yield stress of reinforcement bar
- Ultimate stress of reinforcement bar
- Elongations of reinforcement bar under tensile axial stress.

SKY GEOTECHNICAL CONSTRUCTION MATERIAL LABORATORIES

Deformed and Plain Carbon-Steel Bars for Concrete Reinforcement
ASTM A615/A 615M -09a

Client:	Alberoni University	Lab. Ref. No.:	SGCL-034/STLT-005
Contractor:	Ahmad Zaker Mudaser	Request No.:	Feb. 005
Project:	Comparison of tensile strength of (Khan Steel) reinforcement bar with imported reinfocement bar (Toshkendi and Isfahani)	Date of Request:	14-Feb-2023
Source:	Khan Steel Mill/Afghanistan	Testing Date:	18-Feb-2023

Sr. No.	Sample No.	Required Grade	Approx Dia	Mass/m.	Pls Dia	Effective Dia	Area	Perimeter	Maximum Average Spacing	Minimum Average Height	Maximum Gap	Yield Load	Ultimate Load	Yield Stress	Ultimate Stress	% Elong	Bend Test	Remarks
			mm	Kg/m	mm	mm	mm^2	mm	mm	mm	mm	kN	kN	Mpa	Mpa	%	180°	
1	STL-01	60	25.0	3.845	87.5	24.80	482.806	79.7	17.5	1.22	9.7	246.79	325.50	511.16	674.18	11.25	OK	Deformed
2	STL-02	60	22.0	3.005	77.0	21.70	369.649	69.7	15.6	1.09	8.6	206.86	273.24	559.61	739.19	10.21	OK	Deformed
3	STL-03	60	18.0	1.972	63.0	17.80	248.719	56.8	12.0	0.83	6.7	113.02	172.11	454.41	691.98	9.52	OK	Deformed
4	STL-04	60	14.0	1.203	49.0	13.97	153.201	40.4	9.7	0.54	5.5	72.89	110.04	475.78	718.27	10.03	OK	Deformed
6	STL-05	60	12.0	0.873	42.0	11.97	112.476	35.3	8.0	0.41	4.1	57.02	79.53	506.95	707.09	12.56	OK	Deformed
6	STL-06	60	10.0	0.521	35.0	9.88	76.627	29.7	6.5	0.38	3.6	51.65	58.46	674.042	762.91	19.50	OK	Deformed

Specification Tensile Strength Yield Strength Elongation	Grade 40 60,000 Psi (420 Mpa) 40,000 Psi (280 Mpa) 10 mm = 11%, More then 10 mm = 12%	Grade 60 90,000 Psi (620 Mpa) 60,000 Psi (420 Mpa) 10 to 19 mm = 9%, 22 to 25 mm=8% More than 25 = 7%	Grade 75 100,000 Psi (690 Mpa) 75,000 Psi (520 Mpa) 19 mm to 25 mm = 7% More than 25mm = 6%	Gauge Length: 8" OG-Fracture outside gauge length

Disclaimer:

Remarks: All Information Provided By The Client Representative.

Tested by:	Mohmmad Nwroz	Lab. Manager:	Aziz Azizi
Client Q.A.:		E-mail:	sgcl.afgco@gmail.com
Coctractor Q.C.:		Date:	

Figure 2. The result of laboratory test (Khan Steel) reinforcement bar

SKY GEOTECHNICAL CONSTRUCTION MATERIAL LABORATORIES

Deformed and Plain Carbon-Steel Bars for Concrete Reinforcement
ASTM A615/A 615M -09a

Client:	Alberoni University	Lab. Ref. No.:	SGCL-034/STLT-005
Contractor:	Ahmad Zaker Mudaser	Request No.:	Feb. 005
Project:	Comparison of tensile strength of (Khan Steel) reinforcement bar with imported reinfocement bar (Toshkendi and Isfahani)	Date of Request:	14-Feb-2023
Source:	IRAN/Isfahan	Testing Date:	16-Feb-2023

Sr. No.	Sample No.	Required Grade	Approx Dia	Mass/m.	Pin Dia	Effective Dia	Area	Perimeter	Maximum Average Spacing	Minimum Average Height	Maximum Gap	Yield Load	Ultimate Load	Yield Stress	Ultimate Stress	% Elong	Bend Test	Remarks
			mm	Kg/m	mm	mm	mm^2	mm	mm	mm	mm	kN	kN	Mpa	Mpa	%	180°	
1	STL-01	60	25.0	3.789	87.5	24.78	482.40	mm	mm	mm	mm	241	322	499.59	667.50	22.5	OK	Deformed
2	STL-02	60	22.0	2.941	77.0	21.26	354.81	69.60	15.30	1.13	8.40	173.9	276.0	490.01	777.91	19.3	OK	Deformed
3	STL-03	60	18.0	1.988	63.0	17.70	245.933	55.3	12.4	0.82	6.6	125.10	192.01	508.68	780.74	10.25	OK	Deformed
4	STL-04	60	14.00	1.220	49.0	13.69	147.120	43.20	9.63	0.58	5.30	80.24	119.12	545.41	809.69	15.66	OK	Deformed
5	STL-05	60	12.00	0.937	42.0	12.00	113.040	34.90	8.16	0.47	4.46	71.20	96.88	629.87	857.04	16.29	OK	Deformed
6	STL-06	60	10.0	0.520	35.0	9.55	71.594	29.7	6.5	0.38	3.6	53.23	60.57	743.498	846.02	17.50	OK	Deformed

Specification Tensile Strength Yield Strength Elongation	Grade 40 60,000 Psi (420 Mpa) 40,000 Psi (280 Mpa) 10 mm = 11%, More then 10 mm = 12%	Grade 60 90,000 Psi (620 Mpa) 60,000 Psi (420 Mpa) 10 to 19 mm = 9%, 22 to 25 mm=8% More than 25 = 7%	Grade 75 100,000 Psi (690 Mpa) 75,000 Psi (520 Mpa) 19 mm to 25 mm = 7% More than 25mm = 6%	Gauge Length: 8" OG-Fracture outside gauge length

Disclaimer:

Remarks: All Information Provided By The Client Representative.

Tested by:	Mohammad Nwroz	Lab. Manager:	Aziz Azizi
Client Q.A.:		E-mail:	sgcl.afgco@gmail.com
Codtractor Q.C.:		Date:	

Figure 3. The result of laboratory test (Isfahan) reinforcement bar

SKY GEOTECHNICAL CONSTRUCTION MATERIAL LABORATORIES

Deformed and Plain Carbon-Steel Bars for Concrete Reinforcement
ASTM A615/A 615M -09a

Client:	Alberoni University	Lab. Ref. No.:	SGCL-034/STLT-005
Contractor:	Ahmad Zaker Mudaser	Request No.:	Feb. 005
Project:	Comparison of tensile strength of (Khan Steel) reinforcement bar with imported reinfocement bar (Toshkendi and Isfahani)	Date of Request:	15-Feb-2023
Source:	Uzbekistan/(Toshkendi)	Testing Date:	16-Feb-2023

Sr. No.	Sample No.	Required Grade	Approx Dia	Mass/m.	Pls Dia	Effective Dia	Area	Perimeter	Maximum Average Spacing	Minimum Average Height	Maximum Gap	Yield Load	Ultimate Load	Yield Stress	Ultimate Stress	% Elong	Bend Test	Remarks
			mm	Kg/m	mm	mm	mm^2	mm	mm	mm	mm	kN	kN	Mpa	Mpa	%	180°	
1	STL-01	60	25	3.7270	87.50	24.58	474.566	69.1	15.5	1.12	8.5	211	328	444.617	691.158	17.8	OK	Deformed
2	STL-02	60	22.0	2.992	77.0	21.50	362.866	69.4	15.4	1.10	8.4	169.16	265.65	466.18	732.09	11.84	OK	Deformed
3	STL-03	60	18.0	1.893	63.0	17.60	243.162	52.7	12.1	0.83	6.7	116.95	177.34	480.96	729.31	12.25	OK	Deformed
4	STL-04	60	14.0	1.218	49.00	13.71	147.550	43.20	9.63	0.58	5.30	77.73	120.18	526.80	814.50	15.25	OK	Deformed
5	STL-05	60	12.0	0.828	42.0	11.61	105.812	34.1	7.9	0.44	4.3	54.77	79.26	517.62	749.07	12.41	OK	Deformed
6	STL 06	60	10.0	0.579	35.0	9.60	72.3456	29.7	6.7	0.35	3.1	38.09	60.87	526.501	841.378	11.68	OK	Deformed

Specification Tensile Strength Yield Strength Elongation	Grade 40 60,000 Psi (420 Mpa) 40,000 Psi (280 Mpa) 10 mm = 11%, More then 10 mm = 12%	Grade 60 90,000 Psi (620 Mpa) 60,000 Psi (420 Mpa) 10 to 19 mm = 9%, 22 to 25 mm=8% More than 25 = 7%	Grade 75 100,000 Psi (690 Mpa) 75,000 Psi (520 Mpa) 19 mm to 25 mm = 7% More than 25mm = 6%	Gauge Length: 8" OG-Fracture outside gauge length

Disclaimer:

Remarks: All Information Provided By The Client Representative.

Tested by:	Mohmmad Nwroz	Lab. Manager:	Aziz Azizi
Client Q.A.:		E-mail:	sgcl.afoco@gmail.com
Codtractor Q.C.:		Date:	

Sky Geo Technical Construction Material Laboratory

Figure 4. The result of laboratory test (Tashkent) reinforcement bar

3.2. Effective diameter

Reinforcement bars are manufactured according to (ASTM, A615) standard in specific approximate diameters from 6 mm to 50 mm. but the approximate diameters are different from the actual diameter of the reinforcement bar, the diameter that shows the size of the reinforcement after the manufacturing is called the effective diameter[5].

The effective diameter should be obtained by careful testing. And this effective diameter is considered by the designer engineer in the design of building members.

One of the parts of this research which is effective in the tensile capacity and elongation of the reinforcement bar is to get the effective diameter of the rebar.

This research, whose experimental models are made of the approximate diameters of the rebar's of 25mm, 22mm,18mm, 14mm, 12mm and 10mm, after testing the models, obtained the effective diameters of the rebar's and showed them in the table 2 and figure 5.

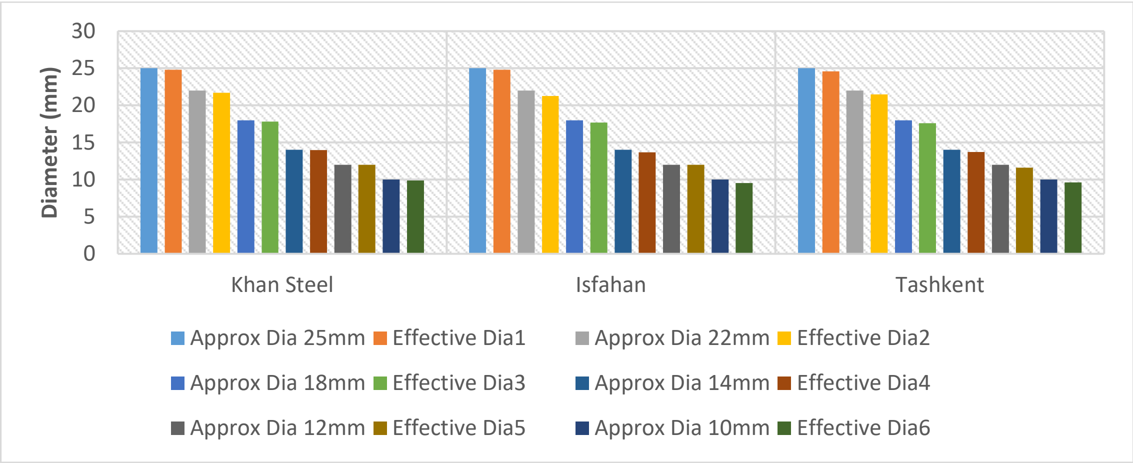

Figure 5. Approximate and effective diameters of the tested models reinforcement bars

Table 2. Approximate and effective diameters of the tested models reinforcement bars

Khan Steel	*Approximate Diameter*	25	22	18	14	12	10
	Effective Diameter	24.80	21.70	17.80	13.97	11.97	9.88
Isfahan	*Approximate Diameter*	25	22	18	14	12	10
	Effective Diameter	24.78	21.26	17.70	13.69	12	9.55
Tashkent	*Approximate Diameter*	25	22	18	14	12	10
	Effective Diameter	24.58	21.50	17.60	13.71	11.61	9.60

Values in figure 5. and table 2, shows the result of laboratory testing of specific models, that the reinforcement bars produced by khan steel company have larger effective diameters than the reinforcement bars produced by (Isfahan and Tashkent) companies; this indicates a better feature of (Khan steel) reinforcement bars.

3.3. Yield stress of reinforcement bar

The yield stress represents the maximum force that can be applied without causing permanent deformation in steel; this properties are one of the good features of steel[11]. Point B in figure 6, shows the location of the yield stress.

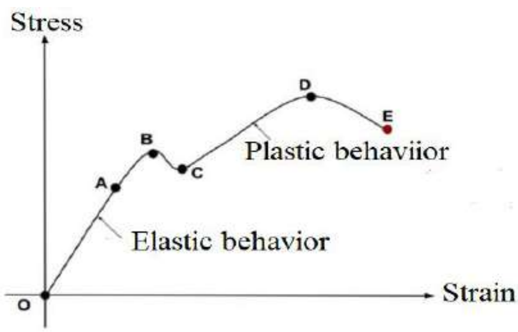

Figure 6. Stress and strain curve

According to (ASTM, A615) standard, the yield stress of grade 60 reinforcement bars is 420 Mpa. However, the tested models can be acceptable when they have a minimum yield stress of 420 Mpa[1].
In this research, all the tested, models meet the yield stress required in the (ASTM, A615) standard, which is shown in figure 7 and table 3.

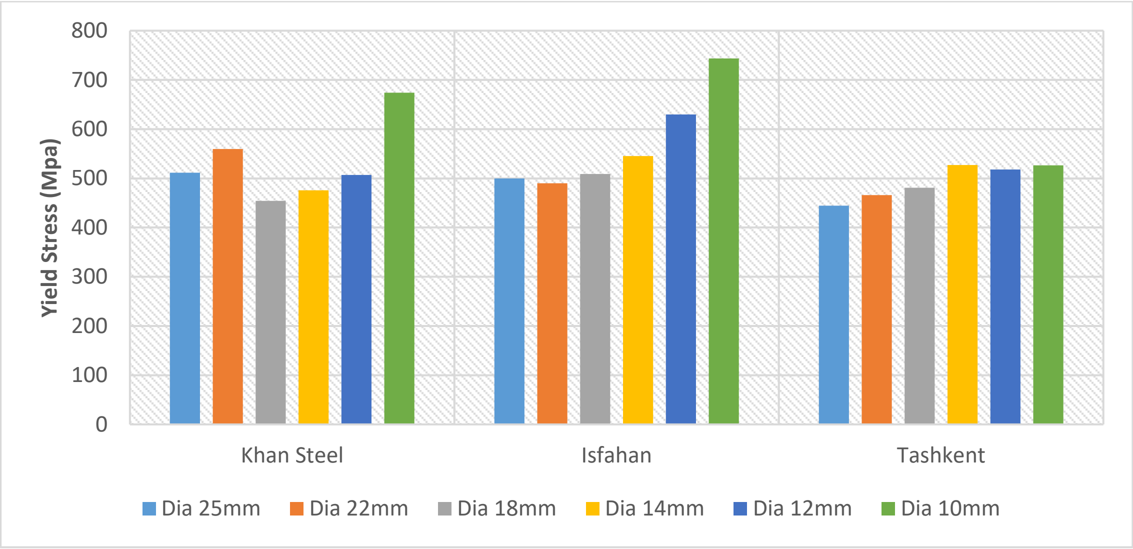

Figure 7. Yield stress of tested models

Table 3. Yield stress of tested models

Diameter (mm)		25	22	18	14	12	10
Khan Steel	*Yield Stress (Mpa)*	511.16	559.61	454.41	475.78	506.95	674.042
Isfahan	*Yield Stress (Mpa)*	499.59	490.01	508.68	545.41	629.87	743.498
Tashkent	*Yield Stress (Mpa)*	444.617	466.18	480.96	526.80	517.62	526.501

values in figure 7. and table 3, shows the result of laboratory testing of specific models, that the reinforcement bars produced by Khan steel company have better yield stress in some cases and similar yield stress in some cases compared to the reinforcement bars produced by (Isfahan and Tashkent) companies, and it should be remembered that Isfahani 10 mm diameter reinforcement bar shows excellent yield stress among reinforcement bar from two other companies.

3.4. Ultimate stress of reinforcement bar

The maximum force that steel tolerates before failure is called ultimate stress. After the yield point, with increasing stress, the strain increases and the material exhibits plastic behavior, Point D in figure 6. Shows the location of the ultimate stress[8].
According to (ASTM, A615) standard, the ultimate stress of grade 60 reinforcement bars is 620 Mpa. However, the tested models can be acceptable when they have a minimum ultimate stress of 620 Mpa[1].
In this research, all the tested models meet the ultimate stress required in the (ASTM, A615) standard, which is shown in figure 8 and table 4.

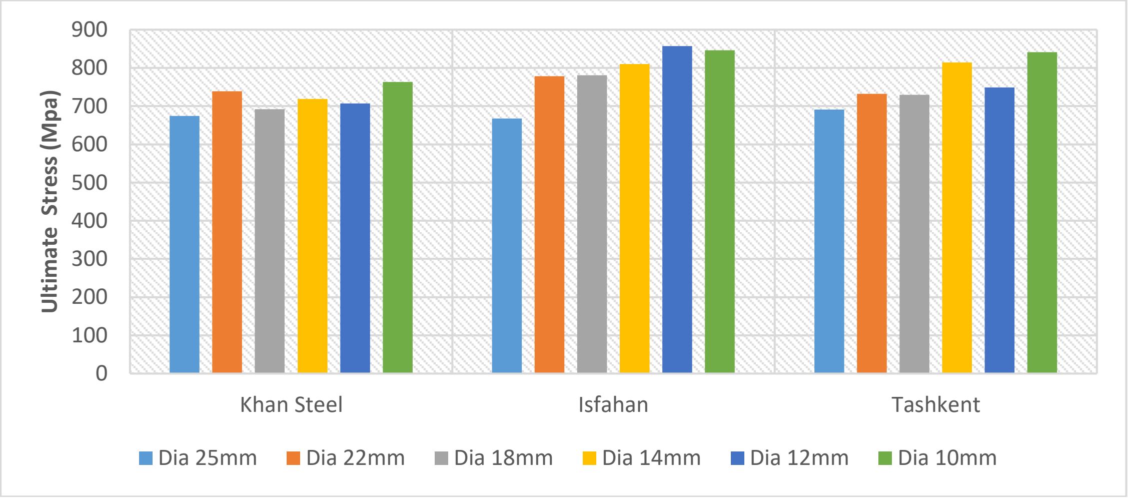

Figure 8. Ultimate stress of tested models

Table 4. Ultimate stress of tested models

Diameter (mm)		25	22	18	14	12	10
Khan Steel	*Ultimate Stress (Mpa)*	674.18	739.19	691.98	718.27	707.09	762.91
Isfahan	*Ultimate Stress (Mpa)*	667.50	777.91	780.74	809.68	857.04	846.02
Tashkent	*Ultimate Stress (Mpa)*	691.158	732.09	729.31	814.50	749.07	841.378

Values in figure 8. and table 4, shows the result of laboratory testing of specific models, that the reinforcement bars produced by khan steel company have better ultimate stress in some cases, similar ultimate stress in some cases and lower ultimate stress in some cases compared to the reinforcement bars produced by (Isfahan and Tashkent).

3.5. Elongation

Elongation refers to the ability to change longitudinal shape under tensile axial loads[2]. The part that can be seen in figure 3, steel after ultimate stress, it has a decrease in width and an increase in length; and finally it breaks at a point where the stress is less than the ultimate stress; this point is called failure stress, shows in figure 9&10[8].

Considering the above, research has shown that steels have different elongation, and this elongation changes due to their physical, chemical and mechanicals properties.

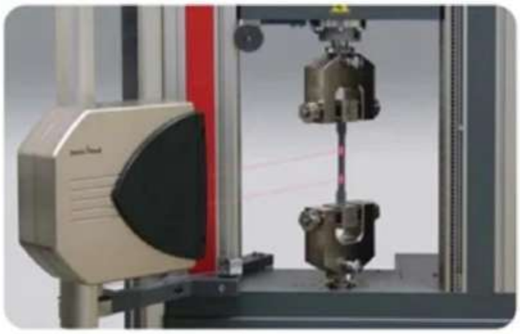

Figure 9. Reinforcement bar in the state of stretching under the experimental machine

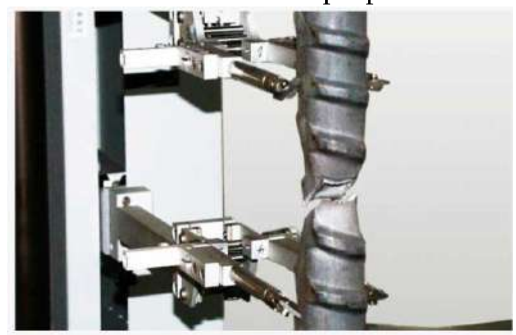

Figure 10. Reinforcement bar is broken due to tensile axial load under the experimental

Research's show that the greater the longitudinal deformability; in case of applying additional loads on reinforcement concrete buildings, the steel reinforcement bars are significantly deformed, thus preventing the spread of cracks in concrete [6].

(ASTM, A615) standard has determined the minimum elongation of grade 60 steel reinforcement bar according to the diameter of the reinforcement bar as follows: reinforcement bars with a diameter of 10 mm to 19 mm have minimum elongation of 9%, reinforcement bars with a diameter of 22 mm to 25 mm have minimum elongation of 8% and reinforcement bars more than diameter of 25 mm have minimum elongation of 7%[1].

In this research, all tested models, meet the percentage of minimum elongation required in the (ASTM, A615) standard, which is shown in figure 11 and table 5.

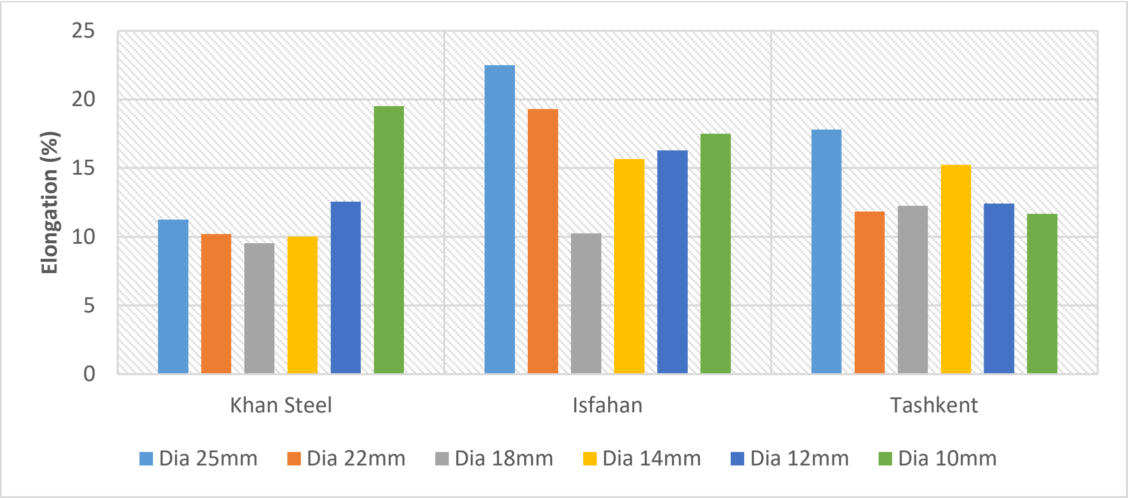

Figure 11. Elongation of tested models

Table 5. Elongation of tested models

Diameter (mm)		25	22	18	14	12	10
Khan Steel	*Elongation (%)*	11.25	10.21	9.52	10.03	12.56	19.50
Isfahan	*Elongation (%)*	22.5	19.3	10.25	15.66	16.29	17.50
Tashkent	*Elongation (%)*	17.8	11.84	12.25	15.25	12.41	11.68

Values in figure 11. And table 5, which shows the result of laboratory testing of specific models, that the reinforcement bars produced by Isfahan Company have better elongation compared than the reinforcement bars produced by (Khan Steel and Tashkent) companies. But elongation of the reinforcement bars of the other two mentioned companies also meet the (ASTM, A615) standard.

4. Conclusion

The testing of the tensile capacity and elongation of the reinforcement bar, which was performed on the tested models from three reinforcement manufacturing companies (Khan Steel, Esfahan and Tashkent), considering the (ASTM) standards, the results of the models testing were acceptable, and it can be used in the structure of the buildings. Also, considering the results of the research, the following points can be mentioned:

- The reinforcement bars produced by Khan Steel Company have more effective diameter than the reinforcement bars produced by the other two mentioned companies.
- In diameters 25 mm and 22 mm, the yield stress of reinforcement bars produced by Khan Steel Company is better, and in diameters 18 mm, 14 mm, 12 mm and 10 mm the yield stress of reinforcement bars produced by Isfahan Company is better. But production reinforcement bars of all three company meet the (ASTM, A615) standard requirement in terms of yield stress.
- The ultimate stress of the reinforcement bars produced by all three companies (Khan Steel, Isfahan and Tashkent) is suitable.

- The elongation of reinforcement bars to produce by Isfahan Company is better. But production reinforcement bars of all three company meet the (ASTM, A615) standard requirement in terms of elongation.
- Khan Steel, as a construction material produced in Afghanistan, can have a good competition in terms of quality with imported steel (Esfahan and Tashkent).

5. Suggestion

After studies and research on the tensile capacity and elongation of the reinforcement produced by Afghanistan, (Khan Steel) and the imported reinforcement that are widely used in Afghanistan such as (Esfahan and Tashkent) reinforcement, the following suggestions can be made:

- Conducting unbiased research by experts and professionals in the field of quality of domestic products.
- The use of domestic products, especially the production of construction materials, because on the one hand it has good quality and on the other hand it has direct impact on economical growth of the country.
- Bringing such research and accurate information to people about better quality of building materials in every possible way.

6. Acknowledgement

I would like to express my gratitude to the professors of Kabul Polytechnic University who have increased the effectiveness and quality of this scientific article with their review and guidance.

References

[1] ASTM A615, Standard Specification for Deformed and Plain Carbon-Steel Bars for Concrete Reinforcement, American Society for Testing and Materials. (2015).

[2] ASTM E8 / ASTM E8M, Standard &Specimens for Metals Tensile Test, American Society for Testing and Materials. (2022).

[3] ASTM A33, Methods of Chemical Analysis of Plain Carbon Steel, American Society for Testing and Materials. (2006).

[4] ASTM A255, Standard Test Methods of Hardenability of Steel, American Society for Testing and Materials. (2007).

[5] ASTM A359, Methods and Definitions for Mechanical Testing of Structural Steel, American Society for Testing and Materials. (2005).

[6] B. Saikia, J. Thomas, A. Ramaswamy, and K. S. N Rao, Performance of rebars as longitudinal reinforcement in normal strength, pp. 857-864, 2005.

[7] Catarina, s.s.(2012). Steel And Concrete Composite Building Structures: star Book services.

[8] Ferdinand P. Beer; E. Russell Johnston; John T. Dewolf, Mechanics of materials, Fourth Edition, pp. 29-36, 2009.

[9] Firoz, A.S., Indian Steel: critical Details, Evolving Structure and Strategic Option, Steel business Briefing, UK. (2007).
[10] L. Lam and J. G. Teng, Strength models reinforced, Journal of Structural Engineering, vol. 128, no. 5, pp.600-605, 2002.
[11] R. C. Hibbeler, Mechanics of materials, Eighth edition, pp.65-69, 2011.

Authors Profile

AHMAD ZAKER MUDASER received his B.Sc. degree in Civil Engineering from Al-Beroni University in 2014, and he obtained his M.tech. Degree in Structural Design from the Maharshi Dayanand University Rohtak, India, in 2018. He is a faculty member of the Civil Engineering Department of Al-Beroni University, Kapisa, Afghanistan. His area of research is Structural Engineering.

MATIULLAH WAHEDI received his B.Sc. degree in Civil Engineering from Al-Beroni University in 2012, and he obtained his master's degree in Structural Design from the Kabul Polytechnic University, in 2021. He is a faculty member of Theoretical and Applied Mechanics Department of Kabul Polytechnic University. His area of research is Earth quake Engineering.

KPU International Journal of Engineering & Technology
Volume 3, Issue1, Sep. 2023
e-ISSN:2790-0819, p-ISSN:2790-0800

Date Received: 2023-03-16
Date Accepted: 2023-08-29
Date Published: 2023-09-15

Climate Change Impacts and Surface Water Accessibility Analysis in the Ghorband Sub River Basin, Afghanistan

MUJEEBULLAH MUJEEB[1*], KAWOON SAHAK[2], LUTFULLAH SAFI[3], MUJIBURAHMAN AHMADZAI[4], SHARIFULLAH PEROZ[5]

[1*]Assistant Professor, Department of Natural Resources Management, Faculty of Environment, Kabul University, Kart-e-Sakhi, Kabul 1001, Afghanistan. Email: mujeebmujeebullah1401@ku.edu.af

[2]Assistant Professor, Department of Environmental science, Faculty of Environment, Kabul University, Kart-e-Sakhi, Kabul 1001, Afghanistan. Email: sahak@ku.edu.af

[3]Assistant Professor, Department of Natural Resources Management, Faculty of Environment, Kabul University, Kart-e-Sakhi, Kabul 1001, Afghanistan. Email: lutfullahsafi7@gmail.com

[4]Assistant Professor, Department of Natural Resources Management, Faculty of Environment, Kabul University, Kart-e-Sakhi, Kabul 1001, Afghanistan. Email: Mujib.ahmadzai@gmail.com

[5]Assistant Professor, Disaster Management, Faculty of Environment, Kabul University, Kart-e-Sakhi, Kabul 1001, Afghanistan. Email: sharifbuarki@gmail.com

Abstract

In this study, impacts of climate change on surface water of the Ghorband Sub-River basin are assessed Ghorband River is located in the Ghorband watershed, which is a part of Afghanistan's Kabul River basin. Numerous communities live within the Ghorband Sub-River Basin, and its surface water assets have been the establishment of their jobs for numerous eras. Climate change impacts, water challenges, hydrological assessment purposes, and long-term hydro meteorological information were analyzed. The cruel yearly temperature has steadily expanded and conversely precipitation and River flow release have slowly diminished. The natural corruption and resultant climatic and characteristic calamities have profoundly influenced the vocation and prosperity of the communities inside this River basin with respect to water, horticulture, and biological system life. In conclusion, the trends show that the hydrology of the basin changed significantly over the last decades. There is not considerable instability due to the data scarcity and gaps in the data, but all results indicate a strong tendency towards different conditions.

Keywords: Water accessibility, Climate change impacts, Trend analysis, River discharge, Ghorband

* Corresponding Author

1. Introduction

Surface water is one of the most important resources of fresh water in every region, and it is very important to investigate the effect of climate change on it. This study aimed to quantify possible climate change impacts on surface water resources in the Ghorband sub-River basin. However, over the last three decades of war and a series of droughts have caused many problems [2]. This research has assessed the hydrological regime of the Ghorband River as well as the quantity of Ghorband River water based on physical parameters, based on which was understood by us. The changes in the River flow of the Ghorband River and also compare the physical parameters of the Ghorband River with international standards, two issues that are closely linked to the impacts of climate change on surface water [2]. The quantity of the Ghorband River is important for the agriculture of Parwan province, the livelihoods of Parwan and Kabul residents, as well as the River flow of the Kabul River basin. After the information gathering on the theoretical basis of the subject and the research, the required data on the water discharge of the Ghorband River sub-basin was acquired [2]. The impacts of climate change on surface water are based on the premise that each landowner has equal rights to the surface water resource below his or her property. There will be cases where one person or entity owns multiple parcels and requests that the total water allotment below all of his or her parcels be considered in the Phase I climate change impacts on surface water [3]. Determining the total threshold based on multiple parcels is acceptable; however, to protect future property owners, certain safeguards must be in place to ensure that the water allotment and transfer between parcels are clearly documented and recorded, especially in cases where the water from more than one parcel will ultimately serve a single parcel [3]. After the analysis, it is inferred that the hydrological regime of the Ghorband River is at an alarming level because there is a huge decline in the annual water discharge, surface run-off, and precipitation [4]. The decline in water discharge due to climate change and the increasing population of Ghorband is an issue of great concern because it will affect every aspect of Ghorband citizens' lives in this research the main objective is the investigation of climate change impacts on the temporal and spatial distribution of precipitation, temperature, and surface runoff in the ghorband Sub-River basin [5].

2. Study Area

2. 1. Ghorband Sub-River Basin

The Ghorband River may be a River in Afghanistan, flowing through the Parwan Territory. It could be a tributary of the Panjshir River, at that point, a sub-tributary of the Indus River, at that point, the Kabul River. Appropriately, Ghorband River joins Panjshir River in the Bagrami locale. The Ghorband runs completely in Parwan province, where it gave its title to the Ghorband Locale. It is born within the eastern Shibar Pass (which interfaces the territories of Parwan and

Bamyan, or watersheds of the Ghorband and Kunduz Rivers) and passes on an eastward course, which it keeps up all the way through most of its course[6]. It runs along the south and the forced central extent of the Hindu Kush, accepting meltwater within the Shibar Pass area of Salang [7]. It Rivers from this in a long valley between the tall peaks of the Hindu Kush (north) and Koh-i-Baba in the south. At that point, it focalizes on the Panjshir, on its right bank, 10 kilometers east of Charikar. It flows through the areas of Sheik Ali, Chinwari, Ghorband, and Surkh Parsa[8].The Ghorband gets numerous tributaries from both left and right, all bolstered basically by snowmelt in spring and summer. Its primary tributary is the Turkman, but the Salang River meets on the cleared out bank, and its valley is a critical get to course to the pass and towards the northern half of the nation. The Salang merges with the Ghorband in the region of Jabal Saraj [9].

2.1.1. Provincial Profile of Ghorband Sub-River Basin

The territory is situated 64 km to the north of Kabul. Charikar, Parwan's common capital, is one of the finest places in the nation for exchange. Inundated farmland of high quality and a distinctive horticulture with noteworthy cultivation and animal generation supplement conventional field crops. The topography of Parwan is composed of the Ghorband River and the Panjshir River. It is a mountainous province with the Kott-I-Baba Range in the southwest, the Panjshir Range in the north, and the Paghman Range in the southeast [10].

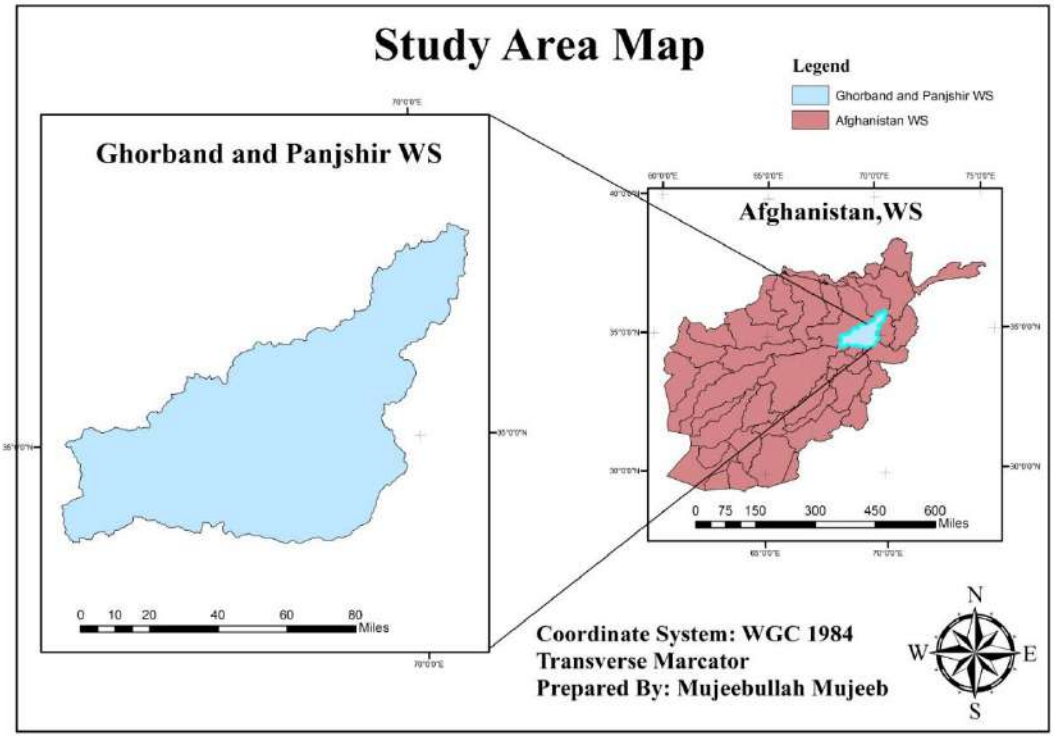

Figure 1: Study area map of Ghorband River Basin

River valleys are prominent and crops are rain fed around the Charikar district, which includes many vineyards and gardens. The majority of the territory is usable as rangeland, with some areas of intense irrigation [9]. In Ghorband and Shinwari districts, there is snow all year round. There are controversial views regarding the exact number of residents and total area of the province, but local sources are of the opinion that Parwan has a total area of 5,715 square kilometers with a total population of 600,000 individuals. Tajik, Pashtun, Hazara, Turkman, and Pashai tribes reside in the province in as many as 1,322 villages. The residents of Kohi Safi are Pashtun, Tajik in Salangare, Turkman, Tajik, Sadaat, and Hazara in Surkh Parsa, Shikh Ali Hazara. The rest of the districts have a mixed population of the tribes [11].

3. Climate

Precipitation and temperature are very heterogeneous in the Ghorband Sub-River Basin due to its large range in elevation. Based on the Köppen–Geiger climate classification scheme, the Kabul River Basin is mainly characterized by a mid-latitude steppe climate (Bsk, cold semi-arid climate), with some areas experiencing a Mediterranean-influenced subarctic climate [12].The Figure2 presents the mean monthly weather average for the recent decade (2008–2022) mean monthly weather average, recorded at Ghorband Sub-River stations. The data was provided from the Afghanistan Meteorological Department [12].

Between 2008 and 2022, the annual minimum, maximum, and average temperatures have had a gradual decline. The maximum air temperature had its highest value of 36.4°C in 2008 and its lowest value of 31.8°C in 2013, whereas its value in 2022 stood at 38.1°C.

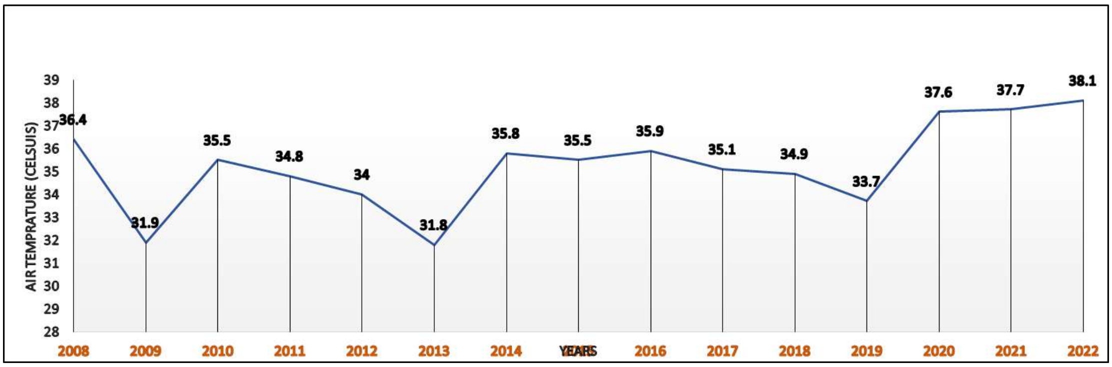

Figure 2: Max Annual Air Temperature (Pul-i-Ashawa station), (2008-2022)

In addition, the minimum air temperature had its highest value of 0.3 in 2008 and its lowest value of -9.3 in 2012.

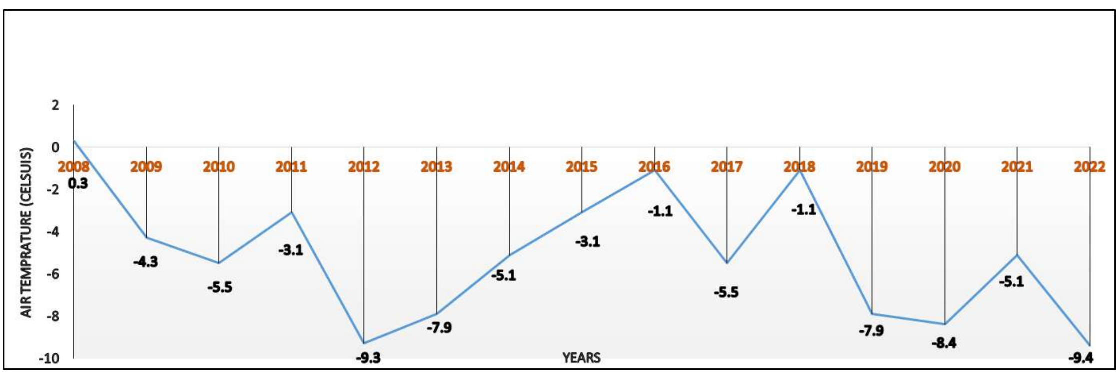

Figure 3: Min, Annual Air Temperature (Pul-i-Ashawa station), (2008-2022)

Besides, the average air temperature had its highest value of 19.5 °C in 2008 and its lowest value of 13.4°C in 2012, whereas its value in 2022 stood at 16.6°C, which indicates a gradual decline in the air temperature [13].

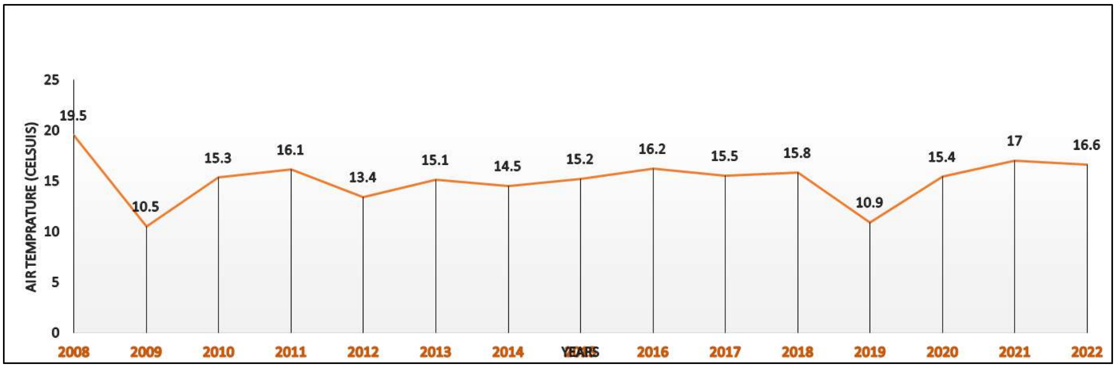

Figure4: Average annual air temperature (Pul-i-Ashawa station), (2008-2022)

4. Hydrology

The Ghorband and Panjshir Sub-River Basin and their tributaries are located in the north of the Kabul basin in Afghanistan. The upper part of the Ghorband River is characterized by high mountains and steep valleys. In the upper part, the Ghorband River is fed by rainfall, snow, and small glaciers. The output of this part of the Parvan plain catchment area is the branches of Golbahar, Shtel, Salang, Ghorband, and other The narrow strip of land covers the water. There are water measuring stations in this area: Shatel, Baghlallah, Pol-e Ashavah, and Shokhi. This sub-area's hydrological stations' average annual flow is presented [14]. Hydrological station Shokhi It is located almost at the exit of this part of the catchment. Most of the water required for consumption, irrigation, drinking and industry in the Parwan plain is from surface water sources of groundwater (deep wells, semi-deep, karezes and springs) provided. Up River, channels are generally narrow and deep and flow throughout the whole year. The runoff regimes are largely controlled by snow-melt, with high discharge from April to June and only close to glaciers in the upRiver parts of the catchment. The small glaciered area has significant influence on the flow regime [15].

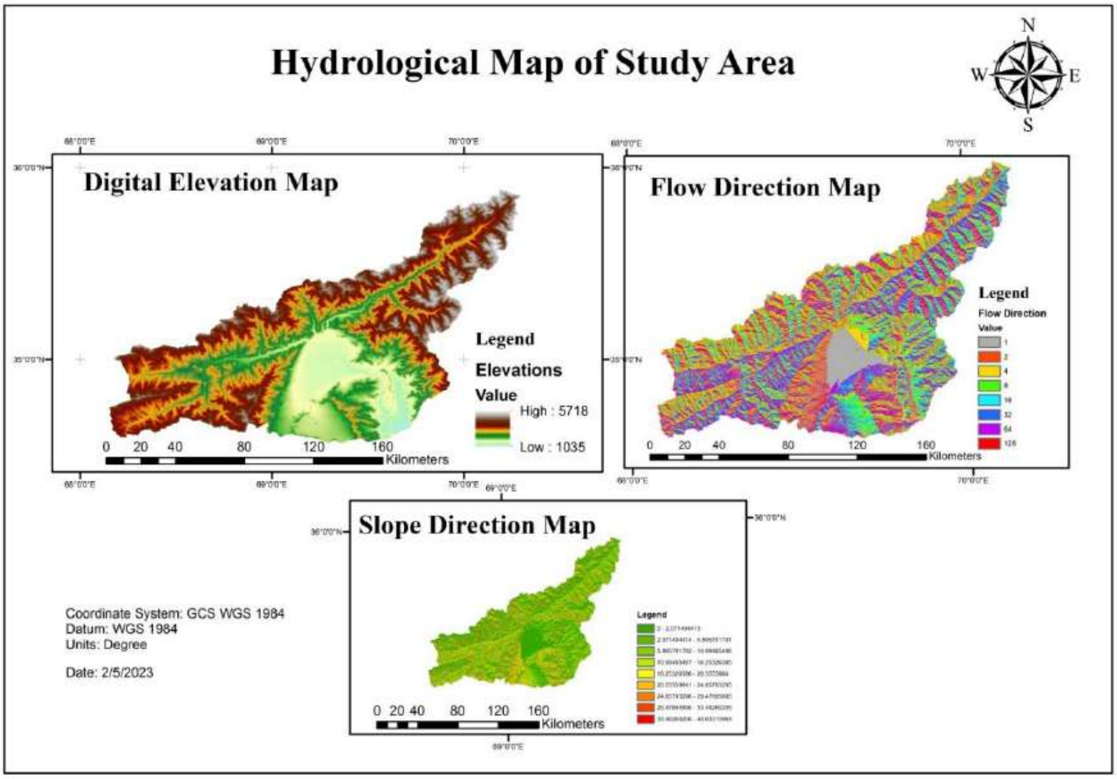

Figure 5: Hydrological map of Ghorband Sub-River Basin

5. Martials and Methods

Based on the data of Pul-i-Ashawa station of the Ghorband River acquired from the Ministry of Energy and Water (MEW), the hydrological regime of the Ghorband River can be assessed in two different time periods. This data is the Annual Mean Water Discharge (m^3/sec) of Pul-i-Ashawa Station between 1960-1980 and 2009-2022. In addition, the physical parameters of Ghorband River water were assessed using the available devices. The Ghorband and Panjshir sub-River basins include the northern heights of the Kabul basin, which has a discharge It is suitable and a large part of the current is required by the downRiver parts, including the flow. It provides access to Naghlo and Sorobi dams. Eastern parts of Panjshir in the range of Pamir Heights have permanent refrigerators and generally a wetter and colder diet. Compared to the western parts of Panjshir, The area of the Ghorband and Panjshir sub-basins is 12963.7 square kilometers, which becomes 1296370 hectares. The Ghorband and Panjshir sub-basins and their tributaries are located in the north of the Kabul basin. The output of this part of the Parvan plain catchment area is the branches of Golbahar, Shtel, Salang, Ghorband, and other The narrow strip of land covers the water [18].

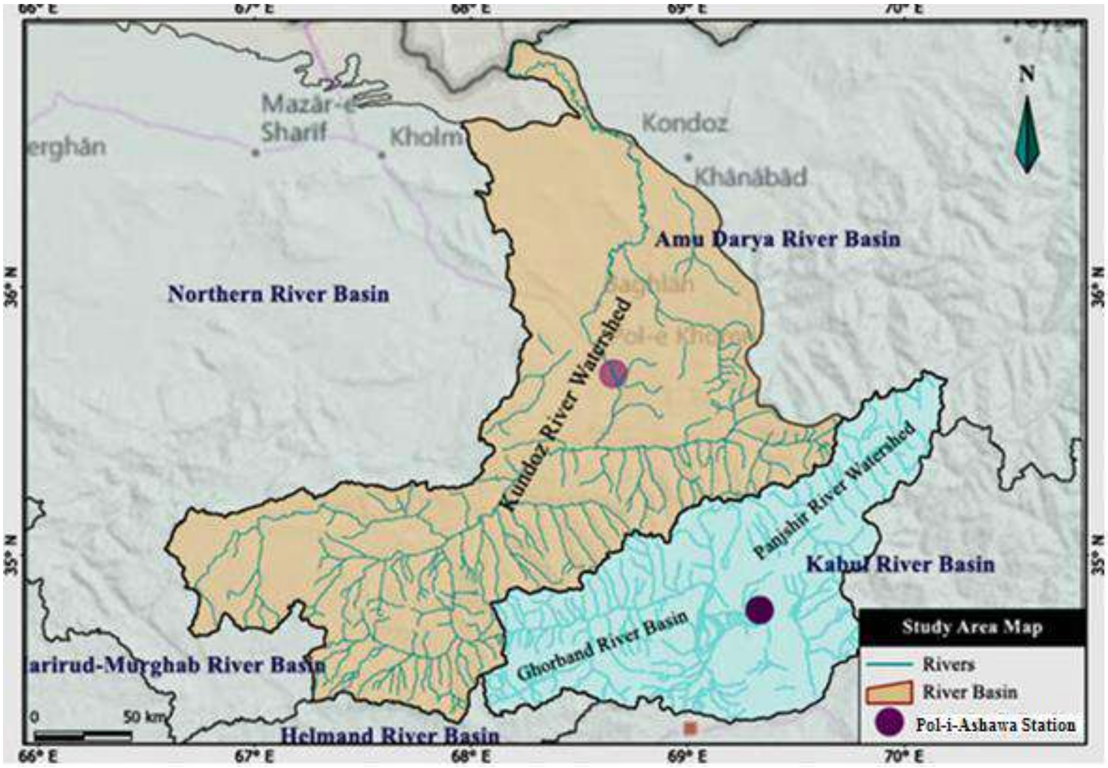

Figure 6: Location map of Pul-i-Ashawa station

5.2. Trend Analysis for Temperature, Precipitation and River Discharge

Linear trends in the time series were analyzed using Excel for trend analysis. It was chosen because it has higher power for non-normally distributed data, which is common in hydrological and meteorological data. Each element is compared with its successors and ranked as larger, equal, or smaller [19].

6. Results

6.1. Change in Precipitation and discharge (Figure 7).

Between 2009 and 2023, the most extreme precipitation had its most elevated esteem of 13 mm in 2012 and its reduced esteem of 1.86 mm in 2023, which appears to be extraordinary variances in one year after another. However, the total precipitation had its highest value of 619 mm in 2020 and its lowest value of 81 mm in 2023, the yearly add up to precipitation, in spite of the increment in most extreme precipitation, has had an incredible continuous decrease.

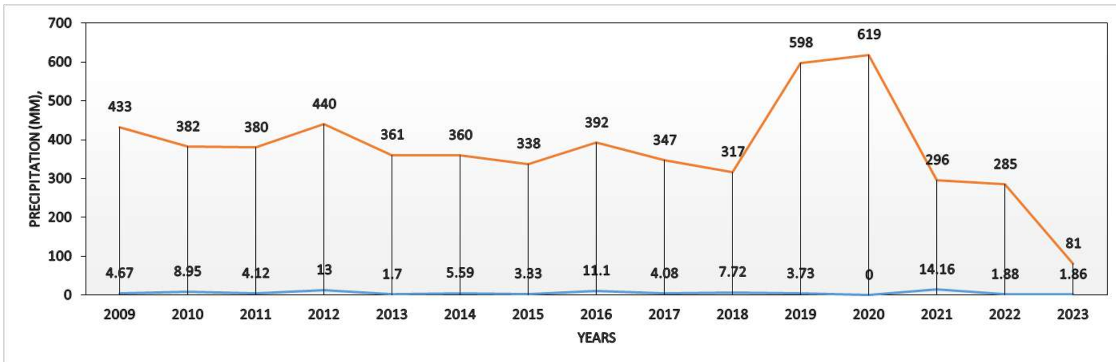

Figure 7: Max and total of precipitation from 2009-2023

As can be seen in the figure, the maximum annual water discharge has had an extremely fluctuating status. There has been a great deal of change in the amount of water discharge which indeed indicates an unstable status of hydrological regime. Specifically, the highest value of maximum annual discharge was 161m^3/sec in 1967, and the lowest value of maximum annual discharge was 63.2m^3/sec in 1974. But if we look at its overall trend, the maximum annual water discharge has declined considerably (Figure 7). In addition, the minimum annual water discharge value has also had a declining trend. Specifically, the highest value of minimum annual water discharge was 10.8m^3/sec in 1961 and its lowest value was 1m^3/sec in 1979. However, it has suddenly soured in 1980 to 11 m^3/sec which also shows the extremity and fluctuation.

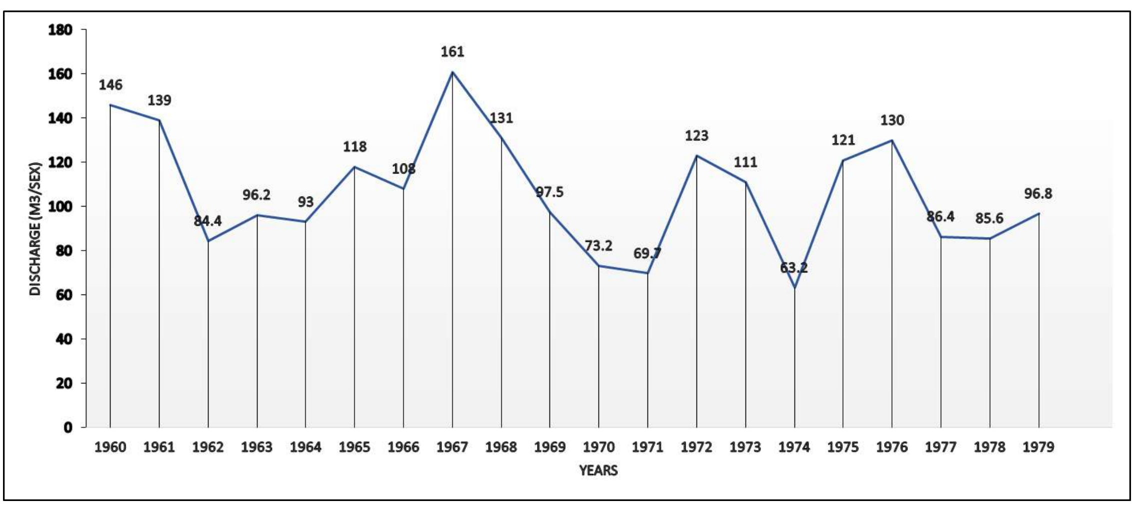

Figure 8: Max annual water discharge from 1960-1979

The mean annual water discharge had its highest value of 36.8m^3/sec in 1960 and its lowest value of 12.5m^3/sec in 1971.

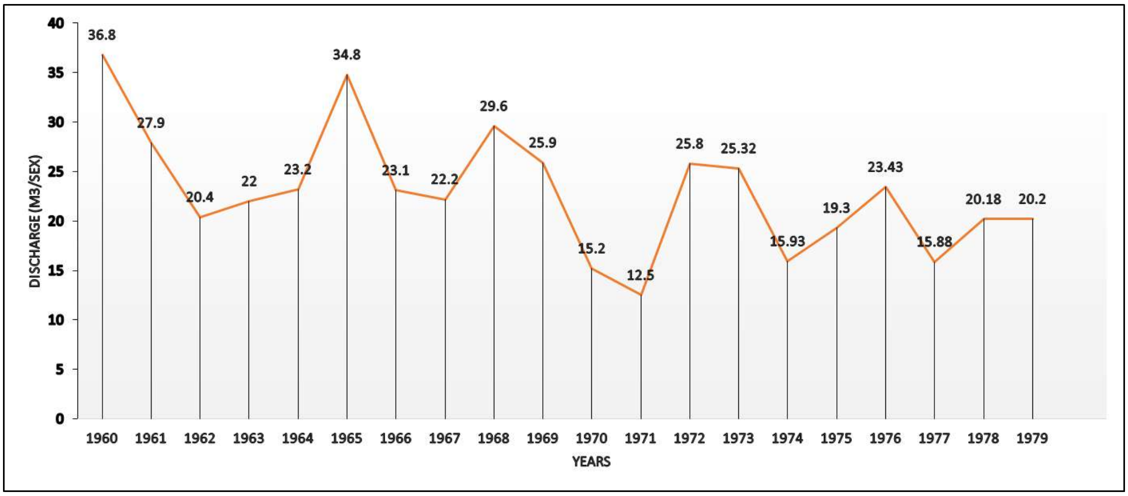

Figure 9: Mean annual water discharge from 1960-1979

As depicted, the overall trend of minimum annual water discharge also has a declining status. Coming to the mean annual water discharge, it also had a similar fluctuating status like maximum annual water discharge (Figure9).

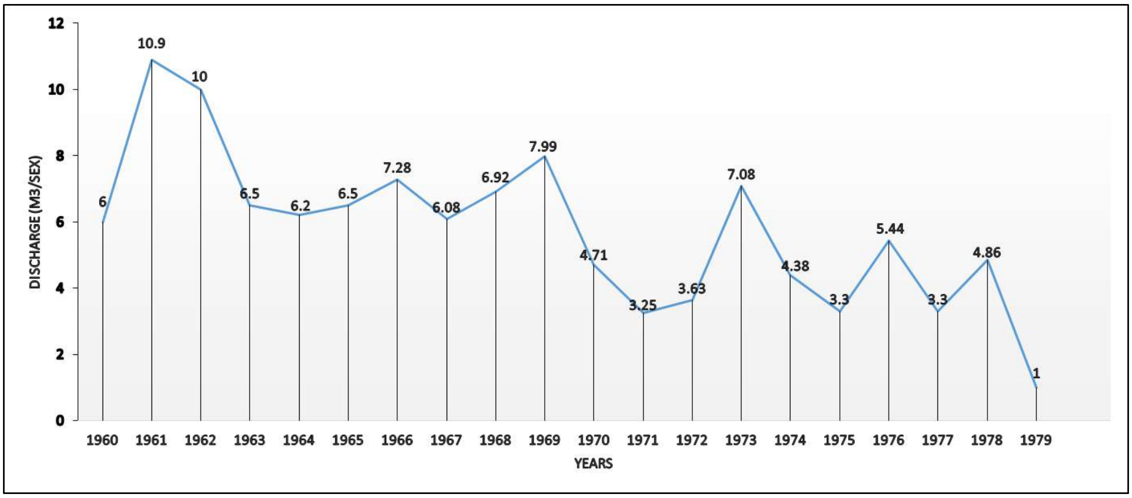

Figure 10: Min annual water discharge from 1960-1979

As can be seen, the mean annual water discharge also has a declining status in addition to the fluctuation (Figure 10).

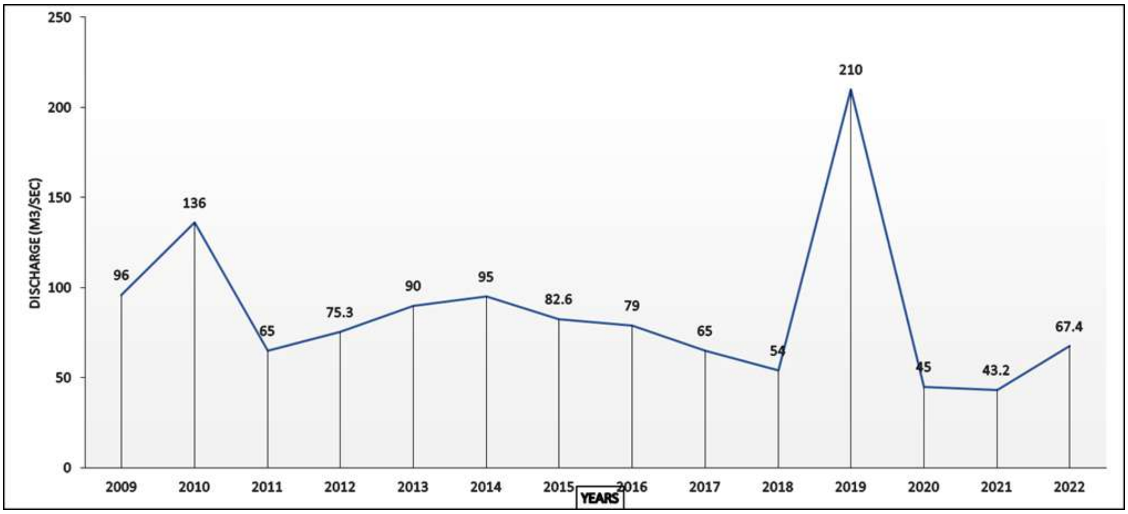

Figure 11: Max annual water Discharge from 2009-2022

As can be seen in figure 10 the maximum annual water discharge had a very dramatic and alarming decline between the years 2009 and 2022.

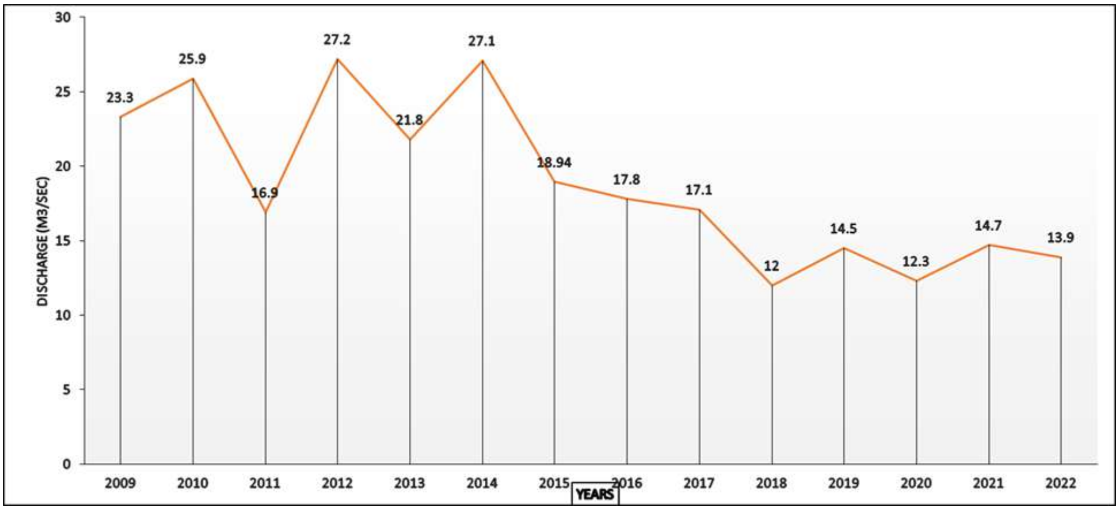

Figure 12: Mean annual water discharge from 2009-2022

The highest value of maximum annual water discharge was 210m^3/sec in 2019, followed by a drastic decline of 45m^3/sec in 2020. However, the lowest value of maximum annual water discharge stood at67.4 m^3/sec in 2022. It can be inferred from (Figure 12) that the maximum annual water discharge has declined continually, which is really concerning.

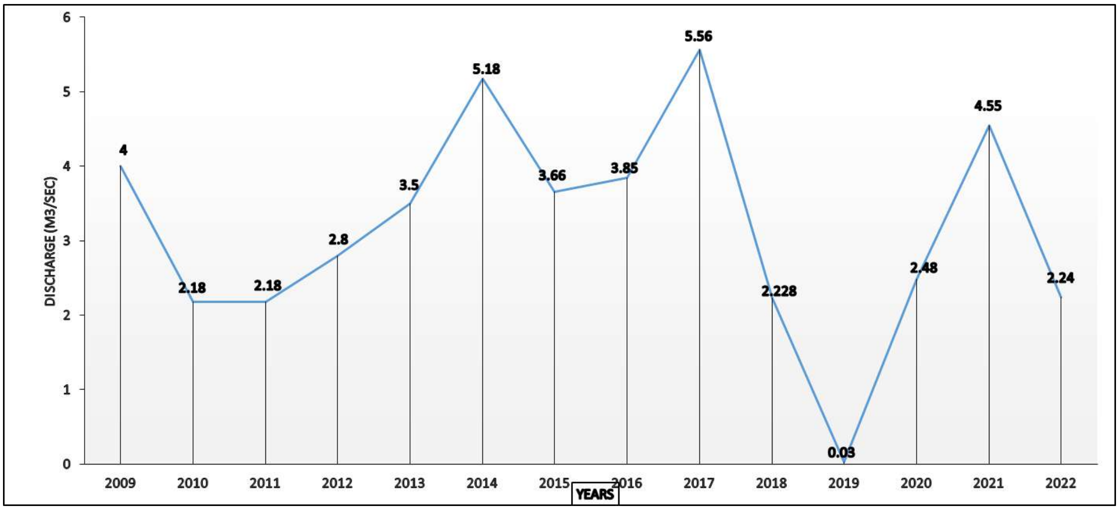

Figure 13: Min annual water discharge from 2009-2022

In addition, the minimum annual water discharge has also declined, as has the maximum annual water discharge (Figure 13).

6.2. Change in annual Run-off

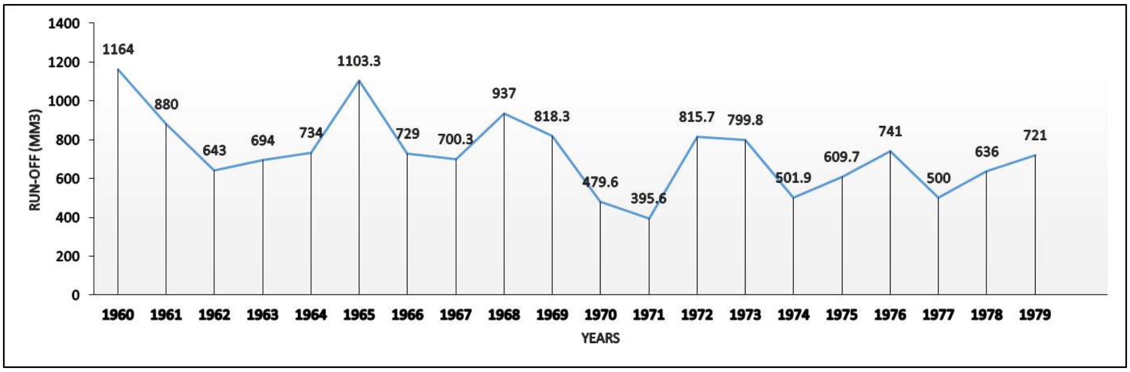

Figure 14: Annual run-off from 1960-1979

Between 1960 and 1979, the annual run-off had its highest value (Figure 14), 1164 MCM, in 1960 and its lowest value, 395.6 MCM, in 1971, whereas the mean run-off value in these years stood at 730.2 MCM.

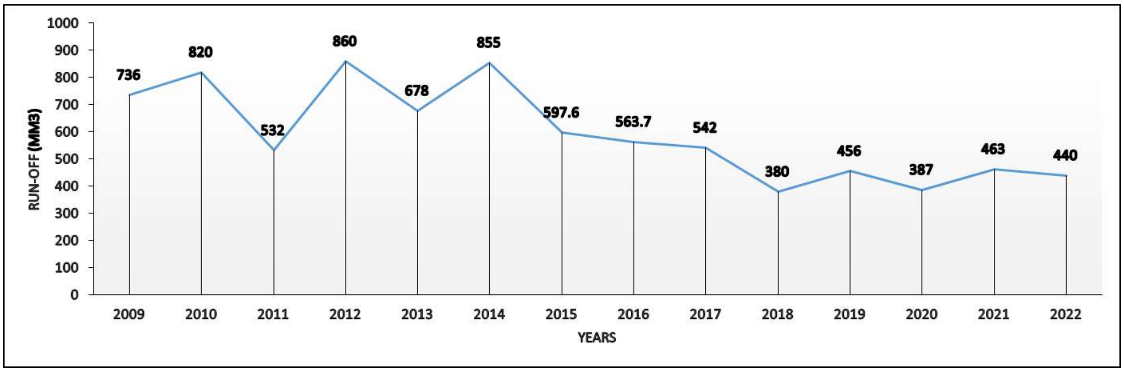

Figure 15: Annual run-off from 2009-2022

Between 2009 and 2022, the annual run-off had its highest value, 860 MCM, in 2012 and its lowest value, 380 MCM, in 2018, whereas the mean run-off value in these years stood at 440 MCM (Figure 15).

7. Discussion

In addition, the study explains that the yearly discharge of the Ghorband Sub-River basin is sufficient for developing the watershed if the water resources are managed in an integrated and sustainable way. The down part of the Ghorband Sub-River basin covers a wide area with large agriculture potential, for example through multiple cropping through irrigation. At the same time, the down River part of the Ghorband Sub-River basin is very vulnerable to flash floods and droughts, which affect the livelihood and socio-economic well-being of the community living within the watershed deeply. Therefore, integrated water resources management is key for agricultural development, livelihoods, and the local economy. Measures like reforestation could reduce the risk of flash floods and droughts. Other measures, which have proven their effectiveness for many catchments in a developing context, could include guidelines on best practices, the establishment of a River basin council, and adapted community-based participation approaches. Using approaches that involve communities directly in management and decision-making processes, we can collectively improve the socioeconomic and livelihoods of the people living in the Ghorband Sub-River basin. However, a comprehensive IWRM strategy is still missing for Afghanistan, and particularly for the Ghorband Sub-River basin. Therefore, it’s hoped that the results of this study will contribute to informing sustainable water resource development and watershed management. In conclusion, this study argues for the establishment of an Integrated Water Resources Management Plan for the Ghorband Sub-River basin to trigger as for the mean annual water discharge, it also had a similar fluctuating status to the maximum annual water discharge. The mean annual water discharge had its highest value of

36.8m3/sec in 1960 and its lowest value of 12.5m^3/sec in 1971. As can be seen, the mean annual water discharge also has a declining status in addition to the fluctuation. In addition, the data from the recent years (2009–2022) of the Pul-i-Ashawa station indicated that the maximum annual water discharge had a very dramatic and alarming decline between the years 2009–2022. The highest value of maximum annual water discharge was 210m^3/sec in 2019, followed by a drastic decline of 43.2m^3/sec in 2021.

However, the lowest value of maximum annual water discharge stood at 67.4m^3/sec in 2022. It can be inferred that the maximum annual water discharge has declined continually, which is really concerning. In addition, the minimum annual water discharge has also declined, as has the maximum annual water discharge. The minimum annual water discharge had its highest value of 5.56 m^3/sec in 2017 and its lowest value of 2.18 m^3/sec in 2011, whereas its value in 2022 stood at 2.34 m^3/sec.

However, the overall trend of the minimum annual water discharge depicts a fluctuating status between 2009 and 2022. Pertinently, if we look at the mean annual water discharge, it has a declining status as well. It had its highest value of 27.2m^3/sec in 2012 and its lowest value of 12m^3/sec in 2018, whereas its value in 2022 stood at 13.9. As can be seen, it has continually declined in the years mentioned. Pertinently, the data analyzed regarding the Pul-i-Ashawa station of the Ghorband River showed that the annual run-off of the Ghorband River has declined alarmingly. As the annual run-off had its highest value of 1164 MCM in 1960-1980, and based on the recent years' data, 2009–2022, it had its highest value of 860 MCM. It can easily be seen that there is a decline of 309 MCM in the highest value of the run-off, which is a really alarming reduction. And if we consider the mean run-off, there has been a decline of 73.8 MCM.

The data analyzed regarding Pul-i-Ashawa station on the Ghorband River in recent years (2008–2022) showed that the annual minimum, maximum, and average temperatures have also had a gradual increase. The maximum air temperature had its highest value of 36.4°C in 2008 and its lowest value of 31.8°C in 2013, whereas its value in 2022 stood at 38.1°C. In addition, the minimum air temperature had its highest value of 0.3 in 2008 and its lowest value of -9.3 in 2012. Besides, the average air temperature had its highest value of 19.5°C in 2008 and its lowest value of 13.4°C in 2012, whereas its value in 2022 stood at 16.6°C, which indicates a gradual decline in the air temperature, which indicates a gradual decline in the air temperature, but this decline is not as alarming as it is a small value of decline.

Moreover, the maximum precipitation had its highest value of 14.16 mm in 2021 and its lowest value of 1.7 mm in 2013, which shows extreme fluctuations in one year after another. However, the total precipitation had its highest value of 619 mm in 2020 and its lowest value of 285 mm in 2022, whereas the mean annual total precipitation stood at 285 mm. As can be seen, the annual total precipitation, despite the increase in maximum precipitation, has had a great gradual decline, which is indeed really concerning.

8. Conclusions

The data analyzed regarding Pul-i-Ashawa station of the Ghorband River showed that the maximum annual water discharge has had an extremely fluctuating status between 1960 and 1980. There has been a great deal of change in the amount of water discharged, which indeed indicates an unstable status of the hydrological regime. Specifically, the highest value of maximum annual discharge was 161m^3/sec in 1967 and the lowest value of maximum annual discharge was 63.2m^3/sec in 1974. But if the overall trend looked by us, the maximum annual water discharge has declined considerably. In addition, the minimum annual water discharge value has also had a declining trend. Specifically, the highest value of minimum annual water discharge was 10.8m3/sec in 1961 and its lowest value was 1 m^3/sec in 1979. However, it suddenly soured in 1980 to 11 m^3/sec, which also shows the extremity and fluctuation. As depicted, the overall trend of minimum annual water discharge also has a declining status. Despite the potential limitations of this type of approach, this is a first step towards the assessment of future projected changes in surface water resources in ghorband Sub-River basin, which needs to be complemented by other studies comparing different hydrological and climate models.

9. Data Availability

The data used to support the findings of this research are available from the Corresponding author upon request.

10. Conflicts of Interest

The authors declare that they have no conflicts of interest regarding the publication of this paper.

11. Acknowledgments

The authors are extremely grateful from the Afghanistan National Meteorological Services Agency for providing climate data and the Ministry of Water and Energy (Afghanistan) for providing water resource data.

References

[1] J. A. Gore, J. Banning, A. F. Casper et al., River Resource Management and the Effects of Changing Landscapes and Climate, pp. 295–312, Wiley, Hoboken, NJ, USA, 2016.

[2] International Federation of Red Cross and Red Crescent Societies. Emergency Plan of Action Operation Update Afghanistan: Drought and Flash Floods. 2020, Volume 2. Available online: https://www.ifrc.org (accessed on 21 September 2020).

[3] Zarrineh, N., & Abad, M. A. N. (2014). Integrated water resources management in Iran : Environmental , socio-economic and political review of drought in Lake Urmia. 6(1), 40–48. https://doi.org/10.5897/IJWREE2012.0380

[4] Nesheim, I., Mcneill, D., Joy, K. J., Manasi, S., Thi, D., & Nhung, K. (2010). The challenge and status of IWRM in four River basins in Europe and Asia. 205–221. https://doi.org/10.1007/s10795-010-9103-9

[5] T. Estrela, M. P´erez-Martin, and E. Vargas, "Impacts of climate change on water resources in Spain," *Hydrological Sciences Journal*, vol. 57, no. 6, pp. 1154–1167, 2012.

[6] S. Huang, Q. Huang, J. Chang, and G. Leng, "Linkages between hydrological drought, climate indices and human activities: a case study in the Columbia River basin,"*International Journal of Climatology*, vol. 36, no. 1, pp. 280–290, 2016.

[7] Mahmoodi, Sultan" Integrated water resources management," Porand Publication, vol. 2, pp. 24–34, 1396.

[8] P. Dey and A. J. Mishra, "Separating the impacts of climate change and human activities on Riverflow: a review of methodologies and critical assumptions," *Journal of Hydrology*, vol. 548, pp. 278–290, 2017.

[9] Mahmoodi, Sultan" Integrated water resources management," Porand Publication, vol. 1, pp. 20–36, 1396..

[10] G .Bala, K . Caldeira and R .Nemani," Fast versus slow response in climate change: implications for the global hydrological cycle," *Climate dynamics.Comp.,* vol. 35, Iss: 2, pp 423-434,Aug 2010.

[11] R. S. Teegavarapu, M. Tufail, and L. Ormsbee, "Optimal functional forms for estimation of missing precipitation data," *Journal of Hydrology*, vol. 374, no. 1-2, pp. 106–115, 2009.

[12] Ghulami, M. Assessment of Climate Change Impacts on Water Resources and Agriculture in Data-Scarce Kabul Basin. Université Côte d'Azur 2018, 146.Available online: https://tel.archives-ouvertes.fr/tel-01737052 (accessed on 22 September 2020)., vol. 38, no. 2, pp. 776–793, 2018.

[13] R. S. V. Teegavarapu, "Missing precipitation data estimation using optimal proximity metric-based imputation, nearestneighbour classification and cluster-based interpolation methods," *Hydrological Sciences Journal*, vol. 59, no. 11,pp. 2009–2026, 2014.

[14] Afghanistan Meteorological Department. Available online: http://www.amd.gov.af/ (accessed on 13 February 2020).

[15] K. H. Hamed and A. R. J. J. Rao, “A modified Mann-Kendall trend test for autocorrelated data,” *Journal of Hydrology*, vol. 204, pp. 182–196, 1998.
[16] A. Tilmant, R. Kelman," A stochastic approach to analyze trade-offs and risks associated with large-scale water resources systems," Water Resour Res., vol.43, pp 43, june 2007.
[17] H. Mann, “Nonparametric tests against trend,” *Econometrica*, vol. 13, pp. 245–259, 1945.
[18] E . Kolokytha and C .Skoulikaris ," WRM and EU policies to adapt to climate change- Experience from Greece *Climate Change-Sensitive Water Resources Management*," *1st ed.*, Ed. London: CRC Press, 2020, pp.1-23.
[19] S. Yue, P. Pilon, and G. Cavadias, “Power of the Mann- Kendall and Spearman’s rho tests for detecting monotonic trends in hydrological series,” *Journal of Hydrology*, vol. 259, pp. 254–271, 2002.
[20] E. Nikzad Tehrani, H. Sahour, and M. J. Booij, “Trend analysis of hydro-climatic variables in the north of Iran,” *theoretical and Applied Climatology*, vol. 136, pp. 85–97, 2019.
[21] R. S. Teegavarapu, M. Tufail, and L. Ormsbee, “Optimal functional forms for estimation of missing precipitation data,”*Journal of Hydrology*, vol. 374, no. 1-2, pp. 106–115, 2009.

Authors Profile

Mujeebullah Mujeeb received the B.Sc degrees in Civil Engineering from Nangarhar University in 2015 and M.Sc degrees in Water Resources and Environmental Engineering from Polytechnic University of Kabul in 2019. Presently, He is working as Assistant Professor in the Department of Natural Resources Management, Faculty of Environment, Kabul University, Kabul Afghanistan. His areas of research include Natural Resources Management, Applied Hydrology and Energy Resources.

Kawoon Shak received the B.S. degrees in Environmental Protection and Disaster Management from Kabul University in 2013 and M.Sc degrees in Environmental Engineering and Management from Asian Institute of Technology (AIT) in 2018. Presently, He is working as Senior Teaching Assistant in the Department of Environmental Science, Faculty of Environment, Kabul University, Kabul Afghanistan. His areas of research include Solid Waste Management, Wastewater Treatment and Pollution Control.

Dr. Lutfullah Safi received the B.Sc. degrees in Plant Science from Al-Beroni University in 2008 and M.Sc. degrees in Biological Diversity from Punjab Agricultural University, Punjab, India, in 2014. He hold his Ph.D. in Agronomy from Sam Higginbottom University of Agriculture, Technology and Sciences (SHUATS), Uttar Pradesh, India, in 2017. Presently, He is Assistant Professor in the Department of Natural Resources Management, Faculty of Environment, Kabul University, Kabul, Afghanistan. His research interests include Biodiversity, Food Security, Agricultural Risk Management and Natural Resource Conservation.

Mujib Rahman Ahmadzai was born on September 15, 1987, in Mohammad Agha District, Logar, Afghanistan. He graduated from Zarghoon Shahr High School. After passing the Kankor Exam (a Nationwide Test for University Entrance in Afghanistan), he joined the Faculty of Agriculture at Alberoni University in 2005 and graduated in 2008. After passing a competitive exam, he earned Islamic Development Bank (IsDB) scholarship and was accepted by University Putra Malaysia (UPM), Malaysia, for his Master's. He took his Master degree in Land Resource Management in 2015. After completing his M.Sc., he returned to Afghanistan and joined the Department of Natural Resources Management Faculty of Environment, Kabul University as a lecturer in December 2016. In March 2020, he enrolled in a Ph.D. program in Forest Management and Ecosystem Science at the Faculty of Forestry and Environment, Universiti Putra Malaysia.

Sharifullah Peroz received the B.S. degrees in Environmental protection and Disaster management in 2015 at Kabul University. Currently, He is working as Assistant Professor in the Department of Disaster Management, Faculty of Environment, Kabul University, Kabul Afghanistan. His areas of research include Disaster Management, Environmental Protection and Climate change.

KPU International Journal of Engineering & Technology
Volume 3, Issue1, Sep. 2023
e-ISSN:2790-0819, p-ISSN:2790-0800

Date Received: 2023-04-16
Date Accepted: 2023-09-02
Date Published: 2023-09-15

Evaluation of Asphalt Mixtures Containing Rejuvenated Reclaimed Asphalt Pavement

KAMALUDDIN KAMAL[1*], MUJTABA AMIN[2]

[1*]Assistant Professor, Faculty of Engineering, Kandahar University, 9th District, Kandahar, Afghanistan. Email: engkamalkamaluddin@gmail.com

[2]Assistnt Professor, Faculty of Transportation Engineering, Kabul Polytechnic University, 5th District, Kabul, Afghanistan. Email: m.amin@kpu.edu.af

Abstract

Reclaimed asphalt pavement (RAP), which is produced from the milling of old asphalt pavement, is one of the most widely recycled materials in the world. The use of reclaimed asphalt pavement (RAP) in freshly hot mixed asphalt (HMA) can save on material costs, preserve energy, and protect the environment. Asphalt mixtures that contain a lower amount of RAP can result in a similar performance to conventional mixtures. However, the use of a high percentage of RAP in hot mix asphalt (HMA) mixtures is limited due to the effect that it has on fatigue and low temperature properties of the mixture. To overcome the adverse effect of the RAP, it is sometimes necessary to rejuvenate the aged binder. This study has the objective of exploring the effect of two commercially available asphalt rejuvenators on the mechanical properties of RAP modified HMA mixture. Six different types of asphalt mixtures, including control mixture, RAP-modified mixture, and rejuvenated RAP mixtures were prepared. The mechanical properties of the mixtures were determined by the Marshall tests. The results of the study indicated that the properties of RAP mixtures were mainly affected by the rejuvenator percentage while the type of rejuvenator statistically has no significant effect. The Marshall test results also indicated that, the addition of 6% soybean and 3% sunflower to the 40% RAP mixture has similar properties values as the control mixture. According to the results of the indirect tensile strength test, it was found that the RAP mixtures with 3% rejuvenator has higher moisture resistance as compared to the 6% rejuvenator. In addition, the sunflower rejuvenator had more pronounced effect on the asphalt mixture properties than that of soybean rejuvenator.

Keywords: Reclaimed Asphalt Pavement, Asphalt binder rejuvenator, Vegetable-oils, Marshall tests.

---

[*] Corresponding Author

1. Introduction

1.1 Study Background

Over the past few decades, asphalt pavement has been widely used around the world due to its better performance, and comfortable driving conditions. As asphalt pavement is subjected to loads and environmental conditions, it loses its strength and deteriorates. It is common practice in asphalt pavement maintenance to mill part of the top layer and replace it with new one. Once these deteriorated parts of the pavements are milled, crushed and removed, they are called reclaimed asphalt pavement (RAP). It is reported that each year, millions of tons of asphalt pavement are milled globally from the road surfaces after being exposed to the long-term effects of climate change and increased traffic loads [1 – 4]. In Europe alone, more than 50 million tons of old asphalt pavement are milled annually [5]. In the USA, the Federal Highway Administration (FHWA) reported that 45 million tons of RAP are produced annually, most of which are dumped in landfills [6]. As a result of the excessive amount of old asphalt pavement being disposed in landfills, the need to increase the use of RAP in the hot mix asphalt (HMA) mixture has continued [7-8]. Besides diverting tons of waste asphalt pavement from landfills, it has been proven that the use of RAP saves on construction materials, and provides significant environmental benefits. Because of these substantial economic and environmental benefits, many countries started the use of RAP in the production of new asphalt mixtures [9-13]. In the United States, it was reported that 66.7 million tons of RAP were used in pavement construction in 2011[14]. Furthermore, according to the European Asphalt Pavement Association (EAPA), 47% of the produced RAP is used in asphalt applications in Europe each year [15].

1.2 The Use of RAP in Afghanistan

RAP is now recycled to a great extent in many countries as a component of HMA asphalt mixtures, however, it is still not frequently used in Afghanistan. After two decades of war when the Islamic Emirate of Afghanistan retook control of Afghanistan in 2021, the government focus more on the rebuilding the existing highways in this country. It is reported that millions of tons of old asphalt pavement are milled annually from the road surfaces in Afghanistan, most of which ends up in landfills. As a result, efforts have been made in this study to assess the feasibility of utilizing a high percentage of old asphalt materials in the production of new hot mix asphalt (HMA). This may result in increased raw material conservation as well as reduction of overburden pressure on landfills and aggregate quarries.

1.3 Problem Statement

It has been demonstrated from the previous researches that RAP collected from old road surfaces still contain valuable materials, including recycled aggregates and a recycled binder, which are materials that can be utilized to create fresh HMA mixtures. However, due to the significant impact that RAP material has on the stiffness of the mixture as a whole, the use of a high percentage of RAP in the production of fresh HMA is restricted because of the increased stiffness, it is sometimes necessary to modify or rejuvenate the aged asphalt binder. Using a modifier to rejuvenate aged asphalt binder may be an option for incorporating high RAP into the fresh HMA mixture [16]. An aged binder rejuvenation is designed to provide a mix capable of resisting fatigue cracking while maintaining permanent deformation resistance [17-21]. Various manufacturers propose different types of rejuvenating agents to rejuvenate aged binder in asphalt mixtures. Among the many rejuvenators available, waste engines and cooking oils are the most commonly used rejuvenators. In contrast, waste oils have been reported with high viscosity and high moisture content, leading to decreased asphalt mixture moisture resistance [22-23]. On the other hand, bio-based vegetable oil is another potential source for rejuvenating aged binders [24]. According to [25-26] the use of a vegetable oil to rejuvenate RAP aged binders can reduce fatigue cracking susceptibilities. Rejuvenators can improve aged binder properties such as binder's brittleness; however, if not used in a proper amount, it can have an adverse effect on the mixture performance. Thus, it is important to emphasize that for a given amount of RAP, the rejuvenator rate should be selected in the optimum percentages to create a mix that is highly resistant to fatigue cracking while maintaining an adequate level of permanent deformation.

1.4 Study Objectives

In order to achieve a mixture with properties similar to those of new paving materials, the RAP recovered binder should be rejuvenated [10]. There have been several types of rejuvenators developed for the asphalt recycling industry so far, most of which have an oily base due to the issue that the RAP recovered binder lacks the oily components of the old asphalt pavement binder over the service life [27]. Rejuvenators can improve RAP recovered binder properties such as binder's binding and adhesion properties. However, if these rejuvenators are not used in a proper amount, they can have an adverse effect on the mixture properties. Thus, the primary objective of the study was to determine and compare the effect of two vegetable-based rejuvenators on the properties of HMA using the Marshall practice in asphalt pavement maintenance and rehabilitation.

2. Experimental Program

2.1 Materials

A brief overview of the materials used in this study is given in the following subsections.

2.1.1 Neat Binder

The 60/70 penetration graded asphalt cement was selected because it is the asphalt grade that is used in most temperature zoning of the country. The neat asphalt binder properties tests included specific gravity test as per [28], binder penetration test as per [29], softening point temperature test as per [30], and rotational viscosity test as per [31]. A summary of the neat asphalt binder physical properties that have been determined from laboratory testing is provided in Table1.

Table 1. Neat asphalt binder physical properties

Test	*Testing methods*	*Test results*
Specific gravity @ 25ºC	*ASTM D70*	1.030
Penetration value (0.1mm) @ 25ºC	*ASTM D5*	64
Softening point (ºC)	*ASTM D36*	45
Rotational viscosity unaged binder at (135ºC) mPa·s	*AASHTO T316*	494
Rotational viscosity unaged binder at (165ºC) mPa·s	*AASHTO T316*	123

2.1.2 Reclaimed Asphalt Pavement

Reclaimed asphalt pavement (RAP) was extracted by the recovering method using trichloroethylene following [32]. During the extraction process, a centrifuge extractor machine with a capacity of 1500 g was used on each representative RAP sample, and the recovered binder for each binder sample was separately stored. Then the recovered binder was subjected to typical standard laboratory tests to determine its physical properties. A summary of the recovered asphalt binder physical properties is shown in Table 2.

Table 2. Recovered RAP binder properties test results and the associated test methods

Test	*Testing method*	*Test results*
Specific gravity @ 25ºC	*ASTM D70*	1.054
Penetration value (0.1mm) @ 25ºC	*ASTM D5*	40.5
Softening point (ºC)	*ASTM D36*	58
Rotational viscosity of aged binder at (135ºC) mPa-s	*AASHTO T316*	1265
Rotational viscosity of aged binder at (165ºC) mPa-s	*AASHTO T316*	342

2.1.3 Rejuvenated Binders

Rejuvenating the recovered RAP binder is intended to restore its physical properties to those of an unaged binder. Two types of rejuvenator agents, namely soybean oil (SOY) and sunflower oil (SnF), were mixed with the RAP recovered binder. Table 3 presents the physical properties of the rejuvenators that are determined after conducting the laboratory tests. The percentage of rejuvenator that are used depends on the desired properties of the binder mix. The rejuvenators were then mixed with the recovered binder at proportions of 3 and 6% (by weight of recovered RAP binder) using a shear force mixer.

Table 3. SOY and SnF rejuvenator physical properties

Properties	***Rejuvenators***	
	SOY	*SnF*
Rotational viscosity @ 25ºC (Pa.S), AASHTO T-316	0.063	0.0608
Specific gravity @ 25ºC, ASTM D70	0.9798	0.9171
Flash point (ºC) ASTM D93	255	275

2.1.4 RAP Binder Content and Aggregate Gradation

First the binder content was determined from the RAP materials. Second aggregate gradation was determined. The residual aggregates were then washed, dried for sieve analysis. Sieve analysis following the [33] was conducted on the residual aggregates as shown in Table 4. The findings after the sieve analysis were tabulated and presented in Table 5.

Table 4. Extraction test results of RAP materials

Wt. of mix	*gm*	1862.0
Wt. Of filter before test	*gm*	20
Wt. Of filter after test	*gm*	21.3
Wt. Of aggregate after test	*gm*	1764.3
Total Wt. of aggregate	*gm*	1765.6
Loss of Wt.	*gm*	96.4
Asphalt % by Wt. of aggregate	*%*	5.46
Asphalt % by Wt. of mix	*%*	5.17

Table 5. Aggregate gradation for the collected RAP

Sieve No	***Retained (%)***	***Passing (%)***
3/4"	0.0	100.0
1/2"	12.2	87.8
3/8"	20.7	79.3
# 4	42.8	57.2
# 10	57.8	42.2
# 40	78.8	21.2
# 80	87.2	12.8

# 200	88.6	11.4

2.1.5 Virgin Aggregate Gradation

In this study, a typical aggregate gradation that is commonly used in producing HMA for the primary highways for asphaltic concrete wearing coarse is selected. To ensure that the aggregate gradation was the same for each mixture, the aggregate was separated into various sized fractions. Table 6 presents the aggregate gradation with the specification limits designated by Marshall method. The selected aggregate properties were then determined in the laboratory in accordance with the application of ASTM standards as shown in Table 7. These properties are used for calculating the mixture volumetric properties.

Table 6. Typical aggregate gradation for asphaltic concrete wearing course

Sieve size	***Retained (%)***	***Passing (%)***	***Specification Limits (Marshall)***
3/4"	0.0	100	100
1/2"	10.3	89.7	75-90
3/8"	22.9	77.1	64-79
# 4	45.2	54.8	41-56
# 10	67.1	32.9	23-37
# 40	81.67	18.33	7-20
# 80	88.2	11.8	5-13
# 200	94.8	5.2	3-8

Table 7. Physical properties of virgin aggregates for asphaltic concrete wearing course

Test	***Specification***	***Coarse Aggregate Results***	***Fine aggregate Results***	***Specifications Limits***
Los Angeles abrasion test (%)	*ASTM C131*	29.5%		*40%. Max*
Angularity (%)	*ASTM D5821*	96%		*90%.Min*
Flat and elongated particles ratio (%)	*ASTM D4791*	2.4%		*(5:1 ratio) 10%. Max*
Bulk specific gravity	*ASTM C127*	2.540		-
Apparent specific gravity		2.653		-

Sand equivalent (%)	*ASTM D2419*		62%	*40%.Min*
Bulk specific gravity	*ASTM C128*		2.52	-
Apparent specific gravity			2.61	-

As shown in Table 8, the combined gradations of asphalt mixture aggregates are presented. Since RAP aggregates are somewhat finer than the virgin aggregates, it is required to determine the proportion of each aggregate percentage to satisfy the desired aggregate gradation. Percentage of both virgin and RAP aggregate must be determined to meet the final gradation of the mixture and satisfy the specified volumetric properties. The combined aggregate gradation is shown in Figure 1.

Table 8. The combined aggregate gradation for asphaltic concrete wearing course

Sieve size	***RAP Aggregate Passing (40%)***	***Virgin Aggregate Passing (60%)***	***Combined Grading (%)***	***Specification Limits (Marshall) (%)***
3/4"	100.0	100	100.0	*100*
1/2"	87.8	89.7	88.9	*75-90*
3/8"	79.3	77.1	77.9	*64-79*
# 4	57.2	54.8	55.7	*41-56*
# 10	42.2	32.9	36.6	*23-37*
# 40	21.2	18.3	19.4	*7-20*
# 80	12.8	11.8	12.1	*5-13*
# 200	11.4	5.2	7.6	*3-8*

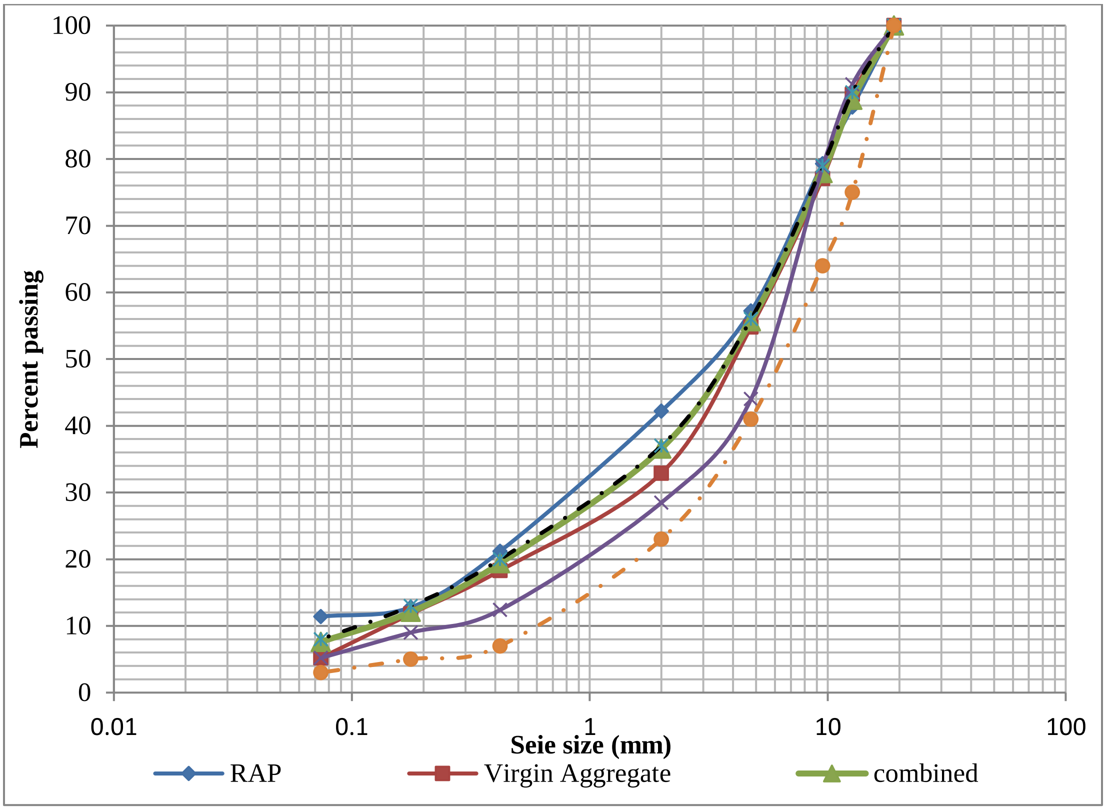

Figure 1. Aggregate gradation blending curves

2.2 Test Methods

In this study, the Marshall method of asphalt mix design accordance with the [34] was used to produce mixture specimens containing control, RAP and rejuvenated RAP mixtures. For the production of specimen, aggregates are heated for 16 hours at 170ºC and binder was heated for 1 hour at 150ºC. The heated aggregate was placed in a mixing bowl preheated to the same temperature as the aggregate; then the bowl was placed on a balance where the appropriate amount of binder was added. The binder was spread into the aggregate with a preheated spoon and then mixed with an electrical mixer. The binder and the aggregate were mixed for about three minutes to produce a mixture with a consistent binder distribution throughout. The mixtures were compacted using 75 impacts of the Marshall compactors, which is designed to handle heavy traffic.

2.2.1 Volumetric Properties

Measuring the volumetric properties of HMA mixture specimen is essential to make sure that the required criteria can be meet. Following [35 - 36], maximum and bulk theoretical densities of the HMA mixture specimens were determined. The air void content, the mineral aggregate voids, and voids in fine aggregates were calculated using the following equations.

$$V_a = \left\{\frac{G_{mm} - G_{mb}}{G_{mm}}\right\} * 100 \quad \text{(Eq. 1)}$$

$$VMA = 100 - \left\{\frac{G_{mb} * P_s}{G_{sb}}\right\} \quad \text{(Eq. 2)}$$

$$VFA = \frac{100\,(VMA - V_a)}{VMA} \quad \text{(Eq. 3)}$$

Where, V_a is the percentage of air voids (%), VMA is the void percentage in mineral aggregates (%) VFA is the void percentage in fine aggregates (%), P_s is the percentage of aggregates in the mixtures, G_{mm} is the maximum theoretical density, G_{mb} is the bulk density of the mixture, G_{sb} is the bulk density of the aggregates.

2.2.2 Marshall Stability and Flow

The Marshall testing apparatus was used to conduct the Marshall stability and flow tests, which were used as parameters for designing the asphalt mixture. As part of the Marshall stability test, the specimen is loaded to failure with a 50 mm/min speed. The required load to produce failure is defined as Marshall stability, while the specimen vertical deformation throughout the test till failure is defined as the Marshall flow. Besides the Marshall test, the asphalt mixture specimens were tested for Indirect Tensile Strength (ITS).

2.2.3 Indirect Tensile Strength (ITS)

The tensile strength test of HMA mixtures plays an important role in identifying the asphalt pavement cracking behavior. ITS is undertaken as a potential testing technique when evaluating the fatigue cracking resistance of asphalt mixtures [12]. The ITS test in this study was conducted at 25ºC as per [37]. Following the fabrication of the mixtures, cylindrical specimens were made with both rejuvenated RAP and non-rejuvenated RAP binder contents. Then, using the Marshall set up, the HMA mixture specimens were loaded along their diameter at a constant rate of deformation of 50 mm/min until they break. Using equation 4, the data achieved from the test can be used to determine the indirect tensile stresses.

$$S_t = \frac{2000P}{\pi t D} \quad \text{(Eq. 4)}$$

where, S_t = Indirect tensile strength (ITS), (kPa), P = The load required for breaking the specimen (in Newton), t = Thickness of the specimen (mm) and D = Diameter of specimen (mm)

2.2.4 Moisture Resistance

Moisture resistance to asphalt pavements is considered to be one of the most significant environmental factors influencing pavement failure [38]. Additionally, earlier researches have shown that adding RAP in the production of HMA mixture causes the mixture

specimen to become more susceptible to moisture resistance, whereas the addition of a small amount of a rejuvenator can enhance moisture resistance [39].
As part of this study, moisture susceptibility was assessed using the [40] method. The test as shown in Figure 2 was carried out on six cylindrical specimens having a diameter of 100 ± 2 mm with a thickness of 65 ± 1.5 mm. These specimens were split into dry and wet subsets. During the saturating process, it is necessary for the dry subsets to be saturated at 25°C in the oven for two hours. Subset of wet specimens are first vacuum saturated to 70-80% saturation, and then conditioned in a water bath for 24 hours. Once the specimens have been removed from the water bath, they are saturated at 25˚C for two hours before being tested for ITS. Finally, the ITS test was conducted at a temperature of 25ºC and a displacement rate that was kept as 50 mm per min.

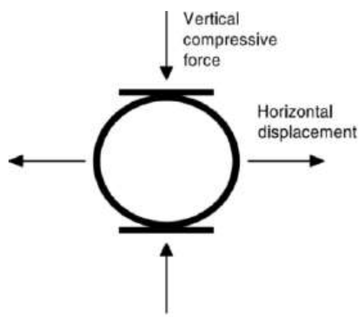

Figure 2. Indirect tensile strength test

Tensile strength ratio (TSR) of saturated (wet) and unsaturated (dry) specimens were then determined using Equation 5.

$$TSR = \frac{ITS_{wet}}{ITS_{Dry}} \quad \text{(Eq. 5)}$$

Where: TSR = Tensile strength ratio (%), ITS_{dry} = Indirect tensile strength of dry (unsaturated) samples, ITS_{wet} = Indirect tensile strength of wet (saturated) samples.

In general, it is recommended that the ratio of ITS_{wet}/ITS_{dry} must not fall below 80% [41].

2.2.5 Statistical Analysis

The statistical analysis consists of the effect rejuvenators on the properties of the RAP modified HMA mixture. In interpreting the data, it was assumed that the effect of the rejuvenators on the properties of rejuvenated RAP mixture would depend primarily on two variables namely rejuvenator type and rejuvenator percentage. It was also expected that in some cases these variables would strongly interact. For this reason, the experiment was statistically designed so that the data would be interpreted through analysis of the variance (ANOVA).
In ANOVA statistical terms, the null hypothesis (also known as H_0) is a statement that a population parameter's value is equal to a certain claim. A direct test is conducted on the null hypothesis. The hypothesis H_0 must either be rejected or not rejected. Contrary to the

null hypothesis, the alternative hypothesis indicates that a parameter differs in some way from that hypothesis. The null hypothesis is considered rejected if the P-value is very small and the alpha level is less than or equal to 0.05.

Independent Variables (Factors): In this analysis, the independent variables are rejuvenator type and rejuvenator percentage are considered.

Dependent Variables (Response Variables): The response variables evaluated were the Marshall stability, Marshall flow and indirect tensile strength.

3. Results and Discussion

The effect of rejuvenated RAP recovered binder was evaluated by examining the properties of HMA mixtures with rejuvenated RAP recovered binder. In order to determine the properties of HMA mixtures, Marshall mix design and Indirect Tensile Strength (ITS) tests were used. Asphaltic mixtures were tested to determine the optimum binder content that would achieve the required stability, density, and air voids.

3.1 Volumetric Properties

In asphalt mixtures, Va, VMA, VFA, and OBC are the significant factors affecting the performance of asphalt mixtures. Where, Va is the percentage of air voids, VMA is the void percentage in mineral aggregates, VFA is the void percentage in fine aggregates, and OBC is the optimum binder content. In order to meet these requirements, optimal binder content (OBC) is important. As can be shown in Table 9, adding RAP recovered binder increased the optimum binder level for the non-rejuvenated RAP mixture specimens. Possibly, this is due to the increase in the percentage of air voids that resulted from the decrease in workability caused by adding the RAP recovered binder, which has been resulted in the need for more binder to fill the air voids and meet the maximum air void content limit.

Table 9. Asphalt Mixture Properties

Samples	***Stability (kg)***	***flow (mm)***	***air void%***	***VMA %***	***VFA%***	***Optimum binder content %***	***Max. Unit weight (gm/cc)***
Specification Limits / Mixture Samples	*750 (min)*	*3.0 – 5.0*	*14 (min)*	*2.0 – 4.0*	*70 – 80*	-	-
Control Mix	1108	4.1	3.90	14.9	71	5.6	2.287
100RAP	1677	3.73	4.20	16.8	78	6.5	2.276
40RAP	1632	3.81	4.15	15.5	74	6	2.271
40RAP3SOY	1644	3.43	3.88	14.88	73.6	5.6	2.276
40RAP6SOY	1596	3.75	3.00	13.86	74.1	5.2	2.273
40RAP3SnF	1527	3.97	3.92	14.22	73.8	5.4	2.269
40RAP6SnF	1488	4.25	3.53	13.12	74.1	5	2.279

Note:

Sample Name	***Mixture type***
Control Mix	*Standard Asphalt Mix*
100RAP	*Mix with 100% RAP materials*
40RAP	*Mix with 40% RAP materials*
40RAP3SOY	*Mix with 40% RAP+3% Soybean oil*
40RAP6SOY	*Mix with 40% RAP+6% Soybean oil*
40RAP3SnF	*Mix with 40% RAP+3% sunflower oil*
40RAP6SnF	*Mix with 40% RAP+6% sunflower oil*

3.2 Marshall Test Results

The Marshall stability test results as shown in Figure 3 indicated that the asphalt mixture specimens comprising RAP asphalt materials have recorded higher stability values than the neat asphalt mixtures. For instance, the asphalt mixture with 40% RAP has a 32% higher Marshall stability rating than the control mixture. The findings given in Figure 3 also shown that the rejuvenated RAP mixtures achieve lesser stability values compared to the non-rejuvenated RAP asphalt mixtures. This is a sign that lubricant level is higher than what is necessary to counteract the hardening brought on by the RAP recovered binder, and as increasing the amount of rejuvenator caused the binder to soften excessively, which decrease its stability. In addition, the asphalt mixture having the SnF rejuvenator resulted in lower Marshall stability as compare to the asphalt mixtures rejuvenated with SOY, which indicating that the SnF rejuvenator has a more softening effect than the SOY rejuvenator.

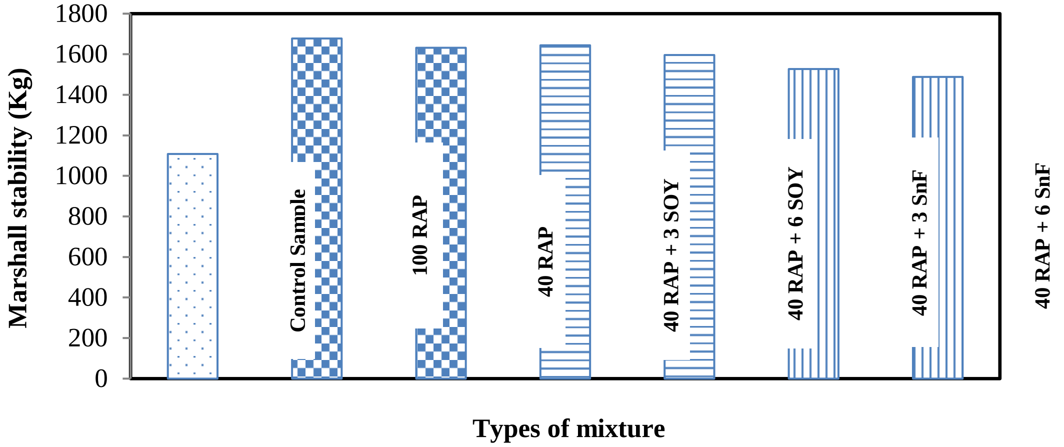

Figure 3. Marshall stability test results of the asphalt mixtures

As presented in Figure 4, the flow value of non-rejuvenated RAP asphalt mixtures increased more as compared to the control asphalt mixture. The increase flow rates were not expected. The reason for this result was that the RAP mixture contained more fines, which followed to the coarse particles. The increase in fines results in more softening and an increase in the flow value.

In addition, rejuvenated RAP mixtures exhibited flow rates within the limits specified by the specification standard. Furthermore, adding the SnF rejuvenator to RAP mixture has resulted in a slight decrease in the flow rate, and this improvement in the flow rate was because of the improved coating of recycled aggregates and the increased workability of the asphalt mixture.

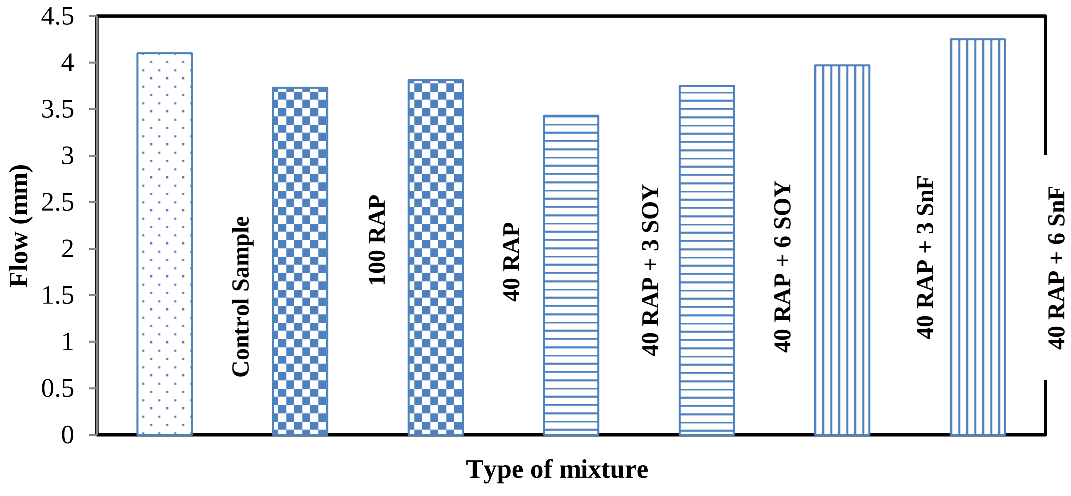

Figure 4. Marshall flow test results of the asphalt mixtures.

3.3 Indirect Tensile Strength Test Results

The observed values of indirect tensile strength (ITS) for control, RAP and rejuvenated RAP mixtures can be found in Figure 5. As shown, the control asphalt mixture exhibited higher ITS values that the RAP asphalt mixtures. For instance, the ITS value of the control mixture was 732 kPa, whereas, it was 535 kPa for 100RAP mixture and 641 for 40RAP mixture.

Furthermore, the rejuvenated RAP asphalt mixtures with 3% rejuvenator shown higher ITS values than the RAP asphalt mixtures, however, for higher rejuvenating content (i.e., 6%), the ITS value was somewhat lower than the asphalt mixture with 3% rejuvenator. This is because of the ITS values dropped as the rejuvenator content increased.

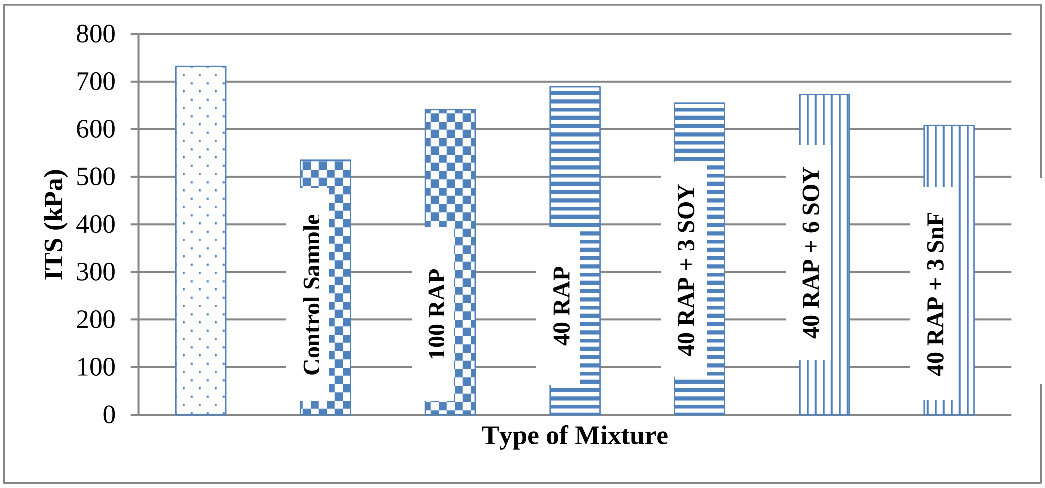

Figure 5. Indirect tensile strength test results of asphalt mixtures

3.4 Moisture Resistance Test Results

The moisture resistance test is performed using the tensile strength ratio (TSR) which is applied to evaluate the effect of rejuvenated RAP on the asphalt mixtures. It should be noted that the increased TSR values leads to better asphalt mixture moisture resistance. The result values of indirect tensile strength test for rejuvenated and non-rejuvenated RAP asphalt mixtures are presented in Figure 6. The indirect tensile strength values of both saturated and unsaturated mixtures increased with rejuvenated RAP asphalt mixtures as compared with non-rejuvenated RAP asphalt mixtures.

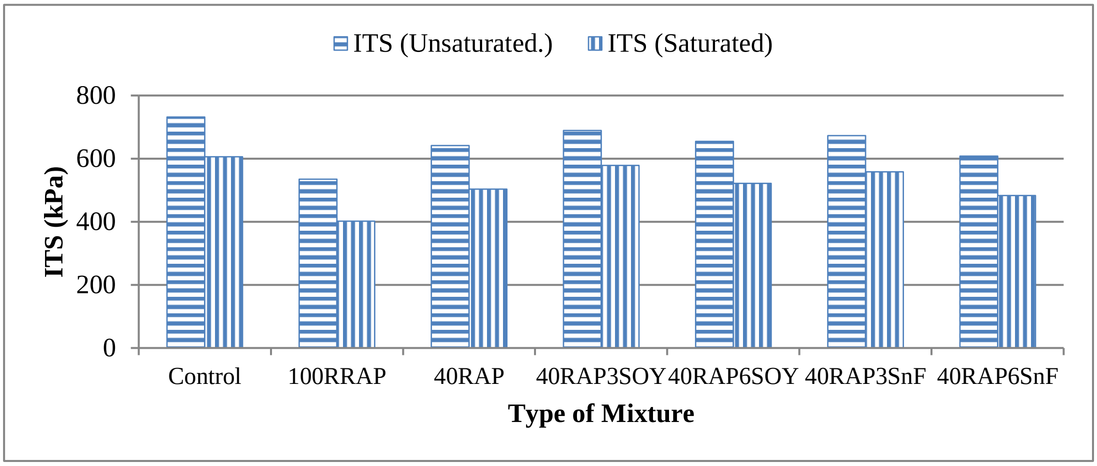

Figure 6. Indirect tensile strength test result of saturated and unsaturated asphalt mixtures

Furthermore, the observed TSR values of RAP mixtures significantly increased when the rejuvenator were added into the mixtures as shown in Figure 7. This indicated that the rejuvenators, improving the adhesion and cohesion bond and had a beneficial effect on tensile strength of asphalt mixtures. Among the different mixtures, highest TSR values were 84% and 83% for asphalt mix having 3% SOY and 3%SnF rejuvenators, respectively. In addition, with increasing rejuvenator percentages the TSR values of asphalt mixtures were reduced indicating lower moisture resistance of the mix with high percentage of rejuvenator.

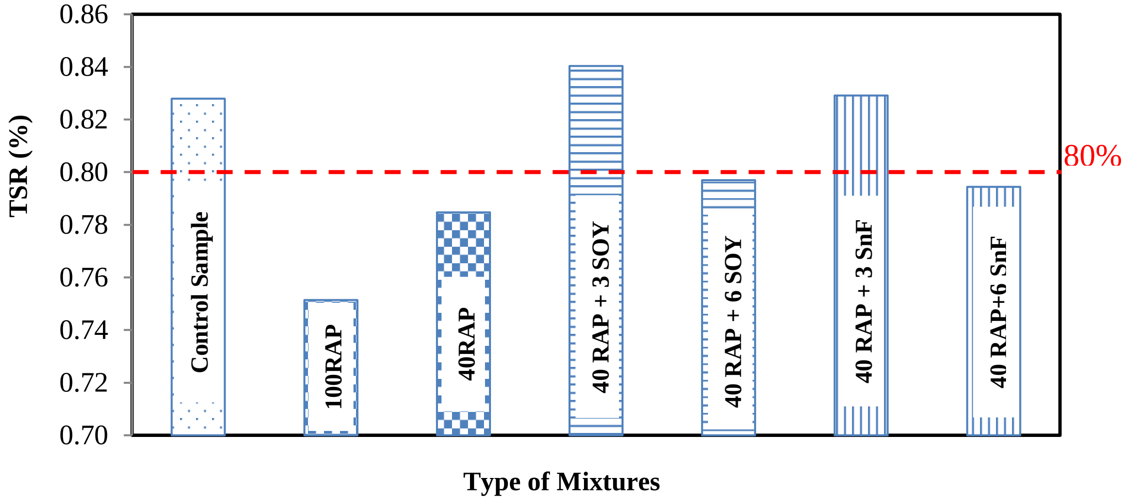

Figure 7. Tensile strength ratio (TSR) result for saturated and unsaturated asphalt mixtures

3.5 Statistical Analysis Results

The effect of rejuvenating agents on the asphalt mixture properties namely (Marshall stability, Marshall flow and indirect tensile strength), were evaluated. A marginal P value of 0.05 was used to base the evaluation, meaning that variables with a P value of less than

0.05 are significant. Based on the stated hypothesis, different observed properties of rejuvenated mixtures were evaluated, including the types and percentages of rejuvenating agents, and their interaction. ANOVA summary as shown in Tables 10, 11 and 12 illustrated that the rejuvenated percentage has statistically significant effect on the given asphalt mixture properties.

Based on the results given in Table 10, it was found that the rejuvenator percentage statistically have significant effect on the Marshall stability values of asphalt mixtures. Whereas, the rejuvenated type and the interaction of rejuvenator type with rejuvenator percentage statistically has no significant effects on the mixture stability value.

Table 10. Statistical analysis (ANOVA) on Marshall stability values of asphalt mixtures

Element	**P-value**	**Status**	**Decision**	**Effect**
Rejuvenator percentage	0.050	$P < 0.05$	Reject H_{01}	Significant
Rejuvenator type	0.14	$P > 0.05$	Do not Reject H_{02}	Insignificant
Percentage of rejuvenator with the type of rejuvenator	0.7	$P > 0.05$	Do not Reject H_{03}	Insignificant

Table 11 provides a summary of the statistical analysis of the asphalt mixtures Marshall flow values. It is shown that the rejuvenator percentage statistically has significant effect on the mixture Marshall flow, while, the rejuvenated type and the interaction of type and percentage of rejuvenator statistically have no significant effect on the mix Marshall flow values.

Table 11. Statistical analysis (ANOVA) on Marshall flow values of asphalt mixtures

Element	**P-value**	**Status**	**Decision**	**Effect**
Rejuvenator percentage	0.030	$P < 0.05$	Reject H_{01}	Significant
Rejuvenator type	0.06	$P > 0.05$	Do not Reject H_{02}	Insignificant
Percentage of rejuvenator with the type of rejuvenator	0.9	$P > 0.05$	Do not Reject H_{03}	Insignificant

The summary of the statistical analysis (ANOVA) of indirect tensile strength (ITS) values is shown in Table 12. The asphalt mixtures ITS values are statistically significantly influenced by the percentage of rejuvenating agents, whereas, the type of rejuvenating agents and its interaction with the percentage of rejuvenating agents have statistically no significant effect on the ITS value.

Table 12. Statistical analysis (ANOVA) for the ITS values of asphalt mixtures

Element	**P-value**	**Status**	**Decision**	**Effect**
Rejuvenator percentage	0.030	$P < 0.05$	Reject H_{01}	Significant
Rejuvenator type	0.150	$P > 0.05$	Do not Reject H_{02}	Insignificant
Percentage of rejuvenator with the type of rejuvenator	0.4	$P > 0.05$	Do not Reject H_{03}	Insignificant

4. Conclusions

The main purpose of the study was to investigate the effects of rejuvenators on the properties of asphalt mixture containing high percentages of RAP, by using both binder conventional and Marshall mixture methods. Based on laboratory test results and statistical analysis conducted during this study, the general conclusions were reached that the properties of rejuvenated RAP mixtures vary and are mainly depended by the type and percentage of rejuvenators added.

As determined by the Marshall mixture test, it was found that by adding sufficient amounts of rejuvenator, the volumetric properties of RAP mixtures reached the desired level. In addition, the rejuvenator, due to its softening properties, has decreased RAP aged binder's stability. In general, Marshall mix test results shown that the rejuvenated RAP samples met the specification limits provided by the specification for the wearing and binder coarse mixtures.

Indirect tensile strength test showed that the TSR ratio (as indicate moisture susceptibility) increased with the addition of rejuvenator, while, with high percentage of rejuvenator it is reduced. It was also found that the 3% SnF and 6% SOY rejuvenated RAP mixture has nearly similar indirect tensile strength values to the control mixture. Furthermore. The SnF rejuvenator more effectively reduced the stability of the rejuvenated RAP mixture than SOY did.

5. Recommendations for future research

During this study, rejuvenators were tested on the properties of the rejuvenated RAP asphalt mixtures using the local paving mixture method. For further research, the author recommends the following:

- The asphalt mixture properties in this study were limited to the Marshall mix practice. Thus, further studies needed to investigate the effect of rejuvenator on using Superpave requirements for mixtures.

- Field testing should be used to validate the test results of this study.

6. Declare of Competing Interest

The author state that he has no competing financial interests that could have influenced the work reported in this paper.

Reference

[1] Farooq, M. A., & Mir, M. S. (2017). Use of reclaimed asphalt pavement (RAP) in warm mix asphalt (WMA) pavements: a review. In Innovative Infrastructure Solutions (Vol. 2, Issue 1). Springer. https://doi.org/10.1007/s41062-017-0058-7

[2] Hettiarachchi, C., Hou, X., Wang, J., & Xiao, F. (2019). A comprehensive review on the utilization of reclaimed asphalt material with warm mix asphalt technology. In Construction and Building Materials (Vol. 227). Elsevier Ltd. https://doi.org/10.1016/j.conbuildmat.2019.117096

[3] Ren, J., Zang, G., Wang, S., Shi, J., & Wang, Y. (2020). Investigating the pavement performance and aging resistance of modified bio-asphalt with nano-particles. PLoS ONE, 15(9 september), 1–16. https://doi.org/10.1371/journal.pone.0238817

[4] Valdés, Pérez-Jiménez, Miró, & Martínez. (2009). Experimental Study of Recycled Asphalt Mixture with High Percentage of Reclaimed Asphalt Pavement (RAP). Transportation Research Record, 2008(November 2008), 1–16.

[5] Dinis-Almeida, M., Castro-Gomes, J., & Antunes, M. D. L. (2012). Mix design considerations for warm mix recycled asphalt with bitumen emulsion. Construction and Building Materials, 28(1), 687–693. https://doi.org/10.1016/j.conbuildmat.2011.10.053

[6] FHWA. (2011). Reclaimed Asphalt Pavement in Asphalt Mixtures: State of the Practice. Report No. FHWA-HRT-11-021, FHWA, McLean, Virginia.

[7] Mamun, A. Al, Al-Abdul Wahhab, H. I., & Dalhat, M. A. (2020). Comparative Evaluation of Waste Cooking Oil and Waste Engine Oil Rejuvenated Asphalt Concrete Mixtures. Arabian Journal for Science and Engineering, 45(10), 7987–7997. https://doi.org/10.1007/s13369-020-04523-5

[8] Yang, X. (2013b). The Laboratory Evaluation of Bio Oil Derived From Waste The Laboratory Evaluation of Bio Oil Derived From Waste Resources as Extender for Asphalt Binder Resources as Extender for Asphalt Binder Part of the Civil Engineering Commons.

[9] Caputo, P., Abe, A. A., Loise, V., Porto, M., Calandra, P., Angelico, R., & Rossi, C. O. (2020). The role of additives in warm mix asphalt technology: An insight into their mechanisms of improving an emerging technology. Nanomaterials, 10(6), 1–17. https://doi.org/10.3390/nano10061202

[10] Hill, B., Asce, A. M., Behnia, B., Buttlar, W. G., Asce, M., & Reis, H. (2013). Evaluation of Warm Mix Asphalt Mixtures Containing Reclaimed Asphalt Pavement through Mechanical Performance Tests and an Acoustic Emission Approach. Journal

of Materials in Civil Engineering, 25(12), 1887–1897. https://doi.org/10.1061/(asce)mt.1943-5533.0000757
[11] Seidel, J. C., & Haddock, J. E. (2014). Rheological characterization of asphalt binders modified with soybean fatty acids. Construction and Building Materials, 53, 324–332. https://doi.org/10.1016/j.conbuildmat.2013.11.087
[12] Zhang, R., You, Z., Wang, H., Ye, M., Yap, Y. K., & Si, C. (2019). The impact of bio-oil as rejuvenator for aged asphalt binder. Construction and Building Materials, 196, 134–143. https://doi.org/10.1016/j.conbuildmat.2018.10.168
[13] Zhu, J., Ma, T., Fan, J., Fang, Z., Chen, T., & Zhou, Y. (2020). Experimental study of high modulus asphalt mixture containing reclaimed asphalt pavement. Journal of Cleaner Production, 263, 121447. https://doi.org/10.1016/j.jclepro.2020.121447
[14] Kent R. Hansen, P. E., & Copeland, A. (2017). Recycled Materials and Warm-Mix Asphalt Usage: 2016. Annual Asphalt Pavement Industry Survey, 05–40.
[15] Key figures of the European. (2011).
[16] Zargar, M., Ahmadinia, E., Asli, H., & Karim, M. R. (2012). Investigation of the possibility of using waste cooking oil as a rejuvenating agent for aged bitumen. Journal of Hazardous Materials, 233–234, 254–258. https://doi.org/10.1016/j.jhazmat.2012.06.021
[17] Al-Qadi, I. L., Elseifi, M., & Carpenter, S. H. (2007). Reclaimed asphalt pavement - A literature review. Federal Highway Administration, 07(FHWA-ICT-07-001), 23.
[18] Ding, Y., Huang, B., & Shu, X. (2016). Characterizing blending efficiency of plant produced asphalt paving mixtures containing high RAP. Construction and Building Materials, 126, 172–178. https://doi.org/10.1016/j.conbuildmat.2016.09.025
[19] Foroutan Mirhosseini, A., Tahami, A., Hoff, I., Dessouky, S., Kavussi, A., Fuentes, L., & Walubita, L. F. (2020). Performance Characterization of Warm-Mix Asphalt Containing High Reclaimed-Asphalt Pavement with Bio-Oil Rejuvenator. Journal of Materials in Civil Engineering, 32(12), 04020382. https://doi.org/10.1061/(asce)mt.1943-5533.0003481
[20] Rodrigues, C., Capitão, S., Picado-Santos, L., & Almeida, A. (2020). Full recycling of asphalt concrete with waste cooking oil as rejuvenator and LDPE from urban waste as binder modifier. Sustainability (Switzerland), 12(19). https://doi.org/10.3390/su12198222
[21] Ziari, H., Aliha, M. R. M., Moniri, A., & Saghafi, Y. (2020). Crack resistance of hot mix asphalt containing different percentages of reclaimed asphalt pavement and glass fiber. Construction and Building Materials, 230, 117015. https://doi.org/10.1016/j.conbuildmat.2019.117015
[22] Elahi, Z., Jakarni, F. M., Muniandy, R., Hassim, S., Ab Razak, M. S., Ansari, A. H., & Ben Zair, M. M. (2021). Waste cooking oil as a sustainable bio modifier for asphalt modification: A review. Sustainability (Switzerland), 13(20), 1–27. https://doi.org/10.3390/su132011506
[23] Ziari, H., Moniri, A., Bahri, P., & Saghafi, Y. (2019). Evaluation of performance properties of 50% recycled asphalt mixtures using three types of rejuvenators.

Petroleum Science and Technology, 37(23), 2355–2361. https://doi.org/10.1080/10916466.2018.1550505
[24] Mcdaniel, R. S., Shah, A., Huber, G. A., Copeland, A., Mcdaniel, R. S., Shah, A., Huber, G. A., & Copeland, A. (2012). Effects of reclaimed asphalt pavement content and virgin binder grade on properties of plant produced mixtures. 0629. https://doi.org/10.1080/14680629.2012.657066
[25] Elkashef, M., Asce, A. M., Williams, ; R Christopher, & Cochran, E. (2018). Effect of Asphalt Binder Grade and Source on the Extent of Rheological Changes in Rejuvenated Binders. https://doi.org/10.1061/(ASCE)
[26] Tarar, M. A., Khan, A. H., Rehman, Z. ur, & Inam, A. (2019). Changes in the rheological characteristics of asphalt binders modified with soybean-derived materials. International Journal of Pavement Engineering. https://doi.org/10.1080/10298436.2019.1600690
[27] Zaumanis, M., & State, L. (2014). Influence of six rejuvenators on the performance properties of Reclaimed Asphalt Pavement (RAP) binder and 100 % recycled asphalt mixtures. July 2015. https://doi.org/10.1016/j.conbuildmat.2014.08.073
[28] ASTM D70-18. (2018). Standard Test Method of Specific Gravity of Bituminous Materials. American society for testing and materials. International. https://standards.globalspec.com/std/3812080/astm-d70-97
[29] ASTM D5-20. (2020). Standard Test Method for Penetration of Bituminous Materials. American society for testing and materials. International. https://standards.globalspec.com/std/3825077/ASTM%20D5-06
[30] ASTM D36-20. (2020). Standard Test Method for Softening Point of Bituminous Materials Ring-and-Ball Apparatus. American society for testing and materials. International. https://webstore.ansi.org/Standards/ASTM/astmd36952000e1
[31] AASHTO T316-20. (2020). Standard Method of Test for Viscosity Determination of Asphalt Binder Using Rotational Viscometer. American Association of State Highway and Transportation Officials. Washington, DC.
[32] ASTM D2172-17. (2017). Standard Test Methods for Quantitative Extraction of Bitumen From Bituminous Paving Mixtures. American society for testing and materials. International. https://webstore.ansi.org/Standards/ASTM/astmd2172d2172m11
[33] AASHTO T30. (2019). Standard Method of Test for Mechanical Analysis of Extracted Aggregate. American Association of State Highway and Transportation Officials. Washington DC.
[34] ASTM D1559-98. (1998). Test Method for Resistance of Plastic Flow of Bituminous Mixtures Using Marshall Apparatus. American society for testing and materials. International. https://www.document-center.com/standards/show/ASTM-D1559
[35] ASTM D2726-21. (2021). Standard Test Method for Bulk Specific Gravity and Density of Non-Absorptive Compacted Bituminous Mixtures. American society for testing and materials. International. https://www.astm.org/d2726-11.html

[36] ASTM D2041-19. (2019). Standard Test Method for Theoretical Maximum Specific Gravity and Density of Bituminous Paving Mixtures https://www.astm.org/standards/d2041
[37] ASTM D6931. (2017). Standard Test Method for Indirect Tensile (IDT) Strength of Asphalt mixture. American society for testing and materials. International. https://www.astm.org/d6931-17.html
[38] Sengoz, B., Topal, A., Oner, J., Yilmaz, M., Dokandari, P. A., & Kok, B. V. (2017). Performance evaluation of warm mix asphalt mixtures with recycled asphalt pavement. Periodica Polytechnica Civil Engineering, 61(1), 117–127. https://doi.org/10.3311/PPci.8498
[39] Ishaq, M. A., & Giustozzi, F. (2020). Rejuvenator effectiveness in reducing moisture and freeze/thaw damage on long-term performance of 20 % RAP asphalt mixes: An Australian case study. Case Studies in Construction Materials, 13, e00454. https://doi.org/10.1016/j.cscm.2020.e00454
[40] AASHTO T283-19 .(2019). Standard Method of Test for Resistance of Compacted Asphalt Mixtures to Moisture-Induced Damage. American Association of State Highway and Transportation Officials. Washington DC. https://standards.globalspec.com/std/13053352/AASHTO%20T%20283
[41] Goli, H., & Latifi, M. (2020). Evaluation of the effect of moisture on behavior of warm mix asphalt (WMA) mixtures containing recycled asphalt pavement (RAP). Construction and Building Materials, 247. https://doi.org/10.1016/j.conbuildmat.2020.118526

Author Profiles

KAMALUDDIN KAMAL received his B.Sc. degree in Civil Engineering Department from Kandahar University in 2006, M.Sc. degree in Civil Engineering from Asian Institute of Technology, Thailand, and Ph.D. in Transportation Engineering, Faculty of Engineering, King Abdul Aziz University in 2023. He is a faculty member of the Civil Engineering Department of Kandahar University, Kandahar, Afghanistan. His research interests include hot mix asphalt pavement, reclaimed asphalt pavement, recycling old asphalt pavement with rejuvenators.

MUJTABA AMIN is a Senior Lecturer in Faculty of Transportation Engineering at Kabul Polytechnic University. He obtained his B.Sc. in Transportation Engineering from Kabul Polytechnic University in 2009, M.Eng, in Structural Engineering from the Asian institute of Technology in 2015, and Ph.D. in Structural Engineering from Kyushu University in 2020. His research interests include impact analysis, bridge pounding, moving load, Structural Dynamics and Earthquake Engineering, Bridge and Structures.